

2-1-1977

Systematic Development Of Methodologies In Planning Urban Water Resources For Medium Size Communities, Application Of Linear Systems Analysis To Ground Water Evaluation Studies

C. T. Bathala

A. R. Rao

J. A. Spooner

Follow this and additional works at: <http://docs.lib.purdue.edu/watertech>

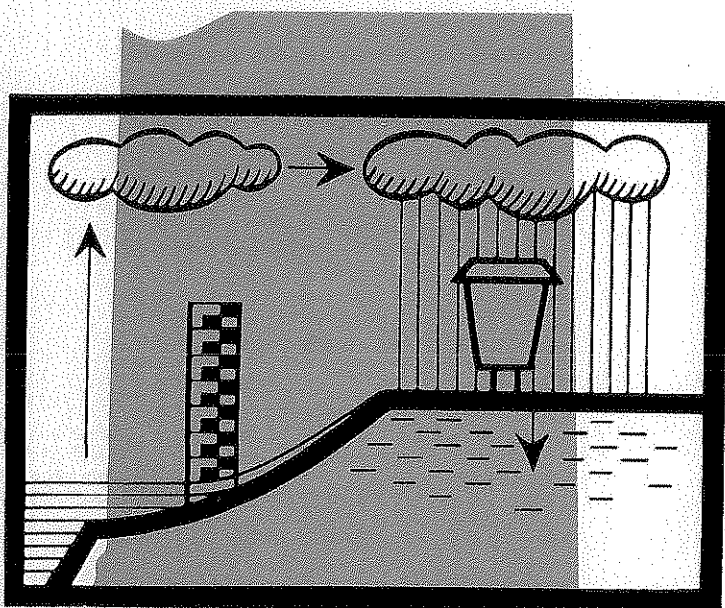
Bathala, C. T.; Rao, A. R.; and Spooner, J. A., "Systematic Development Of Methodologies In Planning Urban Water Resources For Medium Size Communities, Application Of Linear Systems Analysis To Ground Water Evaluation Studies" (1977). *IWRRC Technical Reports*. Paper 91.

<http://docs.lib.purdue.edu/watertech/91>

This document has been made available through Purdue e-Pubs, a service of the Purdue University Libraries. Please contact epubs@purdue.edu for additional information.

*Systematic Development of Methodologies in
Planning Urban Water Resources for Medium Size Communities*

**APPLICATION OF LINEAR SYSTEMS ANALYSIS
TO GROUND WATER EVALUATION STUDIES**



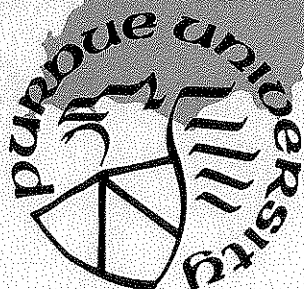
by

C. T. Bathala

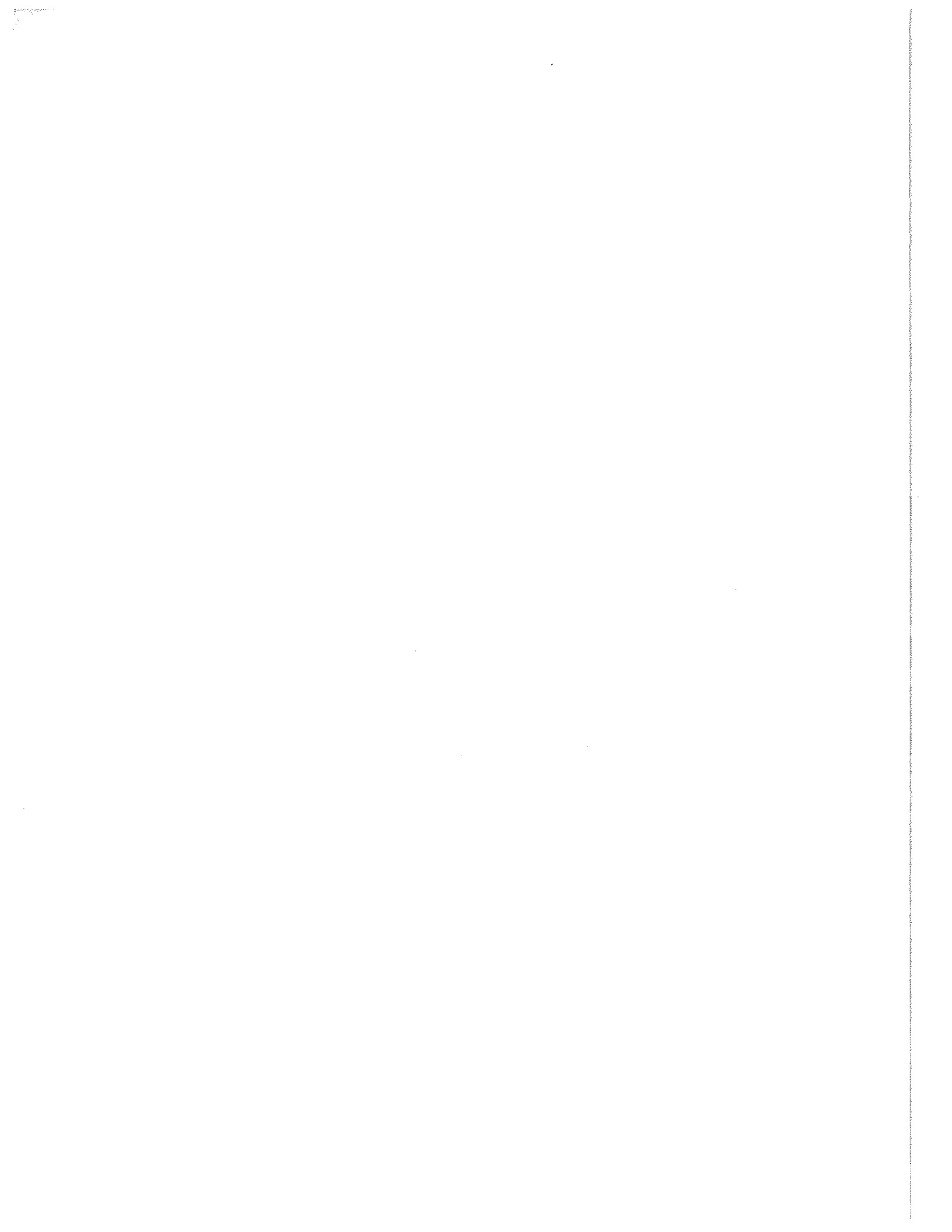
A. Ramachandra Rao

J. A. Spooner

February 1977



**PURDUE UNIVERSITY
WATER RESOURCES RESEARCH CENTER
WEST LAFAYETTE, INDIANA**



Water Resources Research Center
Purdue University
West Lafayette, Indiana

APPLICATION OF LINEAR SYSTEMS ANALYSIS TO
GROUND WATER EVALUATION STUDIES

by

C. T. Bathala

A. Ramachandra Rao

J. A. Spooner

The work upon which this report is based was supported in part by funds provided by the United States Department of the Interior, Office of Water Research and Technology, as authorized by the Water Resources Research Act of 1964 (PL 88-379) as amended.

Partial Completion Report for OWRT-C-6106

Grant No. 14-31-0001-5213

Purdue University Water Resources Research Center

Technical Report No. 91

February 1977

ACKNOWLEDGEMENTS

This report covers part of the work done under the Title II Project C-6106 entitled "Systematic Development of Methodologies in Planning Urban Water Resources for Medium Size Communities - Phase II". The work reported herein is a part of the ongoing work in Urban Water Resources at Purdue University.

The authors wish to express their appreciation to Dr. Dan Wiersma, Director of the Water Resources Research Center, and Dr. J. F. McLaughlin, Head, School of Civil Engineering at Purdue University for their encouragement and excellent administrative support. The authors wish to express their gratitude to their sponsors for their support without which this work could not have been undertaken.

We would like to thank Mrs. Ramona Hill and Mrs. Sherry Miller for their excellent and cheerful secretarial assistance.

The present report is a condensed version of the Doctoral Thesis "The Application of Linear Systems Analysis to Groundwater Evaluation Studies" submitted by C. T. Bathala to the Graduate Faculty at Purdue University in August 1976. The work was performed under the supervision of professors A. Ramachandra Rao and J. A. Spooner. For further details related to this work the reader is referred to the thesis which may be obtained from University Microfilms, Ann Arbor, Michigan.

ABSTRACT

The linear systems approach is used in the present study to formulate deterministic models for analyzing several types of groundwater flow problems. The stochastic nature of groundwater levels and the causal relationships between precipitation, river stages and groundwater levels are also analyzed. The specific objectives are the following:

- 1) To develop a procedure for predicting the response of an aquifer system under different hydrologic stresses by considering only the cause-and-effect relationships of the system.
2. To apply the above procedure for predicting the response of the groundwater system in field situations.
- 3) To investigate the utility of the above procedure to replace the traditional type curve solution for pumping test analysis.
- 4) To investigate the causal relationships between different hydrologic variables affecting groundwater levels.

A generalized linear model is used to analyze groundwater flow in a stream-well-aquifer system. A procedure is developed to predict aquifer response by considering the cause-and-effect relationships of the groundwater flow system. In this procedure, historical records of pumping rates, groundwater levels and stream stages, and estimated storage coefficients are used as inputs. The utility of this procedure for analysis of regional aquifer systems is demonstrated by using both field and hypothetical data and satisfactory results are obtained. The procedure developed in the present study does not require predetermined transmissivity and storage coefficient values. The present procedure is less subjective and appears to be more reliable than the type curve method for determination of the aquifer transmissivity and the storage coefficient from pumping test data.

The causal relationships between precipitation, river stages and groundwater levels are investigated by using the tests based on regression theory and the likelihood approach. Stochastic models for groundwater levels are developed after incorporating these causal relationships. This procedure is found to yield better stochastic models for groundwater levels.

TABLE OF CONTENTS

	<u>Page</u>
ACKNOWLEDGEMENTS	i
ABSTRACT	ii
TABLE OF CONTENTS.	iii
LIST OF TABLES	v
LIST OF FIGURES.	vii
LIST OF SYMBOLS AND NOTATIONS.	ix
CHAPTER 1 - INTRODUCTION	1
1.1 Regional Aquifer Models.	1
1.1.1 Application of Linear Systems Analysis to Groundwater Flow Problems	2
1.1.2 Application of Stochastic Modeling Techniques to Groundwater Flow Problems.	3
1.2 Critique and Motivation.	4
1.3 Objectives of the Present Study.	7
CHAPTER 2 - LINEAR SYSTEMS FORMULATION OF GENERALIZED AQUIFER FLOW PROBLEMS.	9
2.1 Basic Relationships.	9
2.1.1 Stream-Aquifer Interaction Without Pumping.	9
2.1.2 Single Well in an Infinite Aquifer.	10
a) Nonleaky Artesian Condition	10
b) Leaky Artesian Condition.	12
2.1.3 Multiple Well System.	12
2.1.4 Stream-Well-Aquifer System.	14
2.2 Theoretical Formulation.	14
2.2.1 Stream-Well-Aquifer System with Vertical Leakage.	17
2.2.2 Multiple Well System Without Vertical Leakage	18
2.2.3 Other Possible Cases of Groundwater Flow Systems.	18
a) Stream-Aquifer Interaction Without Pumping.	18
b) Non-Steady Radial Flow in an Infinite Leaky Aquifer	19
c) Non-Steady Radial Flow in a Nonleaky Artesian Aquifer	19
CHAPTER 3 - A PROCEDURE FOR THE PREDICTION OF AQUIFER RESPONSE AND ITS APPLICATIONS.	21
3.1 Multiple Well System in a Nonhomogeneous Aquifer	21
3.1.1 Calibration	21
3.1.2 Prediction.	25
3.1.3 Illustrative Example No. 1.	27
3.1.4 Application to a Field Situation.	37
3.2 Multiple Well System in a Homogeneous Aquifer.	40
3.2.1 Drawdowns in One of the Wells and Pumping Rates from All the Wells are Known.	41
3.2.2 Drawdowns in Any Two Wells and Pumping Rates from All the Wells are Known	41
3.3 Analysis of Pumping Test Data.	41
3.3.1 Determination of the Transmissivity and the Storage Coefficient from Pumping Test Data	42
3.3.2 Case Histories of Pumping Test Analysis	43
a) Milton, Illinois.	43
b) Gridley, Illinois	47
c) Grand Island, Nebraska.	49
3.4 Stream-Aquifer Interaction Without Pumping	51
3.4.1 Introduction.	51
3.4.2 Case History: Dunn's Bridge, Kankakee River Basin.	52
3.5 Application of the Present Procedure to a Hypothetical Regional Aquifer Problem.	52
3.5.1 Introduction.	52
3.5.2 Illustrative Example No. 2.	54

	<u>Page</u>
CHAPTER 4 - CAUSALITY AND THE CONSTRUCTION OF STOCHASTIC MODELS FOR GROUNDWATER LEVELS	69
4.1 The Concept of Causality	69
4.1.1 Tests for Causality with Two Variables.	70
4.2 Construction of Stochastic Models.	71
4.2.1 Parameter Estimation.	73
4.2.2 Validation of Models and Selection Criteria	73
4.3 Investigation of the Causal Relationship Between Groundwater Levels, Precipitation and River Stages	74
4.3.1 Data Used in the Study.	74
4.3.2 Statistical Characteristics of the Data	75
4.3.3 Univariate Models for Groundwater Levels, Precipitation and River Stages.	86
4.3.4 Validation Tests on Residuals	86
4.3.5 Checking the Causal Relationships	93
4.3.6 Final Stochastic Models for Groundwater Levels.	96
4.3.7 Characteristics of Groundwater Levels Regenerated from the Final Stochastic Models.	99
4.3.8 Simulation Results.	102
CHAPTER 5 - DISCUSSION AND CONCLUSIONS	111
5.1 Linear Systems Analysis of Aquifer Flow Problems	111
5.1.1 Modeling Regional Aquifer Systems	111
5.1.2 Estimation of Aquifer Storage Coefficients.	112
5.1.3 Data Requirements	112
5.1.4 Analysis of Pumping Test Data	113
5.2 Causal Relationships Between Precipitation, River Stages and Groundwater Levels.	113
5.2.1 Models for Water Levels in Well Tc-7.	113
5.2.2 Model for Water Levels in Well Tc-9	114
5.3 Scope for Further Investigation.	114
5.4 Conclusions.	115
BIBLIOGRAPHY	117
APPENDICES	
Appendix A: Basic Derivations.	120
Appendix B: Well Logs and Time-Drawdown Data	124

LIST OF TABLES

<u>Table</u>	<u>Page</u>
1.1 Cost Distribution of Different Computer Runs	5
1.2 Computational Cost of Modeling	6
3.1 Different Sets of Storage Coefficients Used in Sensitivity Analysis (I.E. No. 1)	29
3.2 Details of Observations Used in Calibration and Prediction	29
3.3 Average Transmissivities Computed After Calibration (I.E. No. 1)	30
3.4 Comparison of Theoretical and Computed Results After Calibration (Well No. 1, Case 1, I.E. No. 1).	31
3.5 Comparison of Theoretical and Computed Results After Calibration (Well No. 3, Case 4, I.E. No. 1).	34
3.6 Comparison of Theoretical and Computed Drawdowns (Ft. Below NPL) Well No. 2, I.E. No. 1.	35
3.7 Comparison of Theoretical and Computed Results After Prediction (Well No. 3, Case 4, I.E. No. 1).	37
3.8 Estimated Storage Coefficients and Computed Transmissivities (Milton).	40
3.9 Details of Pumping Test on Well 3, Milton.	43
3.10 Storage Coefficients and Computed Average Transmissivities Well 3, Milton.	44
3.11 Comparison of Observed and Computed Drawdowns Resulting From Calibration, Well 3, Milton	46
3.12 Comparison of Results From the Present Procedure and the Type Curve Method, Well 3, Milton	47
3.13 Storage Coefficients and Computed Average Transmissivities from Different Trials, Gridley, Illinois	49
3.14 Storage Coefficients and Computed Average Transmissivities from Different Trials, Grand Island, Nebraska	49
3.15 Initial Data for the Illustrative Example No. 2.	54
3.16 Transmissivity and Storage Coefficient Values Used in the Analysis (I.E. No. 2).	56
3.17 Average Transmissivities Computed From Calibration (I.E. No. 2).	60
3.18 Statistics of Observed and Computed Drawdowns and Error Series	65
4.1 Details of Hydrologic Data	77
4.2 Statistics of Data Used in Stochastic Models	80
4.3 Univariate Models Fitted to Monthly Groundwater Levels, Precipitation and River Stages	87
4.4 Parameter Estimates and Their Standard Errors in Univariate Models	87
4.5 Confidence Limits for Correlogram Test and Cumulative Periodogram Test on Residuals.	88
4.6 Critical Values for Portmanteau Test, F-Test and Chi-Square Test on Residuals.	92
4.7 Results of Portmanteau Test, F-Test and Chi-Square Test on Residuals	93
4.8 Sets of Different Variables for Investigating the Causal Relationships	94

<u>Table</u>	<u>Page</u>
4.9 Results from Tests for Checking Causality (Sets A and B)	95
4.10 Results from Tests for Checking Causality (Sets C and D)	96
4.11 Parameter Estimates and Their Standard Errors in Stochastic Models for Residuals	98
4.12 Results of Portmanteau Test, F-Test and Chi-Square Test on Residuals from Models HWA and HWB	98
4.13 Comparison Between the Statistics of Observed and Regenerated Groundwater Levels	100
4.14 Statistics of Residuals Used to Simulate Groundwater Levels.	106
4.15 Statistics of Observed and Simulated Groundwater Levels.	107

Appendix
Table

B.1 Time-Drawdown Data, Well 4, Milton, Illinois	125
B.2 Time-Drawdown Data, Well 3, Milton, Illinois	126
B.3 Time-Drawdown Data, Well 1, Gridley, Illinois.	127
B.4 Time-Drawdown Data, Well 5, Grand Island, Nebraska	127
B.5 Groundwater Levels and River Stages Near the Kankakee River, Dunns Bridge, Indiana	128

LIST OF FIGURES

<u>Figure</u>	<u>Page</u>
2.1 General Aquifer System	16
3.1 Hypothetical Well Field (I.E. No. 1)	22
3.2 Pumping Scheme (I.E. No. 1).	28
3.3 Theoretical Drawdowns (I.E. No. 1)	28
3.4 Comparison of Assumed and Computed Transmissivity Values From Calibration (I.E. No. 1)	28
3.5 Theoretical and Computed Beta Coefficients From Calibration (I.E. No. 1)	32
3.6 Comparison of Theoretical and Computed Drawdowns (Calibration and Prediction, I.E. No. 1).	33
3.7 Theoretical and Computed Beta Coefficients from Prediction (I.E. No. 1).	36
3.8 Pumping Rates in Well 4, Milton, November 1969	39
3.9 Comparison of Observed and Computed Drawdowns (Calibration and Prediction) Well 4, Milton, November 1969.	39
3.10 Comparison of Observed and Computed Drawdowns (Calibration and Prediction) Well 3, Milton, November 1969.	39
3.11 Beta Coefficients Computed From Calibration, Milton, November 1969	39
3.12 Beta Coefficients Computed From Prediction, Milton, November 1969.	39
3.13 Computed Transmissivity Values, Well 3, Milton, June 1969.	45
3.14 Computed Beta Coefficients, Well 3, Milton, June 1969.	45
3.15 Comparison of Observed and Computed Drawdowns, Well 3, Milton, June 1969	45
3.16 Time-Drawdown Graph of Well 3, Milton, June 1969	45
3.17 Computed Transmissivity Values, Gridley, July 1953	48
3.18 Comparison of Observed and Computed Drawdowns, Gridley, July 1953.	48
3.19 Computed Transmissivity Values, Grand Island, July 1931.	50
3.20 Comparison of Observed and Computed Drawdowns, Grand Island, July 1931	50
3.21 Location Map of Dunns Bridge	53
3.22 Computed β_R -Coefficients, Dunns Bridge	53
3.23 Comparison of Observed and Computed Groundwater Levels, Well N-1, Dunns Bridge	53
3.24 Generalized Aquifer Region (I.E. No. 2).	55
3.25 Pumping Demand (I.E. No. 2).	57
3.26 River Stages (I.E. No. 2).	58
3.27 Observed Drawdowns (I.E. No. 2).	59
3.28 Typical Beta Coefficients Computed From Calibration (I.E. No. 2)	61
3.29 Typical β_R -Coefficients Computed From Calibration (I.E. No. 2)	62

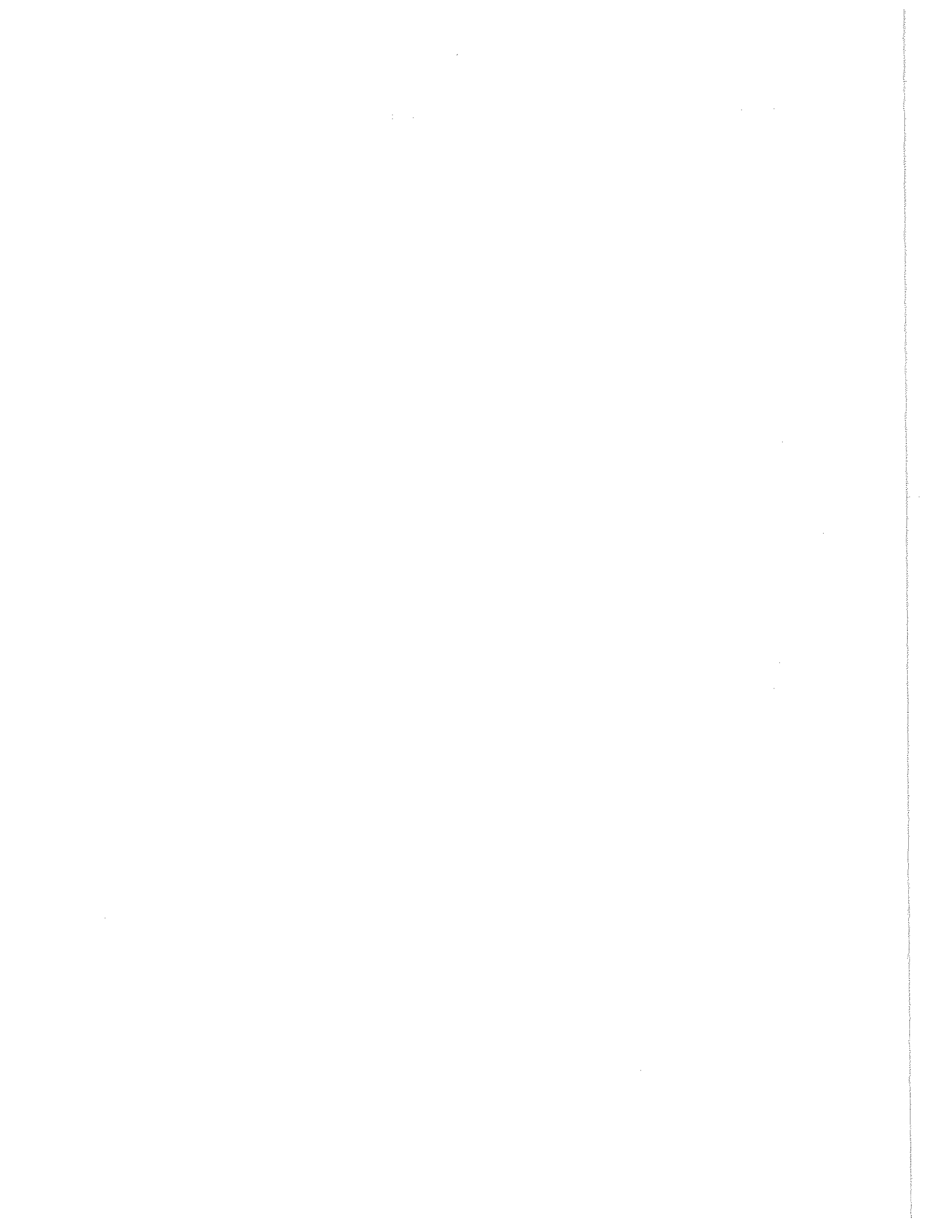
<u>Figure</u>	<u>Page</u>
3.30 Observed and Computed Drawdowns (Calibration and Prediction, I.E. No. 2)	63
3.31 Typical Beta Coefficients Computed from Prediction (I.E. No. 2).	66
3.32 Typical β_R -Coefficients Computed from Prediction (I.E. No. 2).	67
4.1 Location of Stations	76
4.2 Hydrologic Data.	78
4.3 Monthly Means and Standard Deviations of Observed Data	81
4.4 Histograms of Observed Data.	82
4.5 Correlograms and Power Spectra of Observed Data.	84
4.6 Cross Correlations Between Observed Groundwater Level and Precipitation Data	85
4.7 Cross Correlations Between Observed Groundwater Level and River Stages	85
4.8 Correlograms of Residuals.	89
4.9 Cumulative Periodograms of Residuals	91
4.10 Correlograms and Power Spectra of Observed and Regenerated Groundwater Levels.	101
4.11 Monthly Means and Standard Deviations of Observed and Regenerated Groundwater Levels	103
4.12 Comparison Between the Time Series of Observed and Regenerated Groundwater Levels.	104
4.13 Histograms of Residuals.	105
4.14 Histograms of Simulated Groundwater Levels	108
4.15 Correlograms and Power Spectra of Simulated Data	109
 Appendix	
Figure	
A.1 Step Pumping Scheme.	121
A.2 Method of Superposition.	121
A.3 Unit Impulse Response Coefficients for Well 3, Milton, June 1969	121
B.1 Generalized Graphic Logs of Wells.	124

LIST OF SYMBOLS AND NOTATIONS

<u>Symbol</u>	<u>Description</u>	<u>Dimension</u>
AGF	Univariate model for precipitation at the Agronomy Farm	
C_k	Normalized cumulative periodogram ordinate at lag k	
d_j	Serial correlation coefficient at lag j	
erfc [.]	The complimentary error function	
f_k	Frequency at lag k	$[T^{-1}]$
$G(x,j,t)$	Green's function	
$h(x,t)$	Piezometric height at a distance x for any time t	[L]
$h(o,t), h(t)$	River stage at any time t	[L]
H1	Univariate model for water levels in well Tc-4	
H2	Univariate model for water levels in well Tc-7	
H3	Univariate model for water levels in well Tc-9	
HWA	Stochastic model for residuals $W_Y(.)$ and $W_A(.)$	
HHX, HHY	Final stochastic models for water levels in well Tc-7	
i	i^{th} observation	
j	j^{th} well or lag	
k	k^{th} well or lag	
$k_{wr}(x,t)$	Unit impulse response function for the stream-aquifer interflow	
m'	Saturated thickness of the semi-permeable confining layer	[L]
M	Number of wells	
N	Number of observations or number of samples	
NC	Number of observations used for calibration	
NP	Number of observations used for prediction	
ONF	Univariate model for precipitation at the O'Neill Farm	
p	Number of autoregressive terms	
$P(t), P(x,t)$	System unit step function	
P'	Hydraulic conductivity of the semi-permeable confining layer	$[LT^{-1}]$
q	Number of moving average terms	
$q(t)$	Pumping rate as a function of time	$[L^3T^{-1}]$
$q_r(x,t)$	Recharge from the river into the aquifer at a distance x and time t	$[L^3T^{-1}]$
Q	Constant rate of pumping	$[L^3T^{-1}]$
r	Distance from pumping well to observation well	[L]
r_j	Cross correlation coefficient at lag j	

<u>Symbol</u>	<u>Description</u>	<u>Dimension</u>
$r_{k,j}$	Distance between the k^{th} and the j^{th} well	[L]
$s(t), s(r,t),$ $s(k,t), s(x,k,t)$	Drawdown as a function of time at appropriate distances between wells	[L]
S	Storage coefficient	[Dimensionless]
$\bar{S}_{k,j}$	Average storage coefficient of the zones containing the j^{th} and the k^{th} well	[Dimensionless]
t	Time of observation	[T]
T	Aquifer transmissivity	[L ² T ⁻¹]
$\bar{T}_{k,j}$	Average transmissivity of the zones containing the j^{th} and the k^{th} well	[L ² T ⁻¹]
$U(t), U(j,t),$ $U(k,j,t)$	System unit impulse response function	
$w(.)$	Residual series	
$W(.)$	Residuals from univariate models	
$W(u)$	Well function for nonleaky artesian aquifers	
$W(u,R)$	Well function for leaky artesian aquifers	
WAB	Univariate model for Wabash River stages	
$W_A(.)$	Residuals from univariate model AGF	
$W_B(.)$	Residuals from univariate model ONF	
$W_S(.)$	Residuals from univariate model WAB	
$W_X(.)$	Residuals from univariate model H1	
$W_Y(.)$	Residuals from univariate model H2	
$W_Z(.)$	Residuals from univariate model H3	
x	Spatial coordinate in X-direction	[L]
x	Horizontal distance from stream bank	[L]
$x(t)$	System input	
$x'(t)$	Time rate change of the system input	
$X(.)$	Values of variate X	
y	Spatial coordinate in Y-direction	[L]
$y(t)$	System output	
$y_c(t)$	Computed values	
$Y(.)$	Values of variate Y	
$Z(.)$	Values of variate Z	
α	Significance level	

<u>Symbol</u>	<u>Description</u>	<u>Dimension</u>
α, β, γ	Parameters to be estimated in stochastic models	
$\beta(k, j, i)$	Aquifer response coefficient for the i^{th} observation relating the response at well k due to unit pumping at well j	$[TL^{-2}]$
$\beta_R(x, k, i)$	Stream-aquifer response coefficient of the k^{th} well located at distance x from the stream at time t	[Dimensionless]
$\Delta h(i)$	Change in stream stage at the i^{th} observation	[L]
$n_{YA}(\cdot)$	Residuals from model HHX	
$n_{YS}(\cdot)$	Residuals from model HHY	
ν	Aquifer diffusivity	
ν	Number of degrees of freedom	
σ	Standard deviation	
$\hat{\sigma}$	Estimate of standard deviation	



CHAPTER 1

INTRODUCTION

The demand for water is rapidly increasing due to growth in population and urbanization. In many regions, groundwater is an important source to meet this increased demand and hence proper regional planning and utilization of groundwater resources demand our attention. During the past few years, considerable effort has been directed toward the analysis of these groundwater resources. In view of the large expenditures involved in these aquifer evaluation studies, better aquifer modeling techniques are of vital importance.

One of the central problems in the evaluation of groundwater resources is the analysis of the cause-and-effect relationships governing the movement of subsurface water. Fluctuations in groundwater levels and storage are complex phenomena as they are affected by precipitation, streamflow, evapotranspiration, surface detention, infiltration, pumpage and characteristics of the aquifer. A direct field investigation of these phenomena is highly expensive and time consuming. Consequently, several types of closed form solutions, analog models, digital computer techniques and stochastic models have been devised to analyse these relationships.

In the past few years, digital computer models based on numerical methods of analysis have gained importance for evaluating groundwater resources. Although the principles of groundwater flow and the techniques of numerical modeling are well established, there are several limitations on the data and manpower requirements and computational expenditure for developing these models. Bredehoeft and Young (1970) have stated: 'The limited resources available to the project precluded any detailed field studies of the hydrologic, legal, and economic relationships necessary to represent a specific area accurately.' Bathala, Spooner and Rao (1976) have investigated the problems encountered in formulating digital models, especially those related to the data, manpower and computational expenditure. They have concluded that the results from digital models developed by using limited available data should be interpreted with caution. Several other investigators have also emphasized the restrictions imposed by the lack of data and budgetary constraints.

In view of these considerations, there is a need for developing less expensive methodologies for the evaluation of groundwater resources. It would be highly desirable if these methodologies could use essentially the historical record of groundwater levels, pumping rates, precipitation and streamflow. Therefore, the development of such simpler methodologies is the main objective of this study.

1.1 Regional Aquifer Models

Most complex regional aquifer flow problems have been analysed using analog models or numerical-digital computer techniques. A detailed discussion of these modeling techniques, their relative merits

and several case studies may be found in Prickett (1975). In the recent past, linear systems approach and stochastic modeling techniques have been found to be useful to solve several types of groundwater flow problems. The salient features of these techniques are reviewed in this section.

1.1.1 Application of Linear Systems Analysis to Groundwater Flow Problems

A great majority of engineering problems have been analysed by assuming linearity, atleast within certain specified ranges. Also, exact solutions of the behavior of a linear system can usually be found by standard techniques. The linear systems approach has been applied extensively to problems in electrical engineering (Cheng, 1959). In the past few years several researchers have recognized the utility of this method for analysing groundwater flow problems especially those related to stream-aquifer systems.

Any system which is stationary and satisfies the laws of superposition and proportionality can be considered linear (Cheng, 1959). One of the important theorems in linear systems analysis is the "convolution theorem." This theorem enables us to evaluate the response of a linear system to an arbitrary excitation in terms of its response to a unit impulse. The convolution theorem can be expressed in the form of the "convolution integral" (Eq. 1.1) or the "superposition integral" (Eq. 1.2) as

$$y(t) = \int_0^t x(\tau) U(t-\tau) d\tau \quad (1.1)$$

$$y(t) = \int_0^t x'(\tau) P(t-\tau) d\tau \quad (1.2)$$

where, $x(t)$ = system input,
 $x'(t)$ = time rate change of the system input,
 $U(t)$ = system unit impulse response function,
 $P(t)$ = system unit step function,
 and $y(t)$ = system output.

The convolution integral (Eq. 1.1) is also known as the Faltung integral. The relationship between the unit impulse response function, $U(t)$ and the unit step function, $P(t)$ is given as

$$U(t) = \frac{d P(t)}{dt} \quad (1.3)$$

Several types of input-output relationships of a groundwater flow system are linear, thus the laws of superposition and proportionality are valid. For example, the resultant drawdown at any well in a multiple well system can be obtained by superimposing the effects of each pumping well. Solutions to these problems are often obtained from those of analogous problems in linear flow of heat discussed in Carslaw and Jaeger (1959). These relationships can be expressed in the form of the integrals shown in Eqs. 1.1 and 1.2 and can be used to evaluate the output of an aquifer flow system to a given input such as pumpage and streamflow.

The problem of a stream-aquifer interaction is analogous to that of the linear flow of heat in a semi-infinite solid. The convolution relationship and expressions for the unit impulse response function and the unit step function for the heat conduction problem have been derived by Carslaw and Jaeger (p.305, 1959). Several researchers have applied these derived impulse response relationships to analyse different aspects of stream-aquifer flow problems. Pinder et al., (1969) determined the diffusivity of a homogeneous isotropic aquifer from the response of the aquifer to fluctuations in river stage. A linear model that could be used to calculate the recharge of an ephemeral stream was developed by Moench and Kisiel (1970). Veneti (1971) examined the interaction between recharge and depletion of groundwater levels. Hall and Moench (1972) considered four highly idealized cases involving finite and semi-infinite aquifers, with or without a semipervious stream bank. Theoretical equations were presented for the instantaneous unit impulse response function, the unit step response function and its derivative for all the four different cases.

The well known Theis equation (Theis, 1935) was derived from the solution of an analogous problem in heat conduction. In its original form, the Theis equation was presented in the form of the convolution integral. An analytical expression for the unit impulse response function for this problem has been given by Carslaw and Jaeger (p. 261, 1959). Moench (1971) demonstrated the utility of this impulse response function simulating the water level variation due to pumping from the Cambrian-Ordovician aquifers of the Chicago region. He also identified the unit impulse response function for a leaky artesian aquifer from the basic derivations given by Hantush and Jacob (1955). However, in all his computations, Moench used predetermined values of aquifer transmissivity and storage coefficient (Suter et al., 1959).

Maddock (1972, 1974a) has used linear systems theory and Green's functions for the solution of aquifer flow problems involving multiple well systems and stream-aquifer interflow due to pumping. Morel-Seytoux and Daly (1975) and Morel-Seytoux (1975) extended Maddock's approach and presented modified computational procedures.

1.1.2 Application of Stochastic Modeling Techniques to Groundwater Flow Problems

As mentioned earlier, groundwater levels are considerably affected by hydrologic stresses as precipitation, streamflow, evapotranspiration and pumpage. These stresses are often considered to be stochastic processes. Consequently, the groundwater levels may also be considered to be a stochastic process. In the past few years, several investigators have characterized the variations in groundwater levels by using stochastic modeling techniques.

Eriksson (1970) was probably the first hydrologist to apply methods of spectral analysis for analysing hydrogeological time series. He developed a stochastic model of the water balance to give estimates of mean annual infiltration by using groundwater levels from a riparian esker, a glaciofluvial deposit, and local streamflow, air temperature and precipitation records. Jackson et al., (1973) employed the methods

of time series analysis to examine climatological and hydrological variables associated with a groundwater discharge area in Manitoba, Canada. The hydrological variables such as evapotranspiration and infiltration were "adequately" modeled by a first-order Markov process. Rao et al., (1973, 1975) made a detailed investigation of the stochastic modeling of groundwater levels in relation to rainfall and streamflow. They considered both univariate and multivariate models and concluded that valid univariate models with excellent one step-ahead prediction capabilities can be developed for modeling the groundwater level process. Gelhar (1974) developed three different analytical models viz. linear reservoir, Dupuit aquifer and Laplace aquifer to describe the spectral response characteristics of phreatic aquifers subject to time variable accretion and fluctuations in an adjacent stream stage. Bathala et al., (1976) have noted that the cross correlation studies between rainfall, groundwater levels and river stages were quite useful in introducing recharge and base flow into a deterministic groundwater model.

The general principles of spectral analysis and its applications may be found in Jenkins and Watts (1968). Different stochastic modeling techniques are illustrated in Box and Jenkins (1970); and Kashyap and Rao (1976).

1.2 Critique and Motivation

Digital computer models and R-C networks are well suited for analysing complex regional aquifer flow problems. But the utility of these models is highly restricted by the data requirements and economic limitations. In the case of R-C networks, the hardware (resistors, capacitors, and other electronic equipment) and the time taken up for assembly of the model are expensive. Alterations to the network will cause considerable delay and additional expenditure. In the case of digital models, smaller time steps and closer grid spacing, which are usually required to arrive at an adequate or accurate solution, increase the computational expenditure excessively. Bredehoeft and Young (1970) pointed out that it costs about \$400 per study consisting of 6 or 7 computer runs using a 2000 node finite difference network. Some of these aspects of cost and effort involved in the development of digital computer models were investigated by Bathala et al., (1976). The main objective of this study was to explore the feasibility of constructing a digital model for the aquifers underlying medium size communities and to explore the difficulties that may arise due to limitations on the data, computational expenditure and availability of skilled manpower. The glacial aquifer underlying Lafayette and West Lafayette, Indiana, covering an area of about 26 sq. miles, was selected as a test site. A digital computer model was formulated by using a rectangular finite difference grid system consisting of 24 columns and 33 rows with 792 nodes. Only the historical record of water levels, pumping rates and pumping test data were used in developing this model. These data were not sufficient either to prepare reasonably accurate piezometric surface maps or to estimate the aquifer properties satisfactorily. However, considerable effort and expenditure was involved in the development of this model. About 1000 skilled (undergraduate students guided by a graduate research assistant at Ph.D. level) man-hours were required for the preliminary phase in the model development.

This phase consisted of data acquisition from past records, preparation of piezometric maps and flow nets, delineation of aquifers, analysis of pumping tests and estimation of aquifer properties. The effort expended in the specification of the aquifer characteristics such as hydraulic conductivity, storage coefficient, piezometric head, depth to bedrock and aquifer thickness at each node point of the finite difference grid is proportional to the number of nodes in the grid. About 300 skilled man-hours were spent on this phase in the study. The initial computer trial runs and calibration of the digital model were tedious and time consuming. These trials and the final computer runs required about 2500 hours at the skill level of a graduate research assistant. The cost distribution of different computer runs as a function of number of nodes in the grid system using a CDC 6500 digital computer is shown in Table 1.1. The cost per single run for the Model X (3,055 nodes) is about three times as high as that for the Model Y (792 nodes). The above costs are based on an average rate of \$250 per hour (Purdue internal rate struc-

TABLE 1.1
COST DISTRIBUTION OF DIFFERENT COMPUTER RUNS

Item	MODEL - X	MODEL - Y
Grid size (square)	500 ft	1000 ft
No. of nodes	3,055	792
Core storage (Octal)	110,000	67,000
Central processor time	1,100 Sec	400 Sec
Cost per run	\$75 - \$90	\$25 - \$40

ture) of central processor time. The major practical limitation to adopt larger number of grids (finer mesh) was the computing cost. The approximate overall computer related expenditure corresponding to different stages during the development of the digital model is presented in Table 1.2. It was concluded from the above study that the data requirements and budgetary constraints play a major role in the formulation and operation of the digital models. The study also suggested the need for developing less expensive methodologies for estimating aquifer capacities.

Aquifer problems which can be analysed by using the basic theory of well hydraulics are comparatively less expensive and can yield highly valuable results if they are formulated with sound professional judgment and analytical discretion. With appropriate recognition of hydrogeologic controls, there are many practical ways of circumventing analytical difficulties posed by complicated field conditions. However, the use of these techniques have been restricted to relatively uniform aquifers of small areal extent.

TABLE 1.2
COMPUTATIONAL COST OF MODELING

S.No.	Item	Approx. Cost
1	Data processing and preliminary computer runs	\$ 2,000
2	Calibration of the Digital Model	\$ 4,500
3	Development of Stochastic Models	\$ 800
4	Estimation of Aquifer Capacity (Final Runs)	\$ 2,900
5	Miscellaneous	\$ 500
	Total	\$10,700

The linear systems approach which has been gaining favor for the past few years appears to be an efficient tool for developing less expensive and comprehensive models for regional groundwater resource evaluation. However, there is a common drawback with most of these deterministic models presently used. As far as the authors are aware, these models [except those on stream-aquifer interactions (Pinder et al., 1969)] use the predetermined values of aquifer transmissivity and storage coefficient as the primary input variables. It is difficult to obtain this information where there is lack of suitable pumping test data. It is, therefore, highly desirable to couple the theory of well hydraulics with the linear systems approach to develop a model which considers only the cause-and-effect relationships of the groundwater system.

Another aspect that is of interest in the development of aquifer flow models is the stochastic nature of the groundwater levels. Rainfall is the major source of recharge to the groundwater basin in many situations. The amount of this recharge is dependent on the infiltration characteristics of the soil. The depth of water levels below ground surface also affect recharge in terms of time of travel and intermediate losses. Where circumstances are favorable, surface streamflow also interacts with the groundwater system. When groundwater levels are near the surface, the effects of evaporation and transpiration may be significant. Pumpage from wells constitute the major artificial discharge of groundwater. The groundwater levels will go down when the pumping rates are higher than the recharge rates. In essence, groundwater levels in an aquifer system are affected by several stochastic processes such as precipitation, infiltration, evapotranspiration, streamflow and pumpage. Consequently, groundwater levels also constitute a stochastic process.

Several investigators (Sec. 1.1.2) have formulated stochastic models for groundwater level processes by considering the hydrologic variables such as precipitation, streamflow and evapotranspiration as inputs. The time series of precipitation and streamflow are also used as inputs in formulating deterministic models

for evaluating groundwater resources. Therefore, before using any of these variables as inputs into these models, it is necessary to investigate if these processes are really the cause of the variations in groundwater levels. This can be done in several ways. For example, when groundwater levels are relatively close to the surface, it is possible to identify the dependency of these levels on variations in precipitation by examining the time series relationships or by water balance studies or by performing cross correlation studies. The above techniques can also be applied when a well is located relatively close to a river which is hydraulically connected with the aquifer. Obviously, variations in groundwater levels are directly proportional to the pumping rates. Based on this preliminary information stochastic or deterministic models can be formulated by using streamflow, precipitation and evapotranspiration as input variables at the appropriate locations in the groundwater system.

On the other hand, when groundwater levels are at relatively greater depths below the surface, it is difficult to determine if these levels are affected by precipitation at all. Examination of the time series or the water balance studies or the cross correlograms may not yield reliable information about the relationship between the groundwater levels and the precipitation. The above statement is also valid when the causal relationship of the water levels in a well located at a relatively long distance away from a stream is to be investigated with reference to variations in the stream stages. Under these circumstances, the causal relationship of the different hydrologic processes such as precipitation and streamflow with the groundwater levels must be investigated in a different manner than by simply examining the time series or correlograms. Alternatively, the causal relationship among different variables affecting a process must be investigated before formulating any model.

Therefore, in the present study, it is proposed to investigate the causal relationship between precipitation, stream stages and groundwater levels by using some statistical tests.

1.3 Objectives of the Present Study

Based on the foregoing discussion the objectives of the present study are as follows:

- 1) To develop a procedure for predicting the response of an aquifer system under different hydrologic stresses by considering only the cause-and-effect relationships of the system.
- 2) To apply the above procedure for predicting the response of the groundwater system in field situations.
- 3) To investigate the utility of the above procedure to replace the traditional type curve solution for pumping test analysis.
- 4) To investigate the causal relationship of different hydrologic variables affecting groundwater levels.

The results of the present study are organized as follows. The linear systems formulation of generalized aquifer flow problems is presented in Chapter 2. A procedure for prediction of aquifer response by considering only the cause-and-effect relationships of the groundwater system is discussed in Chapter 3. This chapter also deals with the use of the above procedure for analysing pumping test data. Numerical

results from several types of aquifer flow problems which are analysed by using the present procedure are included in Chapter 3. Chapter 4 is concerned with the definition of causality, general principles of formulating stochastic models, method of parameter estimation and the investigation of causal relationships among different hydrologic variables. Application and numerical results of the stochastic models formulated in this study are also presented in Chapter 4. Discussion and conclusions are given in Chapter 5.

CHAPTER 2
 LINEAR SYSTEMS FORMULATION OF
 GENERALIZED AQUIFER FLOW PROBLEMS

Most deterministic models used for the evaluation of groundwater resources need predetermined values of the aquifer transmissivity and the storage coefficient as primary input variables. It is often difficult to obtain this information due to lack of adequate pumping test data. Therefore, one of the primary objectives (Sec. 1.3) of the present study is to develop a procedure for estimating the aquifer response by considering only the cause-and-effect relationships of the groundwater flow system. A linear systems approach is used in this study to investigate the above problem. The basic relationships used in the present approach and the theoretical formulation of the problem for different types of aquifer flow systems are explained below.

2.1 Basic Relationships

The basic principles of linear systems theory and the concept of convolution were briefly explained in Sec. 1.1.1. A brief review of the existing literature regarding the application of linear systems analysis to groundwater flow problems was also presented (Sec. 1.1.1). The basic relationships governing the solution of a few pertinent groundwater flow problems by using the linear systems approach are given below.

2.1.1 Stream-Aquifer Interaction without Pumping

The convolution relation giving the response of an aquifer at a specified distance from a stream can be expressed (Venetis, 1970) in two ways similar to the convolution integral and the superposition integral expressions given in Eqs. 1.1 and 1.2. These expressions are

$$h(x,t) = \int_0^t h(0,\tau) U(x,t-\tau) d\tau \quad (2.1)$$

$$h(x,t) = \int_0^t \frac{\partial h(0,\tau)}{\partial \tau} P(x,t-\tau) d\tau \quad (2.2)$$

where, $h(x,t)$ = piezometric height at distance x for any time t (L),

$h(0,t)$ = piezometric height at the origin (river stage) for any time t (L),

$U(x,t)$ = unit impulse response function of the system (T^{-1}),

and $P(x,t)$ = unit step response of the system, dimensionless.

When $h(x,t)$ and $h(0,t)$ are discrete time series, Eqs. 2.1 and 2.2 can be expressed in the equivalent forms as (Eagleson et al., 1966),

$$h(x,N) = \sum_{i=1}^N h(0,i) U(x,N-i+1)\Delta \quad (2.3)$$

$$h(x,N) = \sum_{i=1}^N \Delta h(0,i) P(x,N-i+1) \quad (2.4)$$

where, $\Delta h(0,i)$ is the change in piezometric height at the origin (river stage) at the i^{th} time step, N is the upper limit of summation, i is the variable of summation, and Δ is the time interval.

The expressions for $U(x,t)$ and $P(x,t)$ (Eqs. 2.1 and 2.2) are based on the type of hydraulic connection between the stream and the aquifer. Hall and Moench (1972) have considered four different cases; (i) the semi-infinite aquifer, (ii) the finite aquifer, (iii) the semi-infinite aquifer with semipervious stream bank and (iv) the finite aquifer with semipervious stream bank. When the stream bank is pervious and semi-infinite, the problem is analogous to that of a plane source of heat in a semi-infinite solid. The unit impulse response function and the unit step response for this case have been given by Carslaw and Jaeger (p. 305, 1959) and can be expressed as

$$U(x,t) = \frac{x \exp(-x^2/4vt)}{(4\pi v)^{1/2} t^{3/2}} \quad (2.5)$$

$$\text{and} \quad P(x,t) = \text{erfc}(x/\sqrt{4vt}) \quad (2.6)$$

where, $\text{erfc}[-]$ = the complimentary error function,

v = aquifer diffusivity (equal to T/S),

T = aquifer transmissivity ($L^2 T^{-1}$),

S = storage coefficient (dimensionless),

x = horizontal distance from the stream bank (L),

and t = time (T).

Equations 2.5 and 2.6 can be written in discrete form as follows:

$$U(x,i) = \frac{x \exp(-x^2/4vi\Delta)}{(4\pi v)^{1/2} (i\Delta)^{3/2}} \quad (2.5a)$$

$$P(x,i) = \text{erfc}(x/\sqrt{4vi\Delta}) \quad (2.6a)$$

The relationships for $U(x,t)$ and $P(x,t)$ for other cases of stream-aquifer boundaries have been summarized by Hall and Moench (1972).

2.1.2 Single Well in an Infinite Aquifer

a) Nonleaky Artesian Condition

When a well fully penetrating a nonleaky artesian aquifer of infinite areal extent is pumped, water is continuously withdrawn from storage within the aquifer and the cone of depression progresses radially outward from the well. The nonequilibrium equation for the time-distribution of drawdown at any distance from the pumping well was derived by Theis (1935) from the solution of an analogous problem in heat conduction (Carslaw and Jaeger, p. 261, 1959). In its basic form, the nonequilibrium equation can be expressed as

$$s(r,t) = \int_0^t q(\tau) \frac{\exp\left[-\frac{r^2 S}{4T(t-\tau)}\right]}{4\pi T(t-\tau)} d\tau \quad (2.7)$$

where, $s(r,t)$ = drawdown as a function of distance and time (L),

$q(t)$ = pumping rate as a function of time (L^3/T),

r = distance from pumping well to observation point (L),

and t = time after pumping started (T).

By comparing Eq. 2.7 with the convolution integral (Eq. 1.1) the unit impulse response function for a well in an infinite aquifer, $U(r,t)$ can be written as shown in Eq. 2.8 (Moench, 1971).

$$U(r,t) = \frac{\exp\left[-\frac{r^2 S}{4Tt}\right]}{4\pi Tt} \quad (2.8)$$

When $s(r,t)$ and $q(t)$ are discrete time series, Eq. 2.7 is expressed in the equivalent form as

$$s(r,N) = \sum_{i=1}^N q(i) \frac{\exp\left[-\frac{r^2 S}{4T(N-i+1)\Delta}\right]}{4\pi T(N-i+1)\Delta} \Delta \quad (2.9)$$

which is more convenient for computational purposes.

When the well is pumped at a constant rate Q , Eq. 2.7 can be reduced to the Theis equation (Eq. 2.10) (Theis, 1935) after carrying out the necessary steps of integration as detailed in Appendix A.1,

$$s(r,t) = \frac{Q}{4\pi T} \int_u^\infty \frac{e^{-v}}{v} dv \quad (2.10a)$$

where,

$$u = r^2 S / 4Tt. \quad (2.10b)$$

In Eq. 2.10, the integral $\int_u^\infty \frac{e^{-v}}{v} dv$ is a function of the lower limit u and is known as the "exponential integral." In groundwater terminology, the exponential integral is symbolically expressed as $W(u)$ and stands for the "well function for nonleaky artesian aquifers." The well function (or the exponential integral) is expanded in a convergent series as shown in Eq. 2.11 and is extensively tabulated (Abramowitz and Stegun, 1965).

$$W(u) = \int_u^\infty \frac{e^{-v}}{v} dv = (-0.5772 - \ln u + u - \frac{u^2}{2.2!} + \frac{u^3}{3.3!} + \frac{u^4}{4.4!} + \dots) \quad (2.11)$$

Values of $W(u)$, in terms of practical range of u for application in groundwater flow problems are found elsewhere (Wenzel, 1942; Todd, 1959; Johnson, 1966; and Walton, 1970). For small values of r and large values of t , u is small, so that the series in Eq. 2.11 can be truncated after the first two terms (Cooper and Jacob, 1946). As a result the well function (Eq. 2.11) can be approximated as given by Eq. 2.12 for values of u less than 0.01. This is commonly known as "Jacob's method" (Cooper and Jacob, 1946).

$$W(u) = \ln\left(\frac{2.25Tt}{r^2 S}\right) \quad (2.12)$$

b) Leaky Artesian Condition

When a confined aquifer is overlain by a confining bed of slightly permeable material, the vertical leakage into the aquifer must also be considered. Hantush and Jacob (1955) derived the following expression (Eq. 2.13) for the drawdown around the pumping well by using an extension of the analysis done by Theis (1935),

$$s(r,t) = \frac{Q}{4\pi T} W(u,R) \quad (2.13)$$

$$\text{where, } R = \frac{r}{\sqrt{T/(P'/m')}}$$

P' = hydraulic conductivity of the aquitard, L/T,

and m' = saturated thickness of aquitard, L.

$W(u,R)$ stands for the "well function for leaky artesian aquifers with fully penetrating well without water released from storage in the aquitard and constant discharge conditions." This well function is expressed as,

$$\begin{aligned} W(u,R) = & 2K_0(R) - I_0(R) \left[-E_i\left(-\frac{R^2}{4u}\right) + \exp\left(-\frac{R^2}{4u}\right) \right] \\ & \left\{ 0.5772 + \ln u + \left[-E_i(-u) \right] - u + u \frac{[I_0(R)-1]}{R^2/4} \right. \\ & \left. - u^2 \sum_{n=1}^{\infty} \sum_{m=1}^n \frac{(-1)^{n+m} (n-m+1)! \left(\frac{R^2}{4}\right)^m}{(n+2)!^2} u^{n-m} \right\} \end{aligned} \quad (2.14)$$

where, $K_0(R)$ is the modified Bessel function of the second kind and zero order and $I_0(R)$ is the modified Bessel function of the first kind and zero order.

2.1.3 Multiple Well System

When a homogeneous and isotropic aquifer of uniform thickness is pumped by several fully penetrating wells, the drawdown at any time due to pumping of these wells is given by (Maddock 1972; and Morel-Seytoux, 1975),

$$s(k,t) = \sum_{j=1}^M \int_0^t q(j,\tau) \frac{\exp\left[-\frac{r_{k,j}^2 S}{4T(t-\tau)}\right]}{4\pi T(t-\tau)} d\tau \quad (2.15)$$

where, M = number of wells,

$s(k,t)$ = drawdown at the k^{th} well at time t (L),

$q(j,t)$ = pumping rate at the j^{th} well at time t ($L^3 T^{-1}$),

and x,y = spatial coordinates of the wells (L).

When there is no previous groundwater development in the area, the initial and boundary conditions at the drawdowns are shown in Eq. 2.16.

$$s(x,y,0) = 0, \text{ and } s(\pm\infty, \pm\infty, t) = 0 \quad (2.16)$$

The following assumptions are made in the above formulation.

- (1) The aquifer is homogeneous, isotropic and of infinite areal extent.
- (2) The aquifer thickness is uniform and the wells are fully penetrating the aquifer.
- (3) The groundwater flow in the aquifer is approximately two-dimensional, i.e., vertical flow is insignificant.
- (4) The aquifer is confined and nonleaky.

If $s(k,t)$ and $q(j,t)$ are discrete time series, Eq. 2.15 can be reduced to the form as shown in Eq. 2.17 by using the Theis equation (Eq. 2.10a) and the method of superposition. The details of the mathematical derivation for Eq. 2.17 are shown in Sec. A.3 of Appendix A.

$$s(k,N) = \sum_{j=1}^M \sum_{i=1}^N \beta(k,j,i) q(j,N-i+1) \quad (2.17)$$

In Eq. 2.17, $s(k,N)$ = drawdown at the k^{th} well at the end of the N^{th} time step due to pumping from M wells (L),

$q(j,i)$ = pumping in the j^{th} well at the i^{th} time step ($L^3 T^{-1}$),

and $\beta(k,j,i)$ = response coefficient for the i^{th} time step relating the response at well k to unit pumping at well j ($T L^{-2}$).

The β -coefficients in Eq. 2.17 are expressed in a form given as (Maddock, 1972)

$$\begin{aligned} \beta(k,j,i) &= \alpha(k,j,i) \text{ for } i=1 \\ &= \alpha(k,j,i) - \alpha(k,j,i-1) \text{ for } i>1 \end{aligned} \quad (2.18a)$$

where,
$$\alpha(k,j,i) = \frac{1}{4\pi T} W[u_{k,j}(i)], \quad (2.18b)$$

$W[u_{k,j}(i)]$ = well function given by Eq. 2.11 with appropriate subscripts,

$$u_{k,j}(i) = \frac{r_{k,j}^2 S}{4Tt_i} \quad (2.18c)$$

$r_{k,j}$ = distance between the k^{th} and j^{th} well (L),

= radius of the well (if $k=j$),

and t_i = time at the i^{th} step (T).

Equation 2.17 is identical with the "algebraic technological function" derived by Maddock (1972) by using the partial differential equation governing the aquifer system and the method of Laplace transforms. Maddock has also shown that the β -coefficients in the functional relationship (Eq. 2.17) exist even for aquifer systems with irregularly shaped boundaries and nonhomogeneous parameters, but did not explicitly suggest methods for computation.

In general, if there are M wells in an aquifer system, Eq. 2.17 will have (M^2N) β -coefficients at the N^{th} observation (Maddock, 1975).

The β -coefficients given in Eq. 2.18a can be computed theoretically for any time step if the well geometry and the aquifer parameters (T and S values) are known. A more general method of estimating the β -coefficients for any aquifer configuration by using the predetermined values of the aquifer transmissivity and the storage coefficient has been developed by Maddock (1974b).

2.1.4 Stream-Well-Aquifer System

The pumping wells are often located very near the streams which may be hydraulically connected to the aquifer. The drawdown $s(x,t)$ at any distance x from a stream due to pumping from M fully penetrating wells is given as (Maddock, 1974a)

$$s(x,t) = \sum_{j=1}^M \int_0^t G(x,j,t-\tau) q(j,\tau) d\tau \quad (2.19)$$

where, $G(x,j,t-\tau)$ is the Green's function related to the well geometry, distance from the river, the aquifer transmissivity, the storage coefficient, the boundary conditions, the initial conditions and the type of partial differential equation governing the groundwater flow.

The above problem can also be solved as shown in Eq. 2.20 by treating the river reach as a special well and by using the principle of superposition (Morel-Seytoux, 1975 and Morel-Seytoux and Daly, 1975),

$$s(x,t) = \sum_{j=1}^M \int_0^t q(j,\tau) U(j,t-\tau) d\tau + \int_0^t q_r(x,\tau) k_{wr}(x,t-\tau) d\tau \quad (2.20)$$

where, $U(j,t)$ = the unit impulse response function for the j^{th} well (similar to Eq. 2.8),

$q_r(x,t)$ = the recharge from the river into the aquifer at a distance x and time t ,

and $k_{wr}(x,t)$ = the unit impulse response function for the stream-aquifer interflow.

Equation 2.20 can be reduced to a form similar to that of Eq. 2.17 and the resulting response coefficients can be computed numerically (Morel-Seytoux, 1975; and Morel-Seytoux and Daly, 1975) by using the predetermined values of the transmissivity and the storage coefficient.

2.2 Theoretical Formulation

Pumping wells located near a stream hydraulically connected to an aquifer draw most of their discharge from the river. Under favorable conditions, the groundwater system is recharged by precipitation. Consequently, the drawdowns in these wells are related to pumpage, fluctuations in the river stage, the vertical recharge, the aquifer properties, the initial conditions, the boundary conditions and the type of theoretical relationship governing the flow in the aquifer system. Therefore, any model developed to study the water level changes in these wells should consider all these aspects. Maddock (1974a) and Morel-Seytoux (1975) have developed (Sec. 1.1.1 and Sec. 2.1) generalized relationships (Eqs. 2.19 and

2.20) for analysing the groundwater level changes in a stream-well-aquifer system without considering the effects of vertical recharge. In this section, a general relationship similar to, but slightly different from that of Eq. 2.20 is used for analysing the flow through a stream-well-aquifer system.

Consider a multiple well field with M fully penetrating wells and intersected by a hydraulically connected stream as shown in Fig. 2.1. Let the irregular grid system divide sections of the aquifer having different values of transmissivity and storage coefficient. Let there be a real or imagined well, pumping, nonpumping or recharging, at the center of each of these subdivided sections. If the groundwater flow is approximately two-dimensional, and if there has been no previous groundwater development in the aquifer system, the drawdown in the k^{th} well at a distance x from the river can be expressed by using the basic relationships given in Sec. 2.1 and the theory of linear systems (Cheng, 1959), as

$$s(x,k,t) = \sum_{j=1}^M \int_0^t q(j,t-\tau) U(k,j,\tau) d\tau + \int_0^t \frac{\partial h(t-\tau)}{\partial \tau} P(x,k,\tau) d\tau \quad (2.21)$$

where, $s(x,k,t)$ = drawdown in the k^{th} well located at a distance x from the river at time t (L),

$q(j,t)$ = pumping rate in the j^{th} well at time t ($L^3 T^{-1}$),

$h(t)$ = stage in the river at time t (L),

$U(k,j,t)$ = unit impulse response function of the k^{th} well due to pumping at the j^{th} well at time t (L^{-2}),

and $P(x,k,t)$ = unit step response of the k^{th} well located at a distance x from the river at time t (dimensionless).

Equation 2.21 can be written in the discretized form, following the methods presented by Eagleson et al (1966) and Maddock (1972), as

$$s(x,k,N) = \sum_{j=1}^M \sum_{i=1}^N q(j,N-i+1) \beta(k,j,i) + \sum_{i=1}^N \Delta h(N-i+1) \beta_R(x,k,i) \quad (2.22)$$

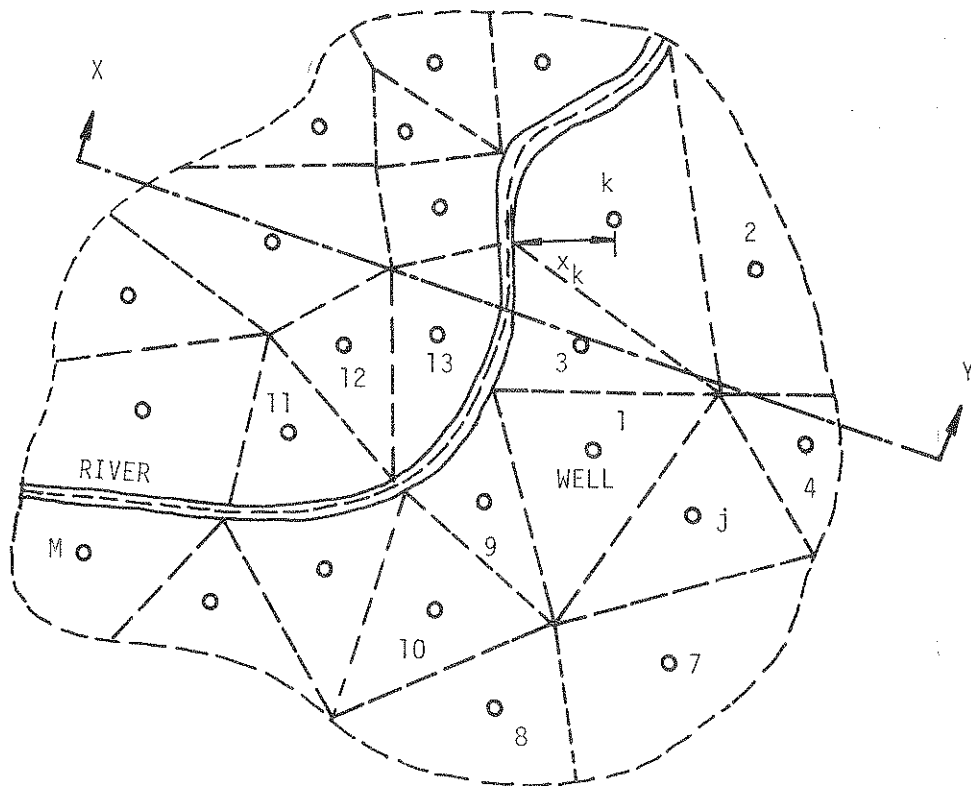
where, N = N^{th} observation (T),

$\beta(k,j,i)$ = aquifer response coefficients of the k^{th} well at the i^{th} time step due to pumping from j^{th} well ($T L^{-2}$),

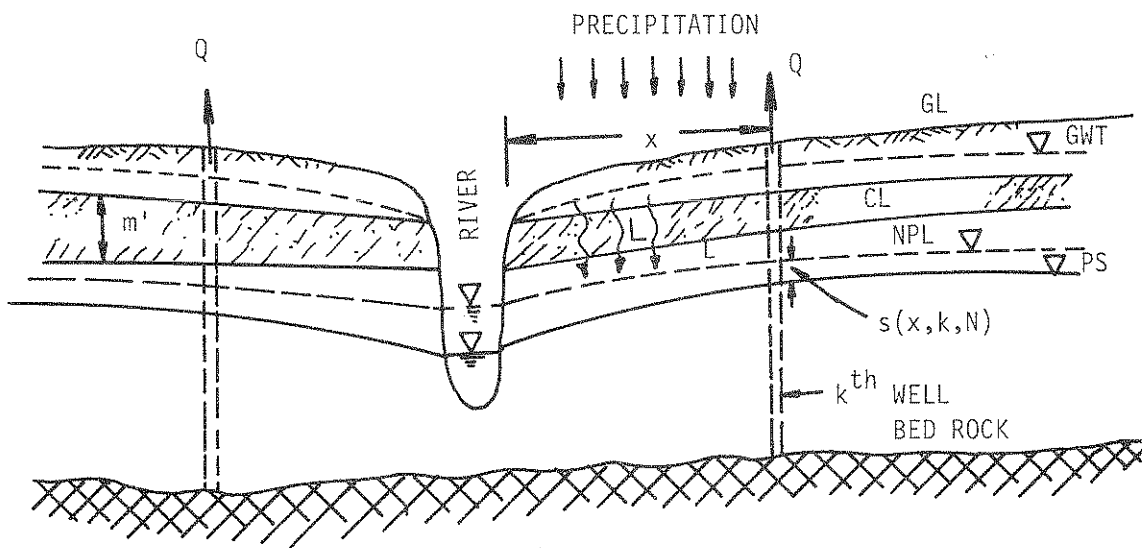
$\Delta h(i)$ = change in the stream stage at the i^{th} time step (L/T),

and $\beta_R(x,k,i)$ = stream-aquifer response coefficients of the k^{th} well located at a distance x from the stream at time t (dimensionless).

In Eq. 2.22 the β -coefficients are related to the well radius, the distance between the wells, the transmissivity and the storage coefficient of the subsections (Fig. 2.1), the initial conditions, the boundary conditions, the time period since the start of pumping and the theoretical relationship governing the aquifer flow system. The β_R -coefficients are based on the distance from the river to the point of observation, the aquifer diffusivity, the initial and boundary conditions of the stream, the time period from the start of pumping and the theoretical relationship governing stream-aquifer interaction.



(a) PLAN VIEW



(b) SECTION - XY

GL = GROUND LEVEL
 GWT = GROUNDWATER TABLE
 NPL = NONPUMPING LEVEL

PS = PIEZOMETRIC SURFACE
 CL = CONFINING LAYER (SEMI-PERMEABLE)
 L = LEAKAGE

FIGURE 2.1 GENERAL AQUIFER SYSTEM

The relationship shown in Eq. 2.22 is very flexible in the sense that it can be used, after making suitable simplifications, to solve different cases of aquifer flow problems. A few of these different cases are presented next.

2.2.1 Stream-Well-Aquifer System with Vertical Leakage

Let us consider that the aquifer in Fig. 2.1 is overlain by a semi-permeable confining bed of thickness m' and vertical hydraulic conductivity P' . Let the rate of vertical leakage be proportionate to the difference in head between the water table and the piezometric surface of the aquifer. If the aquifer is assumed to be of semi-infinite extent on both sides of the river, the coefficients $\beta(k,j,i)$ and $\beta_R(x,k,i)$ given in Eq. 2.22 can be expressed as shown in Eqs. 2.23 and 2.24 by using the basic relationships presented in Sec. 2.1,

$$\begin{aligned}\beta(k,j,i) &= \alpha(k,j,i) \text{ for } i=1 \\ &= \alpha(k,j,i) - \alpha(k,j,i-1) \text{ for } i>1\end{aligned}\quad (2.23a)$$

where,

$$\alpha(k,j,i) = \frac{1}{4\pi\bar{T}_{k,j}} W[u_{k,j}(i), R_{k,j}]. \quad (2.23b)$$

In Eq. 2.23b, $W[u_{k,j}(i), R_{k,j}]$ is the same as the well function for leaky artesian aquifers shown in Eq. 2.14 with appropriate subscripts, and the expressions for $u_{k,j}(i)$ and $R_{k,j}$ are given as

$$u_{k,j}(i) = \frac{r_{k,j}^2 \bar{S}_{k,j}}{4\bar{T}_{k,j} t_i} \quad (2.24)$$

$$R_{k,j} = \frac{r_{k,j}}{\sqrt{\bar{T}_{k,j}/(P'_j/m'_j)}} \quad (2.25)$$

where, $\bar{T}_{k,j} = (T_k + T_j)/2$ and $\bar{S}_{k,j} = (S_k + S_j)/2$.

The above relationships (Eqs. 2.23 to 2.25) are formulated by assuming that the drawdown in the k^{th} well due to pumping in the j^{th} well are affected by the average values of transmissivity ($\bar{T}_{k,j}$) and storage coefficient ($\bar{S}_{k,j}$) of the respective subsections.

When the stream aquifer boundary is semi-infinite and pervious, the expression for β_R is the same as that in Eq. 2.6, and can be written in the notation of this theoretical formulation as

$$\beta_R(x,k,i) = \text{erfc} \left[\frac{x_k}{\sqrt{4 \frac{\bar{T}_k}{S_k} t_i}} \right] \quad (2.26)$$

where, x_k = distance of the k^{th} well from the river (L),

\bar{T}_k = transmissivity of the subsection containing the k^{th} well (L^2/T),

S_k = storage coefficient of the subsection containing the k^{th} well (dimensionless).

In Eq. 2.26, the transmissivity (T_k) and the storage coefficient (S_k) refer to that of the k^{th} subsection only.

Substituting Eqs. 2.23 and 2.26 in Eq. 2.22, the relationship for the stream-well-aquifer system with vertical leakage can be expressed as

$$s(x,k,N) = \sum_{j=1}^M \sum_{i=1}^N q(j,N-i+1) \left\{ \frac{1}{4\pi T_{k,j}} W[u_{k,j}(i), R_{k,j}] - \frac{1}{4\pi T_{k,j}} W[u_{k,j}(i-1), R_{k,j}] \right\} + \sum_{i=1}^N \Delta h(N-i+1) \operatorname{erfc} \left[\frac{x_k}{\sqrt{4v_k t_i}} \right] \quad (2.27)$$

where, v_k = aquifer diffusivity, T_k/S_k , and $W[u_{k,j}(i-1), R_{k,j}] = 0$ for $i=1$.

2.2.2 Multiple Well System without Vertical Leakage

When there is no river present in the well field shown in Fig. 2.1 and when the aquifer is overlain by an impermeable confining bed, the problem reduces to that of analysing the groundwater flow in a multiple well system without vertical leakage. If the aquifer is assumed to be of infinite areal extent, the relationship governing the flow of groundwater in this system is the same as that presented by Maddock (1972). The expression for $s(k,N)$ can be obtained by ignoring the second term on the right hand side of Eq. 2.22, which will be the same as Eq. 2.17. The β -coefficients are given by Eq. 2.23a and the related expression for $\alpha(k,j,i)$ is

$$\alpha(k,j,i) = \frac{1}{4\pi T_{k,j}} W[u_{k,j}(i)] \quad (2.28)$$

where, $W[u_{k,j}(i)]$ is the well function for nonleaky artesian aquifers (Eq. 2.11) with appropriate subscripts and $u_{k,j}(i)$ is given by Eq. 2.24. The specific relationship between the drawdowns and the pumping rates is given as

$$s(k,N) = \sum_{j=1}^M \sum_{i=1}^N q(j,N-i+1) \left\{ \frac{1}{4\pi T_{k,j}} W[u_{k,j}(i)] - \frac{1}{4\pi T_{k,j}} W[u_{k,j}(i-1)] \right\} \quad (2.29)$$

where, $W[u_{k,j}(i-1)] = 0$ for $i=1$.

2.2.3 Other Possible Cases of Groundwater Flow Systems

Several other possible cases of groundwater flow systems can be formulated by making suitable simplifications in Eq. 2.22. A few of these cases which are of practical importance are discussed below.

a) *Stream-Aquifer Interaction without Pumping*

When there is only an observation well near a river, the relationship governing the groundwater level fluctuations due to change in the river stage can be easily derived from Eq. 2.22. This relationship is shown as

$$s(x,N) = \sum_{i=1}^N \Delta h(N-i+1) \beta_R(x,i). \quad (2.30)$$

The β_R -coefficients are given by Eq. 2.26 without the subscript k. Several types of stream-aquifer flow problems have been analysed by Pinder et al. (1969); Moench and Kisiel (1970) and Ha11 and Moench (1972) using the relationship given in Eq. 2.30.

b) Non-Steady Radial Flow in an Infinite Leaky Aquifer

If we substitute $M=1$ in Eq. 2.27 and assume that there is no river, then Eq. 2.27 reduces to that of radial flow around a single pumping well located in an infinite aquifer with vertical leakage from the overlying confining bed. This problem has been analysed by Hantush and Jacob (1955).

c) Non-Steady Radial Flow in a Nonleaky Artesian Aquifer

By substituting $M=1$ and $\Delta h(\cdot)=0$ in Eq. 2.22 we obtain a relationship which can be expressed in the present notation as

$$s(r,N) = \sum_{i=1}^N \beta(i) q(N-i+1) \quad (2.31)$$

where, $s(r,N)$ is the drawdown at a distance r from the pumping well at the N^{th} time step, and $\beta(i)$ and $q(i)$ are respectively the aquifer response coefficients and pumping rates as functions of time.

If the aquifer is assumed to be of infinite areal extent, confined and nonleaky, Eq. 2.31 represents the drawdown around a single, fully penetrating pumping well.

In Eq. 2.31, β -coefficients are given as

$$\begin{aligned} \beta(i) &= \alpha_i \text{ for } i=1 \\ &= \alpha_i - \alpha_{i-1} \text{ for } i>1 \end{aligned} \quad (2.32)$$

where, $\alpha_i = W(u_i)/4\pi T$, $W(u_i)$ is the well function for nonleaky aquifers (Eq. 2.11) and $u_i = r^2 S/4Tt_i$.

Equation 2.31 is nothing but the Theis equation (Theis, 1935) expressed in a discretized form. Derivation of Eq. 2.31 from the basic Theis relationship (Eq. 2.7) is given in Secs. A.1 and A.2, Appendix A. Another discretized form of the Theis equation can be obtained from Eqs. 2.8 and 2.9 as

$$s(r,N) = \sum_{i=1}^N U(i) q(N-i+1)\Delta \quad (2.33)$$

where, $U(i)$ is the unit impulse response coefficient and can be expressed as

$$U(i) = \exp\left(\frac{-r^2 S}{4Tt_i}\right) / 4\pi T t_i. \quad (2.34)$$

When the pumping rates are discrete time series, the values of $s(r,N)$ can be computed from Eq. 2.31 if the β -coefficients are known. Similarly, Eq. 2.33 can be used to compute drawdowns if the unit impulse response coefficients (U -coefficients) are given. In the present study (Chapter 3) a procedure is

presented to compute β -coefficients by using the observed pumping rates and drawdowns. The relationship between the β -coefficients and the U-coefficients is given in Sec. A.4, Appendix A.

A PROCEDURE FOR THE PREDICTION OF AQUIFER RESPONSE AND ITS APPLICATIONS

The theoretical formulations presented earlier (Sec. 2.2) are used in this chapter for the prediction of aquifer response. Two steps are involved in this process. The first step is the "calibration" of the model, wherein the aquifer response coefficients (β or β_R values) are estimated by using the historical record such as drawdowns, pumping rates and stream stages. The second step is the "prediction" of the aquifer response due to future pumping stresses, variations in river stage, etc. The results obtained during the process of calibration are used for predicting future drawdowns. The details of the calibration and prediction steps are explained below for a few types of groundwater flow problems. The method can be extended to analyse regional aquifer flow systems as demonstrated for a hypothetical problem in Sec. 3.5.

3.1 Multiple Well System in a Nonhomogeneous Aquifer

Consider a hypothetical aquifer system with three zones of different aquifer properties as shown in Fig. 3.1. Assume that a well is located in each zone with the distances as noted. These wells can be operated in any manner for pumping or recharging the aquifer or can be left unpumped for observation of water level changes. The initial static water levels and a time history of pumping rates and the corresponding water levels are available at uniform time intervals for all the wells. The following assumptions are made in the analysis:

- 1) The aquifer is homogeneous and isotropic within each zone.
- 2) The aquifer is confined, infinite in areal extent and is of uniform thickness.
- 3) The wells fully penetrate the aquifer and the vertical leakage is negligible.
- 4) The input record is sampled at uniform time intervals.

Under these assumptions, the drawdown in any well due to pumping from the three wells is given by either Eq. 2.17 or Eq. 2.29. When $M=3$, Eq. 2.17 is written as

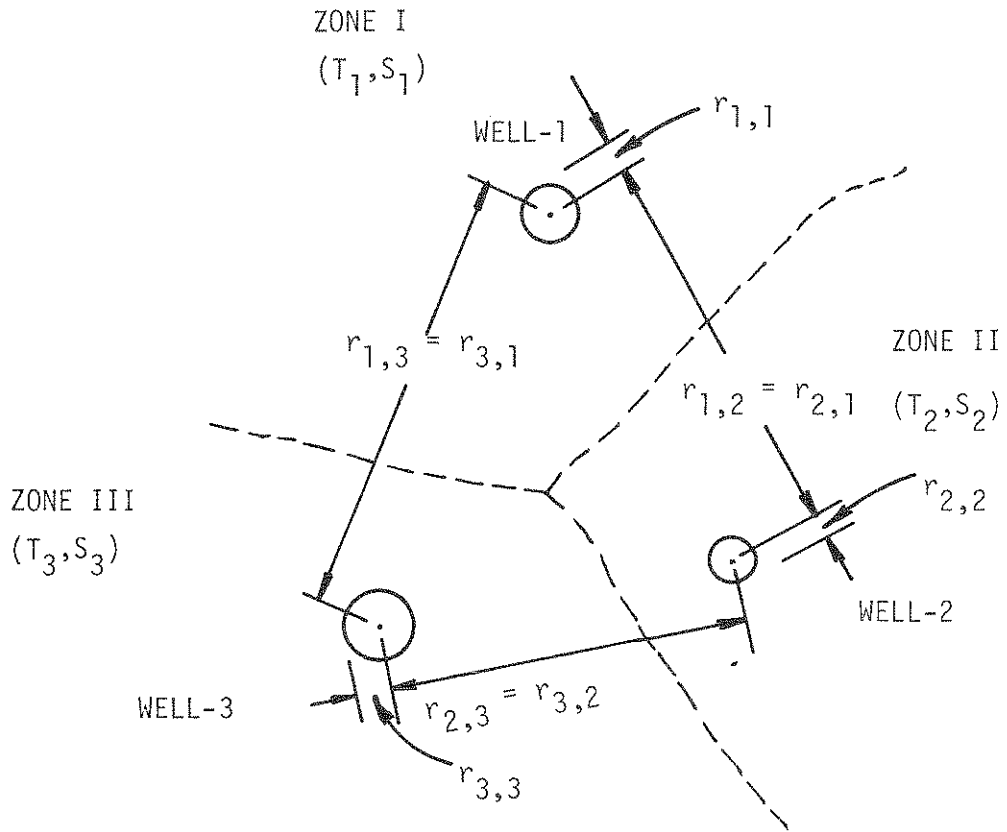
$$s(k,N) = \sum_{j=1}^3 \sum_{i=1}^N \beta(k,j,i) q(j,N-i+1) \quad (3.1)$$

where, the response coefficients $\beta(k,j,i)$ are given by Eqs. 2.23a, 2.28, 2.24 and 2.25.

The main purpose of this method is to compute these β - coefficients using the historical values of pumpages, $q(j,i)$ and the drawdowns, $s(k,i)$ and to further use these computed β - coefficients for prediction of drawdowns under future pumping stresses.

3.1.1 Calibration

Equation 3.1 is expanded for the first two observations as shown below in customary vector notation in order to explain the calibration procedure.



DATA FOR ILLUSTRATIVE EXAMPLE NO. 1

WELL k	DISTANCE, $r_{k,j}$ (FT)			T_k (sft/day)	S_k
	j = 1	j = 2	j = 3		
1	0.5	103.08	106.89	4,000	0.0001
2	103.08	0.375	45.28	6,000	0.01
3	106.89	45.28	0.4	7,000	0.005

FIGURE 3.1 HYPOTHETICAL WELL FIELD (I.E. NO. 1)

$$\begin{array}{c} \text{First Observation (N=1)} \\ \left\{ \begin{array}{l} s(1,1) \\ s(2,1) \\ s(3,1) \end{array} \right\} = \begin{bmatrix} \beta(1,1,1) & \beta(1,2,1) & \beta(1,3,1) \\ \beta(2,1,1) & \beta(2,2,1) & \beta(2,3,1) \\ \beta(3,1,1) & \beta(3,2,1) & \beta(3,3,1) \end{bmatrix} \left\{ \begin{array}{l} q(1,1) \\ q(2,1) \\ q(3,1) \end{array} \right\} \end{array} \quad (3.2)$$

$$\begin{array}{c} \text{Second Observation (N=2)} \\ \left\{ \begin{array}{l} s(1,2) \\ s(2,2) \\ s(3,2) \end{array} \right\} = \begin{bmatrix} \beta(1,1,1) & \beta(1,1,2) & \beta(1,2,1) & \beta(1,2,2) & \beta(1,3,1) & \beta(1,3,2) \\ \beta(2,1,1) & \beta(2,1,2) & \beta(2,2,1) & \beta(2,2,2) & \beta(2,3,1) & \beta(2,3,2) \\ \beta(3,1,1) & \beta(3,1,2) & \beta(3,2,1) & \beta(3,2,2) & \beta(3,3,1) & \beta(3,3,2) \end{bmatrix} \left\{ \begin{array}{l} q(1,2) \\ q(1,1) \\ q(2,2) \\ q(2,1) \\ q(3,2) \\ q(3,1) \end{array} \right\} \end{array} \quad (3.3)$$

In Eq. 3.2, there are nine β - coefficients to be determined from three equations. Equation 3.3 consists of eighteen β - coefficients of which nine are carried over from Eq. 3.2. Assuming that the nine β - coefficients of Eq. 3.2 are known, there will be nine more β - coefficients to be determined from Eq. 3.3 with three equations.

Thus in general, for any time step N, there will be M^2 unknown β - coefficients where, M is the number of equations (number of wells) available. Obviously this is an underdetermined system with more unknowns than the number of equations. Therefore, it is very difficult to directly determine these β - coefficients from the above equations. A possible alternative is to examine the analytical expressions for the β - coefficients used in Eq. 3.1 and to find some means of reducing the number of unknowns to equal the number of equations.

i) First Observation (N=i=1)

The β - coefficients in Eq. 3.1 can be expressed for the first observation as

$$\beta(k,j,1) = \frac{1}{4\pi\bar{T}_{k,j}} W[u_{k,j}(1)] \quad (3.4)$$

where, $W[u_{k,j}(1)]$ is the well function for nonleaky aquifers for the first observation and can be expanded as shown in Eq. 2.11 or can be approximated by using "Jacob's method" as given in Eq. 2.12 with appropriate subscripts. For illustration, Eq. 3.4 can be written in a simple form using Jacob's approximation as

$$\beta(k,j,1) = \frac{1}{4\pi\bar{T}_{k,j}} \ln \left\{ \frac{2.25 \bar{T}_{k,j} t_1}{r_{k,j}^2 \bar{S}_{k,j}} \right\} \quad (3.5a)$$

$$= \frac{C}{\bar{T}_{k,j}} \ln \left\{ D_{k,j} \frac{\bar{T}_{k,j}}{\bar{S}_{k,j}} \right\} \quad (3.5b)$$

where,

$$\bar{D}_{k,j} = \frac{2.25t_1}{r_{k,j}^2} \text{ (known for a given problem),} \quad (3.5c)$$

$$\bar{T}_{k,j} = (T_k + T_j)/2,$$

and

$$\bar{S}_{k,j} = (S_k + S_j)/2.$$

However, when calculations are made with the aid of a digital computer the well function (Eq. 2.11) can be incorporated into the formulation using a sufficiently large number of terms.

Substituting Eq. 3.5b into Eq. 3.2 we have

$$\begin{Bmatrix} s(1,1) \\ s(2,1) \\ s(3,1) \end{Bmatrix} = \begin{bmatrix} \frac{C}{T_1} \ln(D_{1,1} \frac{T_1}{S_1}) & \frac{2C}{T_1+T_2} \ln(D_{1,2} \frac{T_1+T_2}{S_1+S_2}) & \frac{2C}{T_1+T_3} \ln(D_{1,3} \frac{T_1+T_3}{S_1+S_3}) \\ \frac{2C}{T_2+T_1} \ln(D_{2,1} \frac{T_2+T_1}{S_2+S_1}) & \frac{C}{T_2} \ln(D_{2,2} \frac{T_2}{S_2}) & \frac{2C}{T_3+T_2} \ln(D_{2,3} \frac{T_3+T_2}{S_3+S_2}) \\ \frac{2C}{T_3+T_1} \ln(D_{3,1} \frac{T_3+T_1}{S_3+S_1}) & \frac{2C}{T_3+T_2} \ln(D_{3,2} \frac{T_3+T_2}{S_3+S_2}) & \frac{2C}{T_3} \ln(D_{3,3} \frac{T_3}{S_3}) \end{bmatrix} \begin{Bmatrix} q_{1,1} \\ q_{2,1} \\ q_{3,1} \end{Bmatrix} \quad (3.6)$$

which still contains six unknowns, viz. T_1 , T_2 , T_3 , S_1 , S_2 and S_3 . As there are only three equations, any three of these unknowns can be solved if the values of the other three could be reasonably estimated. In the present study the following method is used to solve for these unknowns.

Determination of Transmissivities and Storage Coefficients: The unknowns in Eq. 3.6 are the transmissivities and the storage coefficients of the three aquifer zones considered in Fig. 3.1. Therefore, Eq. 3.6 can be solved for the transmissivities T_1 , T_2 and T_3 if the values of the storage coefficients S_1 , S_2 and S_3 can be reasonably estimated. The alternative way is to solve for the storage coefficients S_1 , S_2 and S_3 by substituting estimated values of transmissivities T_1 , T_2 and T_3 into Eq. 3.6.

In the present study, the values of the storage coefficients for the different aquifer zones are estimated by examining the geological maps of the area and "well-logs" which are usually available. These estimated values of storage coefficients are substituted into Eq. 3.6. The resulting set of equations will contain only three unknowns, viz., T_1 , T_2 and T_3 , which can be determined by a simultaneous solution. However, these equations are nonlinear and the number of equations increases linearly with the number of wells. When the number of equations is large, special iterative techniques are needed to solve these equations even with the aid of a digital computer. The successive substitution method, the Newton-Raphson method and the secant method are the most commonly used iterative techniques for solving a system of nonlinear equations. A few of these methods are illustrated in Carnhan et al., (1969). In the present study, the secant method (Wolfe, (1959)) is used to solve the system of nonlinear equations. A listing of

the subroutine for the secant method, "SECANT" is given in Bathala (1976). The method of solution and the convergence criteria are also briefly explained in the above listing.

After solving for the unknowns, T_1 , T_2 and T_3 in Eq. 3.6 as explained above, these values are substituted into Eq. 3.5a and the coefficients $\beta(k,j,1)$ for the first observation are computed.

ii) Second Observation ($N=2, i=1, 2$)

The drawdown relationship for the second observation is given in Eq. 3.3. In this equation, the β - coefficients corresponding to the first observation ($\beta(k,j,1)$ values) are known. The unknown β - coefficients ($\beta(k,j,2)$ values) are those corresponding to the second time step ($i=2$). These coefficients are written as

$$\beta(k,j,2) = \frac{1}{4\pi T_{k,j}} W[u_{k,j}(2)] - \beta(k,j,1) . \quad (3.7)$$

Equation 3.7 can be simplified and solved once again for the unknowns T_1 , T_2 and T_3 following the same procedure as explained for the first observation. These values of T_1 , T_2 and T_3 are then substituted into Eq. 3.7 for computing the $\beta(k,j,2)$ coefficients.

iii) Subsequent Observations ($N \geq 3, i=1, 2, \dots, N$)

For subsequent observations, β - coefficients are expressed in a form similar to Eq. 3.7 as

$$\beta(k,j,i) = \frac{1}{4\pi T_{k,j}} W[u_{k,j}(i)] - \beta(k,j,i-1) . \quad (3.8)$$

The same procedure as explained for the case with $N=2$ is followed as the values of $\beta(k,j,i-1)$ are known from the previous observations. This process is repeated until the end of the calibration period.

The calibration procedure explained above will result in one set of transmissivity values ($T(j)$, $j = 1,2,3$ wells) for each observation. These values are averaged for the appropriate wells to obtain the "average transmissivity" of the different subsections (Fig. 3.1).

The values of the storage coefficients used for the different aquifer zones in the above computations need not be very accurate as it is well known that even large errors in estimated storage coefficients will result in comparatively small errors in the computed transmissivity values. A sensitivity analysis of the present procedure for different variations in the storage coefficient values is presented in the Illustrative Example No. 1 in this section to substantiate this observation.

3.1.2 Prediction

An important purpose of this method is to use the results obtained from the calibration step for predicting the aquifer response due to future pumping stresses. As discussed earlier (Sec. 2.2) the β - coefficients are functions of time from the beginning of pumping. In addition the other variables such as well geometry, aquifer properties and the theoretical relationship governing the groundwater flow should be considered. Therefore, the β - coefficients computed for different observations during cali-

bration cannot be directly used for predicting aquifer response due to future pumping stresses. However, the average transmissivity values which result at the end of the calibration period for the different aquifer subsections can be used for computing the β - coefficients during the prediction period. This procedure is explained below.

Let NC be the number of observations and Δt be the time interval used for calibration. It is required to predict the aquifer response due to an anticipated pumping scheme with NP values measured at the same time interval Δt . Considering once again the aquifer system shown in Fig. 3.1, the drawdown in any well due to future pumping demand can be expressed as

$$s_p(k, N') = s(k, NC) + \sum_{j=1}^3 \sum_{ii=NC+1}^{N'} \beta_p(k, j, ii) q(j, N'-ii+1) \quad (3.9)$$

where $NC < N' \leq (NC+NP)$,

NC = no. of observations used for calibration,

NP = no. of observations used for prediction,

$s_p(k, N')$ = predicted drawdown in the k^{th} well at the N' -th observation,

$s(k, NC)$ = drawdown in the k^{th} well at the end of the calibration period,

$\beta_p(k, j, ii)$ = aquifer response coefficients of the k^{th} well due to pumping from the j^{th} well at the ii^{th} step during prediction [$(NC+1) \leq ii \leq (NC+NP)$],

and $q_p(j, ii)$ = future pumping rates as a function of time.

The expressions for β_p - coefficients in Eq. 3.9 are similar to those in Eqs. 2.18 and can be expressed in the present notation as

$$\beta_p(k, j, ii) = \alpha(k, j, ii) - \alpha(k, j, ii-1) \quad (3.10a)$$

where,

$$\alpha(k, j, ii) = \frac{1}{4\pi \bar{T}_{k,j}'} W[u_{k,j}(ii)], \quad (3.10b)$$

$$u_{k,j}(ii) = \frac{r_{k,j}^2 \bar{S}_{k,j}}{4 \bar{T}_{k,j}' t_{ii}}, \quad (3.10c)$$

$$\bar{T}_{k,j}' = (T_k' + T_j')/2,$$

T_k' = average transmissivity value of the aquifer subsection containing the k^{th} well which is obtained from calibration,

and T_j' = average transmissivity value of the aquifer subsection containing the j^{th} well which is obtained from calibration.

3.1.3 Illustrative Example No. 1

The procedure explained above is illustrated below by using a hypothetical numerical example. The assumed well configuration and the aquifer properties are shown in Fig. 3.1. The wells 1, 2 and 3 are respectively of 12 in., 9 in., and 9.6 in. diameter and penetrate the complete thickness of the aquifer. The distances between these wells are as shown in Fig. 3.1. The storage coefficients for the aquifer zones I, II and III are respectively assumed to be 0.0001, 0.01 and 0.005. The aquifer transmissivities are 4000 sft/day, 6000 sft/day and 7000 sft/day respectively in the aquifer zones I, II and III. Only daily data are used for analysis in this example.

A pumping period of 40 days is considered and the time series of the daily pumping rates in the three wells are shown in Fig. 3.2. These pumping records show that wells 1 and 3 are recharging the aquifer during some part of the pumping period. The same wells are also inoperative for several different days. However, well 2 is used throughout for pumping only.

Drawdowns that would result in the three wells due to the assumed pumping scheme (Fig. 3.2) are calculated using the Theis equation (Eq. 2.10) and the method of superposition. These drawdowns hereinafter referred to as "theoretical drawdowns" are plotted in Fig. 3.3. In addition β - coefficients are computed for all the observations using the assumed values of well geometry, the transmissivities, the storage coefficients and the Eqs. 2.23a, 2.28, 2.24 and 2.25. These values are designated "theoretical β - coefficients."

The pumping scheme shown in Fig. 3.2 and the theoretical drawdowns given in Fig. 3.3 are considered as the time history of input variables for this example. The theoretical β - coefficients are used for comparison with the β - coefficients which will be obtained from calibration and prediction.

Computational Procedure: A split sample of the data, consisting of a part of the time history of pumping rates (Fig. 3.2) and drawdowns (Fig. 3.3) starting from the beginning of the pumping period is used for calibration. The later part of the pumping data are used for predicting drawdowns. These predicted drawdowns are then compared with the corresponding history of time-drawdown data (Fig. 3.3) thus verifying the procedure. The numerical computations are carried out with the aid of a digital computer. A listing of the computer program is given in Bathala (1976). In all these computations, the well function (Eq. 2.11) is calculated by using a standard subroutine for calculating the exponential integral.

A sensitivity analysis of the procedure is also performed by assuming different storage coefficients for the three aquifer zones shown in Fig. 3.1. These values are given in Table 3.1 and are designated Cases 1-5. The storage coefficient values for the three aquifer zones in Case 1 are the same as those given for the well field (Fig. 3.1). The storage coefficient values used in the model for the other cases and the percentage errors with reference to the assumed values are shown in Table 3.1. The details of different samples of data used for calibration and prediction are given in Table 3.2.

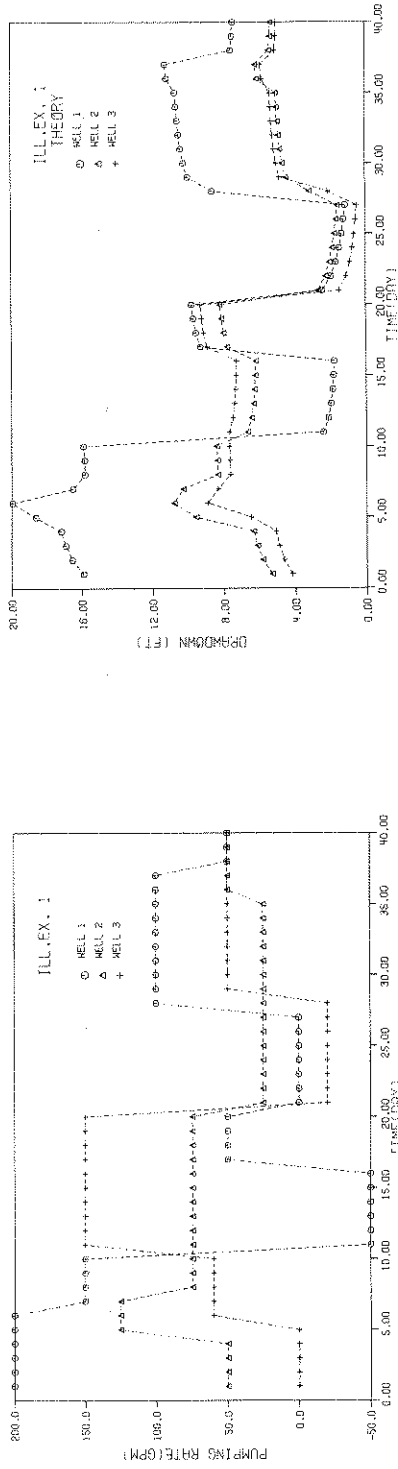


FIGURE 3.2 PUMPING SCHEME (I.E. NO. 1)

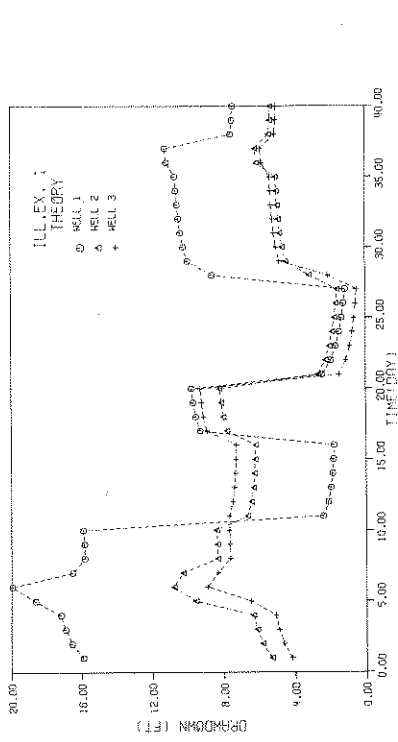


FIGURE 3.3 THEORETICAL DRAWDOWNS (I.E. NO. 1)

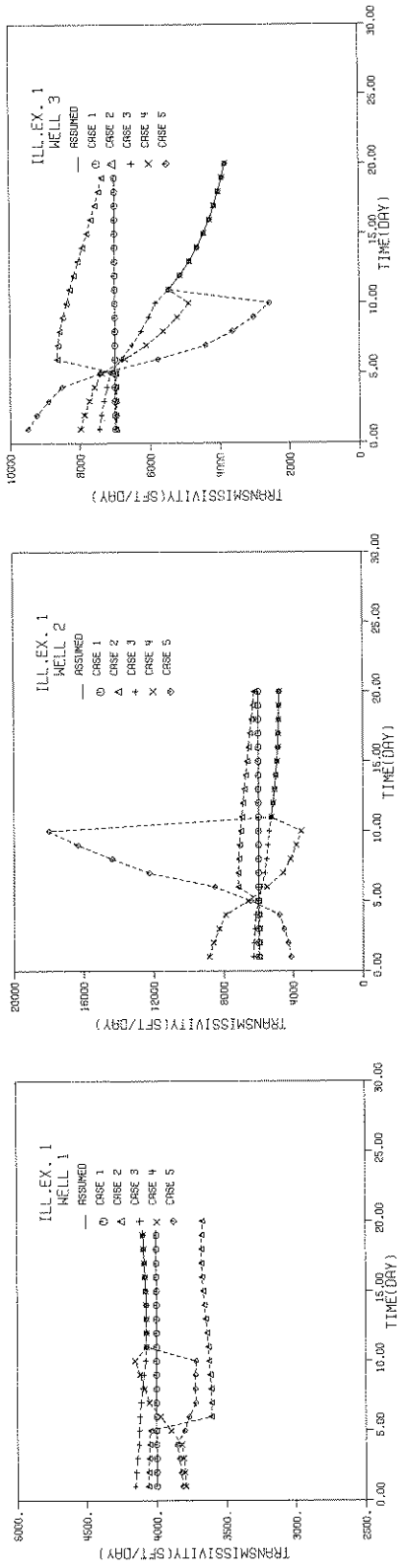


FIGURE 3.4 COMPARISON OF ASSUMED AND COMPUTED TRANSMISSIVITY VALUES

FROM CALIBRATION (I.E. NO. 1)

TABLE 3.1

DIFFERENT SETS OF STORAGE COEFFICIENTS USED IN SENSITIVITY ANALYSIS (I. E. NO. 1)

Well Number (Zone)	GIVEN S_A	CASE-1		CASE-2		CASE-3		CASE-4		CASE-5	
		S	% ERROR (ABS)	S	% ERROR (ABS)	S	% ERROR (ABS)	S	% ERROR (ABS)	S	% ERROR (ABS)
1	0.0001	0.001	0	0.000075	25	0.00005	50	0.003	200	0.0002	100
2	0.01	0.01	0	0.01	0	0.0075	25	0.001	90	0.05	400
3	0.005	0.005	0	0.005	0	0.00375	25	0.003	40	0.001	80

$$\% \text{ ERROR} = (S_A - S) \times 100 / S_A$$

TABLE 3.2

DETAILS OF OBSERVATIONS USED IN CALIBRATION AND PREDICTION

DETAILS	CASE 1	CASE 2	CASE 3	CASE 4	CASE 5
Observations used for calibration	1-20	1-20	1-20	1-10	1-10
Observations used for prediction	21-40	21-40	21-40	11-40	11-40

For example, in Case 4, the sensitivity analysis is performed by assuming the aquifer storage coefficients as 0.0003, 0.001 and 0.003 (Table 3.1) respectively for the zones I, II and III whereas, they are actually assumed to be 0.0001, 0.01 and 0.005 in Fig. 3.1. Therefore, the absolute percentage errors due to these discrepancies in the storage coefficient values used in Case 4 are 200, 90 and 40 respectively for the different aquifer zones. Also for Case 4, the model is calibrated by using the first ten day record of pumping rates (Fig. 3.2) and the theoretical drawdowns (Fig. 3.3). The computed values of transmissivities, β - coefficients and drawdowns resulting during this calibration period are compared with the respective theoretical values and an error analysis is presented. The average transmissivity values resulting at the end of the calibration period are used for computing the β - coefficients and

predicting the drawdowns during the pumping period 11-40 days (Table 3.2). These computed β - coefficients and the drawdowns are compared respectively with the theoretical β - coefficients and the drawdowns for the same period and the results are analysed. This procedure for sensitivity analysis is repeated for each of the different cases listed in Table 3.1.

Calibration Results: A comparison between the assumed transmissivity values for each well and the computed transmissivities during the calibration period for the different cases is presented in Fig. 3.4. From these results it is clear that the computed transmissivity values resulting from Case 1 are the same as those initially assumed for the different aquifer zones. Consequently, where the storage coefficients used during the calibration period are the same as the assumed values (Fig. 3.1) the secant method used for solving the nonlinear simultaneous equations (Sec. 3.1.1) is very efficient. The transmissivities computed during the calibration for the other cases differ from the assumed values for each observation and show either a decreasing or increasing trend with increasing time. However, as we are interested in the β - coefficients only, there is no need to attach much importance to the magnitude of transmissivities computed at each observation. The average transmissivity values obtained for the different aquifer zones at the end of calibration are compared with the respective assumed values (Fig. 3.1) and these results are tabulated in Table 3.3. The average transmissivity values resulting from Case 1 are the same as those assumed for the well field (Fig. 3.1). However, the average transmissivities computed from the other cases (Cases 2-5) are slightly different from the assumed values with the exception of the average transmissivity computed for the aquifer zone II (Well 2) in Case 5. The percentage errors between the assumed and the computed average transmissivities are given in Table 3.3.

TABLE 3.3
AVERAGE TRANSMISSIVITIES COMPUTED AFTER CALIBRATION (I. E. NO. 1)

Well Number	GIVEN T_A (sft/day)	CASE-1		CASE-2		CASE-3		CASE-4		CASE-5	
		T' (sft/day)	% ERROR (ABS)	T' (sft/day)	% ERROR (ABS)	T' (sft/day)	% ERROR (ABS)	T' (sft/day)	% ERROR (ABS)	T' (sft/day)	% ERROR (ABS)
1	4000	4000	0	3748	6.3	4101	2.5	3950	1.3	3778	5.6
2	6000	6000	0	6560	9.3	5408	9.9	6173	2.9	9362	56.0
3	7000	7000	0	7747	10.7	5638	19.5	6710	4.1	6295	10.1

$$\% \text{ ERROR} = (T_A - T') \times 100 / T_A$$

The different values of β - coefficients computed during the period of calibration for different cases are presented in Fig. 3.5. The corresponding theoretical β - coefficients are also plotted in Fig. 3.5 for comparison. All these plots of β - coefficients show an exponential decay with increasing time. These β - coefficients become asymptotic to the time axis as the pumping period increases. The computed β - coefficients are close to their theoretical counterparts. In particular, the computed β - coefficients resulting from Case 1 are the same as those of the theoretical values.

The theoretical drawdowns and those computed during calibration for different cases are depicted in Fig. 3.6. The computed drawdowns for different cases do not differ from the corresponding theoretical values by more than about 25 percent.

A general conclusion from the study of these plots (Figs. 3.4, 3.5 and 3.6) is that the discrepancies between the theoretical and the computed values for the different cases considered are small. Therefore, in order to analyse these discrepancies in a quantitative manner, it is more appropriate to examine some of the typical values presented in Tables 3.4, 3.5 and 3.6.

TABLE 3.4

COMPARISON OF THEORETICAL AND COMPUTED RESULTS AFTER CALIBRATION...
(WELL NO. 1, CASE 1, I. E. NO. 1)
Transmissivity at Well No. 1 = 4000 sft/day (given)

Time since pumping started (Days)	Transmissivity (sft/day)		β - Coefficients $B(k,j,I)$ (day/sft) $k=1, j=2$			Drawdowns (Ft. below SWL)		
	COMPUTED	ABS.PER. ERROR ($\times 10^{-5}$)	Theoretical ($\times 10^{-5}$)	Computed ($\times 10^{-5}$)	ABS.PER. ERROR ($\times 10^{-6}$)	THEORETICAL	COMPUTED	ABS.PER. ERROR ($\times 10^{-6}$)
1	4000	0.0	8.509	8.509	0.0	15.91	15.91	0
2	4000	0.07	1.101	1.101	0.22	16.55	16.55	0.02
3	4000	0.06	0.645	0.645	0.19	16.92	16.92	0.03
4	4000	0.06	0.458	0.458	0.16	17.18	17.18	0.04
5	4000	0.05	0.355	0.355	0.12	18.62	18.62	0.04
6	4000	0.08	0.290	0.290	0.18	19.95	19.95	0.05
7	4000	0.14	0.245	0.245	1.25	16.53	16.53	0.07
8	4000	0.75	0.213	0.213	7.50	15.84	15.84	0.13
9	4000	1.12	0.187	0.187	8.22	15.86	15.86	0.20
10	4000	0.83	0.168	0.168	7.19	15.92	15.92	0.24
11	4000	0.75	0.152	0.152	6.66	2.41	2.41	1.88
12	4000	0.81	0.138	0.138	8.10	2.12	2.12	2.38
13	4000	0.83	0.127	0.127	8.90	1.98	1.98	2.89
14	4000	0.80	0.118	0.118	8.35	1.89	1.89	3.24
15	4000	0.78	0.110	0.110	7.81	1.84	1.84	3.45
16	4000	0.00	0.103	0.103	5.33	1.80	1.80	3.42
17	4000	0.13	0.097	0.097	4.24	9.32	9.32	0.64
18	4000	0.14	0.091	0.091	5.71	9.57	9.57	0.56
19	4000	0.07	0.086	0.086	8.16	9.71	9.71	0.46
20	4000	0.09	0.082	0.082	7.60	9.82	9.82	0.39

SWL = static water level

Avg. computed transmissivity at Well No. 1, $T_1 = 4000$ sft/day

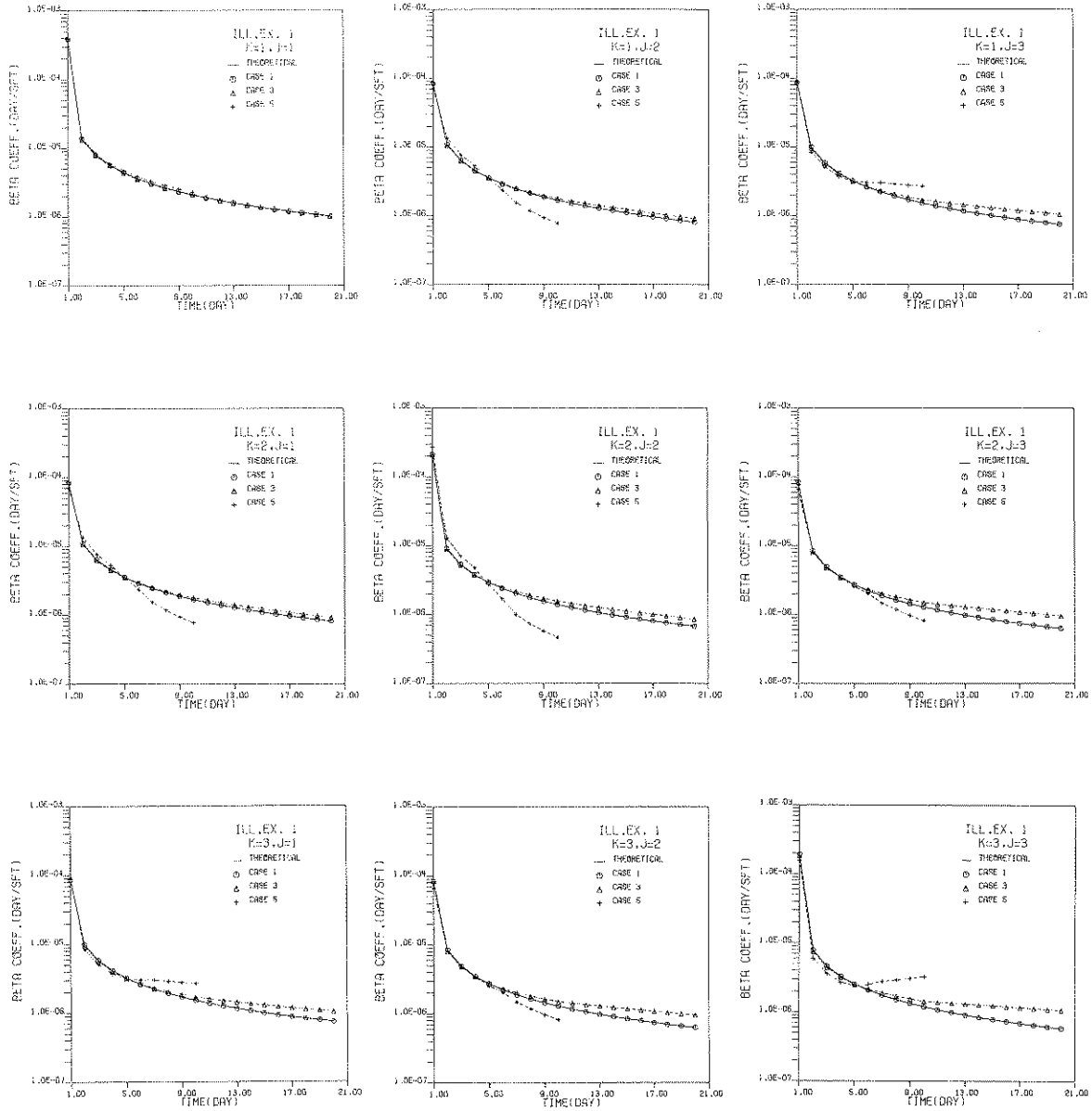


FIGURE 3.5 THEORETICAL AND COMPUTED BETA COEFFICIENTS FROM CALIBRATION (I.E. NO. 1)

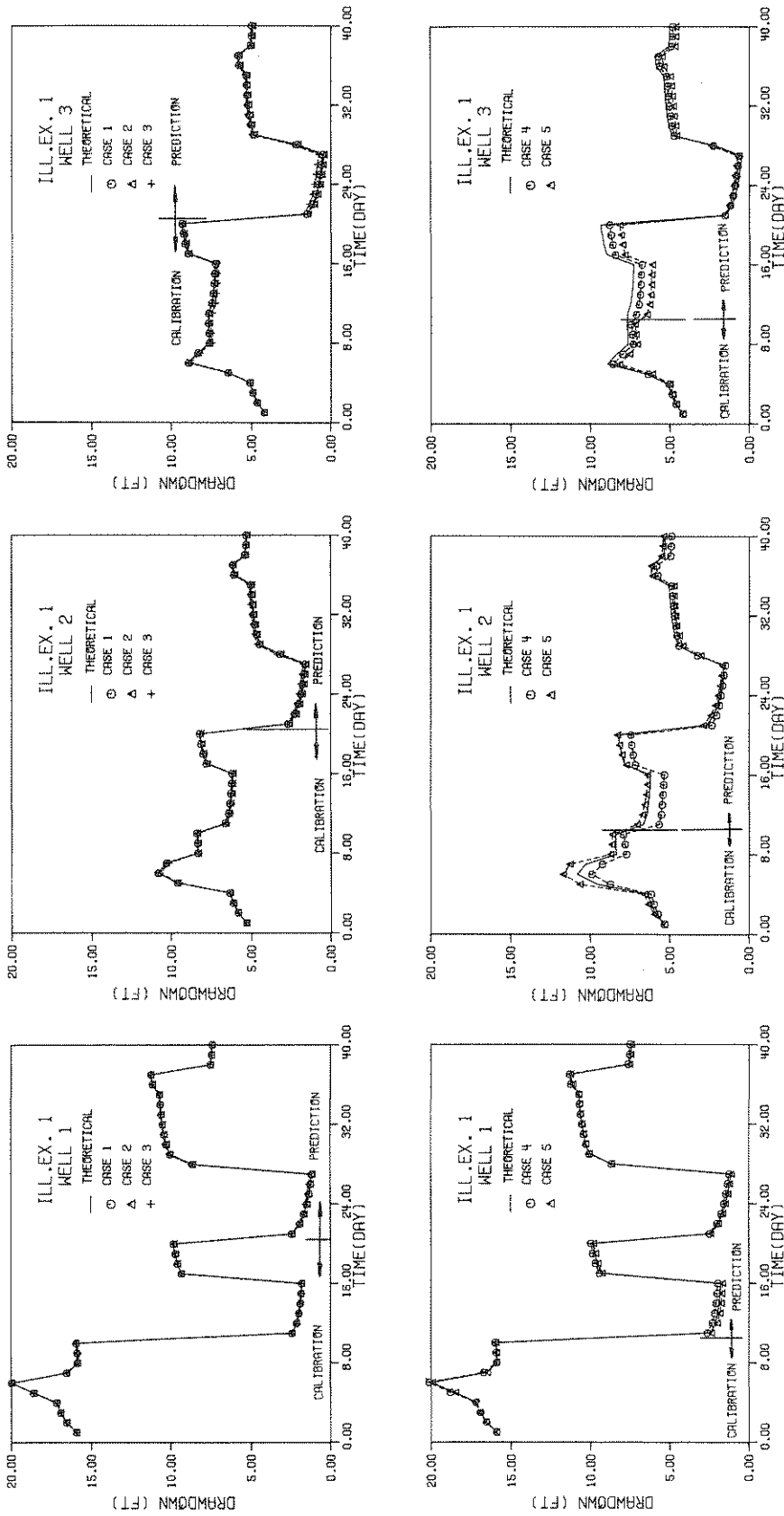


FIGURE 3.6. COMPARISON OF THEORETICAL AND COMPUTED DRAWDOWNS
(CALIBRATION AND PREDICTION, I.E. NO. 1)

Typical values of computed transmissivities, β - coefficients and the drawdowns resulting after calibration for Case 1 (well 1) are given in Table 3.4 along with their theoretical counterparts and percentage errors. The percentage errors between the assumed and the computed transmissivity values are of the order of 10^{-5} . The discrepancies between the theoretical and the computed β - coefficients are also negligible. The maximum absolute error between the theoretical and the computed drawdowns is smaller than 3.5 percent.

A comparison between the theoretical and the computed values of transmissivities, β - coefficients and the drawdowns for Case 4 (well 3) is shown in Table 3.5. The percentage errors between the theoretical

TABLE 3.5
COMPARISON OF THEORETICAL AND COMPUTED RESULTS AFTER CALIBRATION
(WELL NO. 3, CASE 4, I. E. NO. 1)
Transmissivity at Well No. 3 = 7000 sft/day (given)

Time since pumping started (Days)	Transmissivity (sft/day)		β - Coefficients $\beta(k,j,I)$ (day/sft) $k=3, j=1$			Drawdowns (Ft. below SWL)		
	COMPUTED	ABS.PER. ERROR	THEORETICAL ($\times 10^{-5}$)	COMPUTED ($\times 10^{-5}$)	ABS.PER. ERROR	THEORETICAL	COMPUTED	ABS.PER. ERROR
1	7983	14.1	8.755	8.858	1.2	4.18	4.18	0
2	7877	12.5	1.002	0.944	5.8	4.65	4.61	0.8
3	7738	10.5	0.586	0.559	4.7	4.92	4.86	1.2
4	7587	8.4	0.416	0.401	3.6	5.11	5.04	1.4
5	7383	5.5	0.323	0.315	2.5	6.48	6.34	2.1
6	6711	4.1	0.264	0.272	3.0	8.93	8.57	4.0
7	6101	12.8	0.223	0.242	8.3	8.35	7.98	4.5
8	5611	19.8	0.193	0.219	13.4	7.64	7.31	4.3
9	5215	25.5	0.170	0.201	17.9	7.66	7.36	3.9
10	4891	30.1	0.152	0.185	21.6	7.70	7.44	3.5

SWL = static water level
Avg. computed transmissivity at Well No. 1, $T_3 = 6710$ sft/day
Per. Error = (Theoretical Value - Computed Value) $\times 100$ / Theoretical Value

values and the computed results are very small in comparison to the percentage errors between the assumed storage coefficients and those used in calibration. In addition, for a given time step, there is a decreasing trend in the absolute percentage error between the theoretical and the computed of transmissivity values, β - coefficients and drawdowns. For example, referring to the results presented in Table 3.5, the error between the actual and the computed transmissivity at the 9th observation is 25.5 percent whereas that between the theoretical and the computed β - coefficient is 17.9 percent and that for the drawdowns it is only 3.9 percent. Therefore, the large errors in the assumed storage coefficients will result in comparatively small errors in the computed transmissivity values and β - coefficients and even smaller

errors in the computed drawdowns. Typical values of theoretical and computed drawdowns and the percentage errors for the first ten time steps resulting at well 2 for all the cases are shown in Table 3.6. These results indicate that the absolute error between the theoretical and the computed drawdowns for any time step is less than about 12 percent in comparison with the errors in the storage coefficient values used in calibration (Table 3.1) which range from 0 to 400 percent.

Prediction Results: The average transmissivity values for the different aquifer zones used for computing the β - coefficients and drawdowns during the prediction period in the different cases of sensitivity analysis are given in Table 3.3. The details of the number of observations used for prediction under different cases are shown in Table 3.2.

The theoretical β - coefficients and the predicted β coefficients for the different cases are presented in Fig. 3.7. Figure 3.6 shows a comparison between the theoretical and the predicted drawdowns for the various cases. Once again, for Case 1, the errors between the theoretical and the predicted values of β - coefficients and drawdowns are practically zero. The predicted drawdowns plotted in Fig. 3.6 for different cases also show reasonably close agreement with the theoretical drawdowns.

The prediction results for Case 4 (well 3) are tabulated in Table 3.7 along with the theoretical

TABLE 3.6
COMPARISON OF THEORETICAL AND COMPUTED DRAWDOWNS (FT. BELOW NPL) WELL NO. 2, I. E. No. 1

Time since pumping started (days)	THEORETICAL s_A	CASE-1		CASE-2		CASE-3		CASE-4		CASE-5		REMARKS
		s	ABS.PER. ERROR	s	ABS.PER. ERROR	s	ABS.PER. ERROR	s	ABS.PER. ERROR	s	ABS.PER. ERROR	
1	5.33	5.33	0	5.33	0	5.33	0	5.33	0	5.33	0	CALIBRATION
2	5.84	5.84	0	5.84	0.02	5.82	0.34	5.73	1.84	5.97	2.20	
3	6.14	6.14	0	6.14	0.02	6.11	0.50	5.98	2.67	6.33	3.14	
4	6.35	6.35	0	6.35	0.03	6.32	0.57	6.16	3.12	6.58	3.60	
5	9.60	9.60	0	9.61	0.10	9.48	1.26	8.75	8.80	10.66	11.04	
6	10.83	10.83	0	10.84	0.03	10.70	1.23	9.91	8.53	11.72	8.13	
7	10.31	10.31	0	10.30	0.04	10.15	1.46	9.25	10.20	11.30	9.67	
8	8.36	8.36	0	8.34	0.23	8.27	1.08	7.75	7.23	8.74	4.57	
9	8.38	8.38	0	8.35	0.31	8.30	0.96	7.83	6.57	8.66	3.40	
10	8.43	8.43	0	8.39	0.45	8.36	0.85	7.93	5.93	8.63	2.44	
31	4.79	4.79	0	4.74	0.99	4.90	2.23	4.63	3.38	4.55	5.08	PREDICTION
32	4.87	4.87	0	4.83	0.87	4.97	2.00	4.70	3.54	4.63	4.90	
33	4.93	4.93	0	4.89	0.86	5.02	1.80	4.76	3.48	4.69	4.96	
34	4.98	4.98	0	4.94	0.96	5.07	1.64	4.82	3.26	4.72	5.21	
35	5.03	5.03	0	4.97	1.04	5.10	1.51	4.88	2.94	4.75	5.53	
36	6.09	6.09	0	6.04	0.86	6.13	0.69	5.74	5.65	6.07	0.31	
37	6.16	6.16	0	6.11	0.92	6.20	0.55	5.83	5.50	6.14	0.34	
38	5.40	5.40	0	5.34	1.08	5.41	0.24	4.96	8.21	5.52	2.18	
39	5.34	5.34	0	5.28	1.16	5.35	0.22	4.91	8.01	5.43	1.75	
40	5.31	5.31	0	5.25	1.23	5.32	0.18	4.89	7.87	5.39	1.43	

$$\text{PERCENT ERROR} = (s_A - s) \times 100 / s_A$$

NPL = Nonpumping level

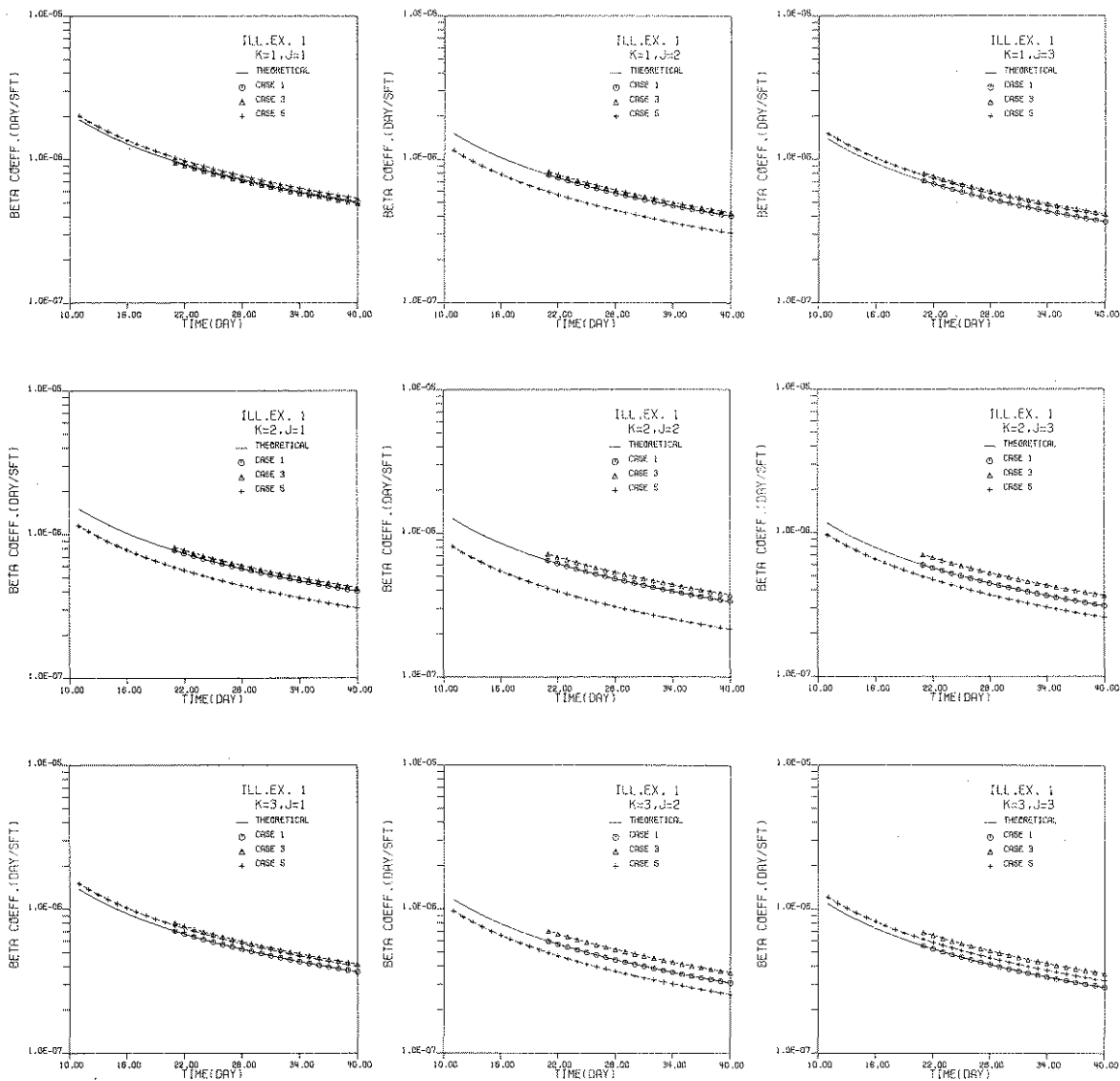


FIGURE 3.7 THEORETICAL AND COMPUTED BETA COEFFICIENTS FROM PREDICTION (I.E. NO. 1)

values of β - coefficients and drawdowns for time steps 11 through 30. The absolute error between the theoretical and the predicted β - coefficients for all the observations is constant and is equal to 3.2%. The reason for this constant error is obvious. The differences between the theoretical and the predicted drawdowns are larger for a few observations, but the maximum absolute difference is less than about 0.6 ft. A comparison of the theoretical and the computed drawdowns at well 2 is presented in Table 3.7 for the different cases. These results are given for time steps 31 through 40 only. The predicted drawdowns of Case 1 are the same as the theoretical drawdowns and those resulting from the other cases are reasonably close to the theoretical drawdowns. The absolute error between the theoretical and the predicted drawdowns resulting from different cases (Table 3.6) ranges from 0 to 9 percent.

TABLE 3.7

COMPARISON OF THEORETICAL AND COMPUTED RESULTS AFTER PREDICTION**
(WELL NO. 3, CASE 4, I. E. NO. 1)

Time since pumping started (days)	β - Coefficients, $\beta(k,j,I)$ (day/sft) $k=3, j=1$			Drawdowns (Ft. below SWL)		
	Theoretical ($\times 10^{-5}$)	Computed ($\times 10^{-5}$)	ABS.PER. ERROR	Theoretical	Computed	ABS.PER. ERROR
11	0.138	0.142	3.2	7.69	7.10	7.63
12	0.126	0.130	3.2	7.49	6.93	7.56
13	0.116	0.120	3.2	7.40	6.85	7.46
14	0.107	0.111	3.2	7.34	6.80	7.36
15	0.100	0.103	3.2	7.31	6.77	7.39
16	0.093	0.096	3.2	7.28	6.73	7.54
17	0.088	0.095	3.2	8.95	8.42	6.00
18	0.083	0.085	3.2	9.14	8.59	6.03
19	0.078	0.081	3.2	9.24	8.69	6.04
20	0.074	0.077	3.2	9.32	8.76	6.05
21	0.071	0.073	3.2	1.49	1.51	1.62
22	0.067	0.069	3.2	1.10	1.18	7.00
23	0.064	0.066	3.2	0.89	1.00	12.00
24	0.062	0.064	3.2	0.75	0.88	16.94
25	0.059	0.061	3.2	0.65	0.79	21.67
26	0.057	0.059	3.2	0.57	0.71	25.04
27	0.055	0.056	3.2	0.50	0.63	25.70
28	0.053	0.054	3.2	2.13	2.26	6.06
29	0.051	0.052	3.2	4.85	4.71	2.80
30	0.049	0.051	3.2	5.03	4.85	3.55

** Prediction results for steps 31-40 are not presented in this table

The above results indicate that the method of solution presented herein is satisfactory for predicting aquifer response.

3.1.4 Application to a Field Situation

The utility of the present method is demonstrated below by using the time-drawdown data resulting from a pumping test. In most pumping tests, drawdowns from the pumping well and a neighboring observation

well are measured. These two wells can be considered to be a multiple well system and the present method (Secs. 3.1.1 and 3.1.2) can be used to compute β - coefficients and to predict drawdowns.

A pumping test was conducted at the well field owned by the Milton Public Water Supply Co., Milton (Pike County, Illinois) on November 24, 1969. The pumping test data, and other details were obtained from the Illinois State Water Survey, Urbana, Illinois.

There are four wells in this well field and the pumping test was conducted at Well 4. The time-drawdown data from the pumping well and a neighboring observation well (well 3) were recorded.

Well 4 is 12 in. in diameter, 53 ft. deep and is located 30 ft. south and 2,250 ft. east of the north-east corner of Section 9, T.6S., R.2W., Pike County (Illinois). Well 3 is of 8 in. diameter, 63 ft. deep and is located 10 ft. west of well 4. The generalized graphic logs of these two wells are shown in Fig. B.1, Appendix B. The aquifer material consists mostly of broken rock, limestone, and shales. The time-drawdown data for this pumping test is tabulated in Table B.1, Appendix B. This data shows that a step drawdown and recovery tests were conducted at well 4. Well 4 was pumped at a constant rate of 30 gpm for the first 150 minutes and was then allowed to recover for the next 30 minutes. The well was then pumped at three different rates; 10, 20 and 30 gpm, from 181 to 210 minutes. The time-drawdown data for the observation well (well 3) include only values for the first 150 minutes (Table B.1). These drawdowns were recorded at larger time intervals.

The procedure illustrated in Secs. 3.1.1 and 3.1.2 is used to analyse the time-drawdown data given in Table B.1 by considering wells 4 and 3 to be a multiple well system in an infinite aquifer. The pumping rates in well 4 during the test period are plotted in Fig. 3.8. The time-drawdown data (Table B.1) which was recorded at nonuniform time intervals are interpolated to obtain drawdowns at uniform time intervals of five minutes. These interpolated drawdown values are plotted in Figs. 3.9 and 3.10 for wells 4 and 3 respectively. A uniform time interval of five minutes is used in all the computations and the total number of observations are 42.

Calibration: The model is calibrated by using the pumping and the drawdown data corresponding to the first 15 time steps. The estimated storage coefficients and the average transmissivity values that resulted at the end of calibration are shown in Table 3.8. The computed β - coefficient values for the first 15 time steps are plotted in Fig. 3.11. These plots also show an exponential decay similar to the theoretical β - coefficients presented in Illustrative Example No. 1 (Sec. 3.1.3). The β - coefficients for the case with $k=1$ and $j=2$ are the same as they should be.

A comparison between the observed and the computed drawdowns of wells 4 and 3 are shown in Figs. 3.9 and 3.10 respectively. There is close agreement between the observed and the computed drawdowns. For example, the computed drawdown in well 4 at the 10th observation is 6.72 ft. as compared with the observed drawdown of 6.94 ft., an error of about 3.2 percent. The highest discrepancy between the observed and

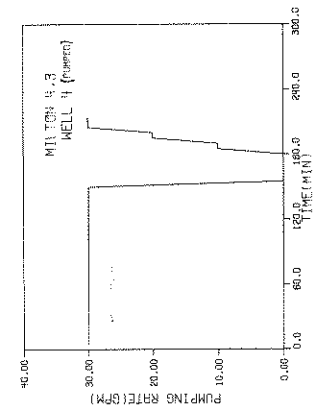


FIGURE 3.8 PUMPING RATES IN WELL 4, MILTON, NOVEMBER 1969

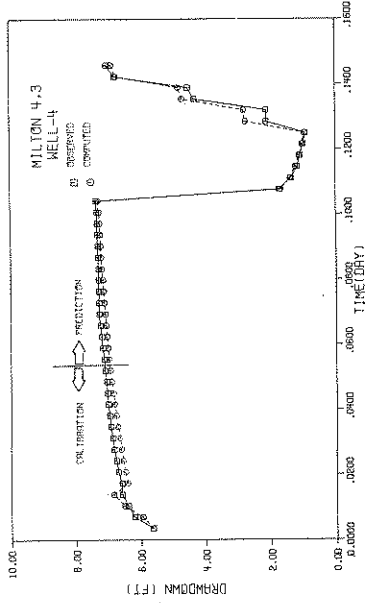


FIGURE 3.9 COMPARISON OF OBSERVED AND COMPUTED DRAWDOWNS (CALIBRATION AND PREDICTION) WELL 4, MILTON, NOVEMBER 1969

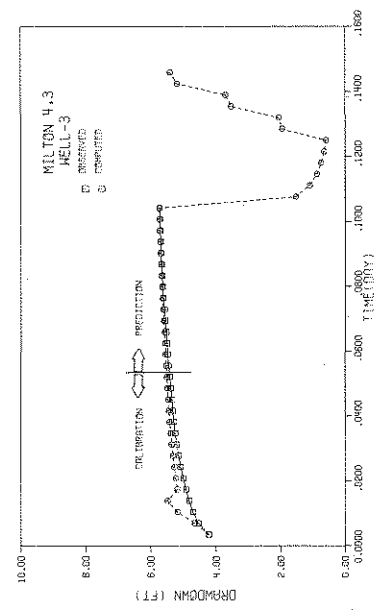


FIGURE 3.10 COMPARISON OF OBSERVED AND COMPUTED DRAWDOWNS (CALIBRATION AND PREDICTION) WELL 3, MILTON, NOVEMBER 1969

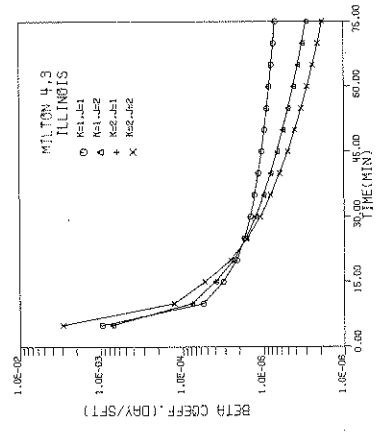
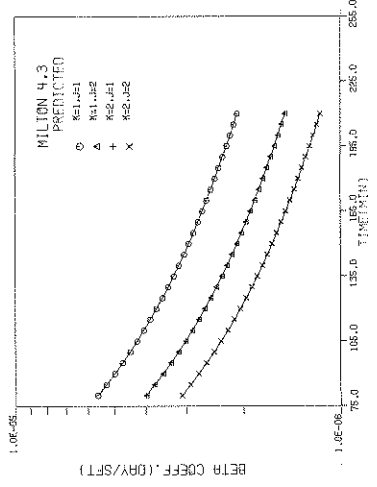


FIGURE 3.11 BETA COEFFICIENTS COMPUTED FROM CALIBRATION, MILTON, NOVEMBER 1969



COMPUTED FROM PREDICTION, MILTON, NOVEMBER 1969

TABLE 3.8
ESTIMATED STORAGE COEFFICIENTS AND
COMPUTED AVERAGE TRANSMISSIVITIES (MILTON)

Well No.	S	T'(sft/day)
4	0.0001	916.8
3	0.0001	1658.3

the computed drawdowns occurs at the 4th observation in well 3 (Fig. 3.10) where the error is about 10 percent. As these discrepancies between the observed and the computed drawdowns are small, the calibration is considered satisfactory and the average transmissivities computed at the end of calibration (Table 3.8) are used for computing β - coefficients and predicting drawdowns for further observations.

Prediction: The β - coefficients computed for the observations, 16 through 42 are plotted in Fig. 3.12. Once again the values of the β - coefficients are the same for the case where $k=1$, $j=2$ and $k=2$, $j=1$. A comparison between the predicted and the observed drawdowns of the wells 4 and 3 are shown in Figs. 3.9 and 3.10 respectively. These plots show close agreement between the observed and the predicted drawdowns at both wells. The discrepancies between the observed and the predicted drawdowns corresponding to most of the time steps are very small with the error being less than about 10 percent. However, the maximum discrepancy is seen at the 38th observation (well 4, Fig. 3.9) where the predicted drawdown is 2.10 ft. as compared with the observed value of 2.80 ft., an error of about 33 percent. The observed drawdowns in well 3 (Fig. 3.10) were not recorded for the pumping period beyond 150 minutes. The predicted drawdowns shown in Fig. 3.10 for time steps beyond 150 minutes reflect the drawdowns that could be expected during this period in this well.

3.2 Multiple Well System in a Homogeneous Aquifer

Often wells are located close enough that the aquifer properties do not vary appreciably within an aquifer flow system. Under these conditions the aquifer response coefficients can be computed even if the water levels in only one of the wells and pumping rates from all the wells are known. The method of solution can be extended to solve for both T and S values simultaneously if the drawdowns in two wells and pumping rates from all the wells are available.

Consider a homogeneous aquifer region with three wells where the distances and the well radii are assumed to be the same as those shown in Fig. 3.1. Since the aquifer is homogeneous, $T_1 = T_2 = T_3 = T$ and $S_1 = S_2 = S_3 = S$ in Eq. 3.6. The analysis is based on the same assumptions stated in Sec. 3.1.

3.2.1 Drawdowns in One of the Wells and Pumping Rates from All the Wells are Known

Using Eq. 3.6, the drawdown in well 2 is written for the first observation as

$$s(2,1) = \frac{C}{T} \left\{ \ln(D_{2,1} T/S)q_{1,1} + \ln(D_{2,2} T/S)q_{2,1} + \ln(D_{2,3} T/S)q_{3,1} \right\}. \quad (3.11)$$

In Eq. 3.11, there are two unknowns, viz. T and S. The value of S, reasonably estimated as explained in Sec. 3.1.1, is substituted into Eq. 3.11 and then solved for the unknown T. The coefficients $\beta(k,j,1)$ are then obtained from Eq. 3.5a. Once again it is stressed that the Jacob's approximation is introduced into Eqs. 3.5a and 3.11 only to make the illustration simpler. The calculations are performed with complete well function (Eq. 2.11) introduced into the governing equations as illustrated in Bathala (1976).

The above procedure is repeated for subsequent observations as explained in Sec. 3.1.1. The transmissivity values resulting at the end of each observation during calibration are used to calculate the average transmissivity of the homogeneous aquifer. This transmissivity value is then used to compute β -coefficients and eventually the drawdowns during the prediction period as explained in Sec. 3.1.2.

3.2.2 Drawdowns in Any Two Wells and Pumping Rates from All the Wells are Known

Once again using Eq. 3.6, the drawdowns $s(1,1)$ and $s(2,1)$ respectively in wells 1 and 2 are written as

$$\begin{Bmatrix} s(1,1) \\ s(2,1) \end{Bmatrix} = \frac{C}{T} \begin{bmatrix} \ln(D_{1,1} T/S) & \ln(D_{1,2} T/S) & \ln(D_{1,3} T/S) \\ \ln(D_{2,1} T/S) & \ln(D_{2,2} T/S) & \ln(D_{2,3} T/S) \end{bmatrix} \begin{Bmatrix} q_{1,1} \\ q_{2,1} \\ q_{3,1} \end{Bmatrix}. \quad (3.12)$$

Eq. 3.12 contains two unknowns, viz., T and S and can be solved simultaneously from the two equations using a suitable iterative technique as discussed in Sec. 3.1.1. The procedure is repeated for subsequent observations as explained earlier.

3.3 Analysis of Pumping Test Data

Pumping tests are often carried out on a single well in order to compute the transmissivity and the storage coefficient of an aquifer. The pumping rates and drawdowns in the pumped well are measured for different time intervals during the test. Where circumstances are favorable, the drawdowns are also measured in a neighboring observation well. A recovery test or a step drawdown test usually follows the first stage of pumping.

The time-drawdown data from these tests are usually analysed by the well known "type curve" method of solution (Todd, 1959 and Walton, 1970) using standard type curves for different aquifer conditions, well penetration, etc. This method is usually tedious and the results are subject to the accuracy in plotting the time-drawdown graphs, mode of superposition and other human errors. The procedure explained

herein can be used as an alternative to the type curve method for the determination of the aquifer transmissivity and the storage coefficient. The present analysis is limited to using the time-drawdown data from either the pumping well or the observation well just as in the type curve method.

3.3.1 Determination of the Transmissivity and the Storage Coefficient from Pumping Test Data

Consider a pumping well and an observation well in an aquifer which is reasonably large in areal extent. The wells are assumed to be deep enough so that the effect of partial penetration is negligible. The aquifer is overlain by a relatively thick confining layer such that the vertical leakage can be ignored. The wells are located close enough that the aquifer enveloping these wells can be assumed homogeneous and isotropic. Under these assumptions, the drawdowns either in the pumped well or the observation well can be expressed by using the Theis equation (Eq. 2.10). The pumping rates and drawdown data are usually measured at discrete time steps and, therefore, it is more convenient to express Eq. 2.10 in the discretized form as shown in Eq. 3.13 following the results of Maddock (1972) and the derivation given in Appendix A.

$$s(r,N) = \sum_{i=1}^N q(i) \beta(N-i+1) \quad (3.13)$$

In Eq. 3.13, $\beta(i)$ are the aquifer response coefficients and are expressed as

$$\beta(i) = \left. \begin{aligned} &= \alpha_i && \text{for } i = 1 \\ &= \alpha_i - \alpha_{i-1} && \text{for } i > 1 \end{aligned} \right\} \quad (3.14a)$$

$$\alpha_i = \frac{1}{4\pi T} W(u_i), \quad (3.14b)$$

where, $W(u_i)$ is the well function for nonleaky artesian aquifers as shown in Eq. 2.11 and,

$$u_i = r^2 S / 4T t_i. \quad (3.14c)$$

Assuming that the drawdown data from the observation well are used for analysis, the drawdown at the first observation can be given as in Eq. 3.15 using the relationships given in Eqs. 3.13 and 3.14.

$$s(r,1) = \frac{q_1}{4\pi T} \left\{ -0.5772 - \ln\left(\frac{r^2 S}{4T t_1}\right) + \left(\frac{r^2 S}{4T t_1}\right) - \frac{1}{2 \cdot 2!} \left(\frac{r^2 S}{4T t_1}\right)^2 + \dots \right\} \quad (3.15)$$

In Eq. 3.15, the values of T and S are unknown. The equation can be solved for T by substituting an estimated values of S as explained earlier. This procedure is repeated for subsequent observations by solving for the transmissivity value.

As all these pumping tests are usually carried out for short periods (2 or 3 days) it can be assumed that the aquifer transmissivity and storage coefficient do not change significantly during this period, which must also be assumed if the type curve procedure is used. Therefore, if the storage coefficient value used in calculations is reasonably correct, the transmissivity values obtained for all the

observations should be fairly constant. If there is a decreasing or increasing trend in the resulting transmissivity values, the entire procedure should be repeated for a different value of S . The trial that yields a fairly constant sequence of transmissivities for all the observations is the correct matching solution. The value of S corresponding to this trial and the average value of T are the aquifer storage coefficient and the transmissivity respectively. However, the above procedure is not valid if there is a transition from artesian to water table condition during the test or if the storage coefficient changes significantly due to delayed gravity drainage from an unconfined aquifer.

The procedure explained above is illustrated by analysing several field pumping tests conducted at different locations in the United States.

3.3.2 Case Histories of Pumping Test Analysis

a) Milton, Illinois

The Milton Public Water Supply Company conducted a pumping test on well 3 of their well field from 11:45 A.M., June 5 to 3:43 P.M., June 7, 1969. The details of this well are given in Sec. 3.1.4. A part of the time-drawdown data which is of interest in the present analysis is tabulated in Table B.2, Appendix B. This time-drawdown data which were measured at nonuniform time increments are interpolated for three minute intervals, and the resulting drawdowns are plotted in Fig. 3.16. A uniform time increment of three minutes is used and this resulted in 54 observations for that part of the pumping period considered in this analysis. The details of pumping rates and other related particulars are given in Table 3.9.

TABLE 3.9
DETAILS OF PUMPING TEST ON WELL 3, MILTON

Diameter of pumping well		= 8 in.
Pumping period considered:	11:45 A.M. to 2:27 P.M., June 5, 1969	
Pumping rates	1- 64 min.	= 105 gpm
	65-100 min.	= 101 gpm
	101-162 min.	= 100 gpm
Time increment considered in the study		= 3 min.
Total number of observations		= 54
Observations used for calibration		= 1 - 21
Observations used for prediction		= 22 - 54

The drawdown data and the pumping rates corresponding to the first 21 observations are used for analysis. During this period the pumping rate was constant at 105 gpm. The storage coefficient values used in various trials for calibrating the model are shown in Table 3.10. The computed transmissivity values resulting from different trials are plotted in Fig. 3.13. The transmissivities computed from trial 1 ($S=0.1$) show a steep increasing trend with increasing time whereas those of trial 2 ($S=0.02$) show a mild increasing trend. The plots of computed transmissivities for the fourth and fifth trials ($S = 0.001$ and 0.005 respectively) show decreasing trends with increasing time. The transmissivity values that resulted from trial 3 ($S=0.012$) are fairly constant throughout calibration period and therefore this can be considered as the best matching solution. The average of transmissivity values computed at the end of calibration for different trials are given in Table 3.10. As the result of trial 3 is the best matching solution, the aquifer transmissivity and the storage coefficient are respectively 473 sft/day and 0.012.

β - coefficients are computed for each observation for all the trials and these are convolved with the pumping rates to obtain the computed drawdowns. The β - coefficients obtained for trials 1, 3 and 5 are shown in Fig. 3.14. A comparison between the observed and the computed drawdowns for a few typical trials is shown in Fig. 3.15. It is obvious that the computed drawdowns from the trial 3 are very close

TABLE 3.10
STORAGE COEFFICIENTS AND COMPUTED AVERAGE TRANSMISSIVITIES
WELL 3, MILTON

Details	Trial 1	Trial 2	Trial 3*	Trial 4	Trial 5
Storage coefficient	0.1	0.02	0.012	0.01	0.005
Transmissivity (sft/day)	785	491	473	467	463

* the best matching solution

to those observed during the test. The discrepancies between the computed and the observed drawdowns for the different trials are given in terms of percentage errors in Table 3.11. Once again, it can be observed that the absolute percentage errors between the observed and the computed drawdowns of trial 3 are smaller than those of the other trials for several observations. These results again confirm that the best matching solution is obtained from trial 3 and the aquifer storage coefficient and the transmissivity are respectively given as 0.012 and 473 sft/day.

Comparison with the Type Curve Solution: The values of the aquifer transmissivity and the storage coefficient computed from the above procedure are compared below with the traditional type curve method of solution.

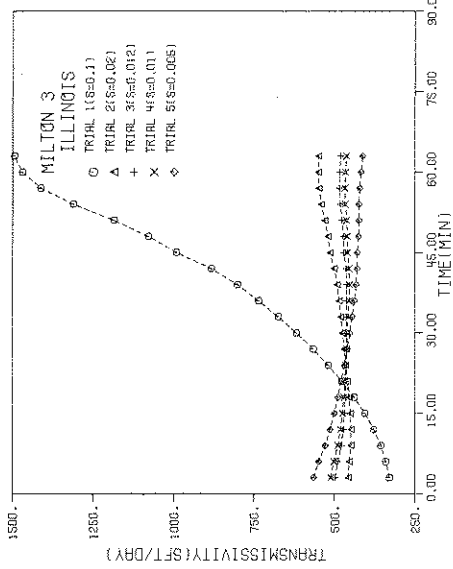


FIGURE 3.13 COMPUTED TRANSMISSIVITY VALUES, WELL 3, MILTON, JUNE 1969

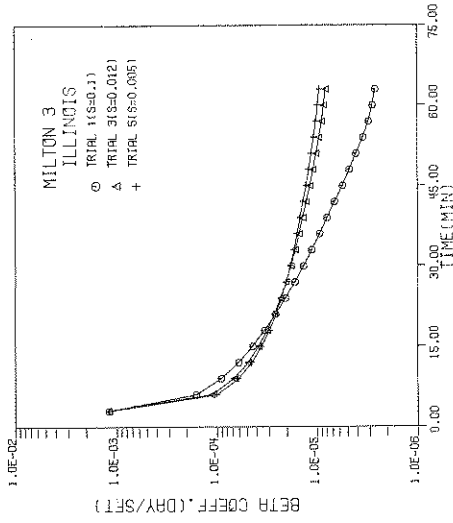


FIGURE 3.14 COMPUTED BETA COEFFICIENTS, WELL 3, MILTON, JUNE 1969

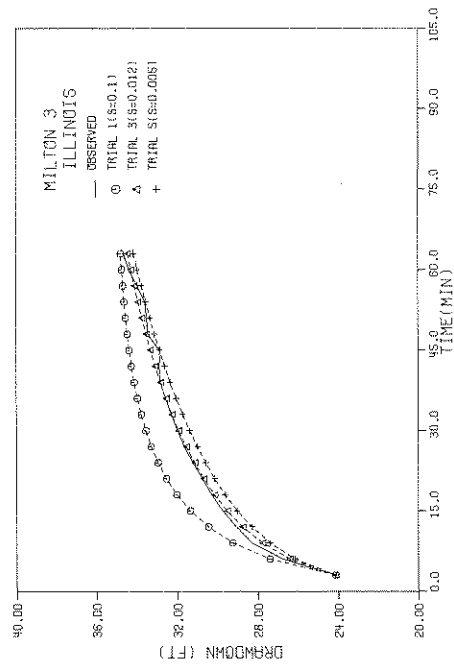


FIGURE 3.15 COMPARISON OF OBSERVED AND COMPUTED DRAWDOWNS, WELL 3, MILTON, JUNE 1969

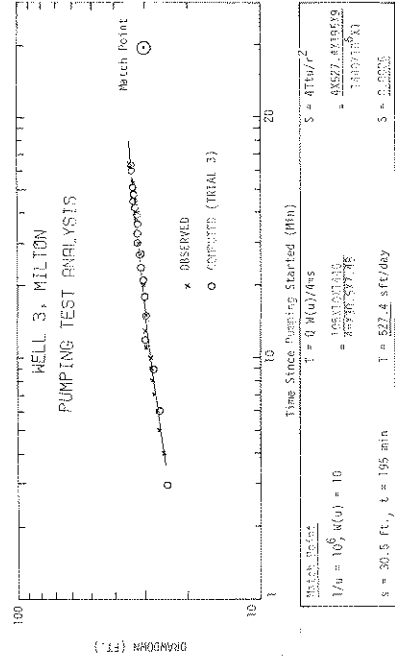


FIGURE 3.16 TIME-DRAWDOWN GRAPH OF WELL 3, MILTON, JUNE 1969

TABLE 3.11

COMPARISON OF OBSERVED AND COMPUTED DRAWDOWNS RESULTING FROM CALIBRATION, WELL 3, MILTON

STEP NO.	Time (Min)	Observed Drawdowns (ft.)	Trial 1 (S=0.1)		Trial 2 (S=0.02)		Trial 3 (S=0.012)		Trial 4 (S=0.01)		Trial 5 (S=0.005)	
			Comp. D.D. (ft.)	ABS.PER. ERROR	Comp. D.D. (ft.)	ABS.PER. ERROR	Comp. D.D. (ft.)	ABS.PER. ERROR	Comp. D.D. (ft.)	ABS.PER. ERROR	Comp. D.D. (ft.)	ABS.PER. ERROR
1	2	3	4	5	6	7	8	9	10	11	12	13
1	3	24.13	24.13	0	24.13	0	24.13	0	24.13	0	24.13	0.0
2	6	26.77	27.40	2.3	26.58	0.7	26.41	1.4	26.35	1.6	26.16	2.3
3	9	28.28	29.23	3.4	28.03	0.9	27.77	1.8	27.68	2.1	27.39	3.1
4	12	29.05	30.45	4.8	29.06	0.0	28.75	1.1	28.64	1.4	28.29	2.6
5	15	29.73	31.34	5.4	29.86	0.4	29.51	0.7	29.40	1.1	29.01	2.4
6	18	30.27	32.00	5.7	30.50	0.8	30.14	0.4	30.02	0.8	29.61	2.2
7	21	30.74	32.52	5.8	31.04	1.0	30.67	0.2	30.55	0.6	30.13	2.0
8	24	31.21	32.94	5.5	31.50	0.9	31.13	0.3	31.01	0.6	30.58	2.0
9	27	31.63	33.27	5.2	31.90	0.9	31.54	0.3	31.42	0.7	30.99	2.0
10	30	31.94	33.54	5.0	32.26	1.0	31.91	0.1	31.79	0.5	31.37	1.8
11	33	32.26	33.77	4.7	32.58	1.0	32.24	0.1	32.13	0.4	31.71	1.7
12	36	32.56	33.96	4.3	32.87	0.9	32.54	0.0	32.43	0.4	32.03	1.6
13	39	32.81	34.12	4.0	33.13	1.0	32.82	0.1	32.72	0.3	32.33	1.5
14	42	32.87	34.26	4.2	33.36	1.5	33.08	0.6	32.98	0.3	32.61	0.8
15	45	32.86	34.37	4.6	33.58	2.2	33.31	1.4	33.22	1.1	32.86	0.0
16	48	33.44	34.47	3.1	33.78	1.0	33.53	0.3	33.44	0.0	33.11	1.0
17	51	33.49	34.55	3.2	33.96	1.4	33.74	0.7	33.65	0.5	33.34	0.5
18	54	33.57	34.62	3.1	34.13	1.7	33.93	1.1	33.85	0.8	33.55	0.1
19	57	33.96	34.68	2.1	34.29	1.0	34.11	0.4	34.04	0.2	33.76	0.6
20	60	34.36	34.74	1.1	34.44	0.2	34.28	0.3	34.21	0.4	33.96	1.2
21	63	34.64	34.79	0.4	34.58	0.1	34.44	0.6	34.38	0.7	34.15	1.4

Drawdowns observed in well 3 (Table B-2, Appendix B) during the first stage of pumping are plotted against time on logarithmic paper as shown in Fig. 3.16. This time-drawdown graph is superposed on the nonleaky artesian type curve (Fig. 4.2, Walton, 1970) because there was no indication of leakage during the test. Match point coordinates and the computations are given in Fig. 3.16. The values of the transmissivity and the storage coefficient computed from the type curve method are respectively 527 sft/day and 0.0026.

The values of the computed drawdowns resulting from trial 3 (Col. 8, Table 3.11) are also plotted in Fig. 3.16 for comparison with the observed time-drawdown graph. It can be seen that it is difficult to differentiate between the observed and the computed time-drawdown graphs and the same match point could be obtained even by using the computed results from trial 3. A comparison of the results obtained from the present procedure and the type curve method is shown in Table 3.12. The transmissivity value computed from the type curve solution is in close agreement to that obtained from the present method. However, there is a large deviation between the storage coefficients obtained from the two methods. It is to be pointed out here that the storage coefficient value cannot be determined accurately from the type-curve solution due to lack of early time-drawdown data.

TABLE 3.12

COMPARISON OF RESULTS FROM THE PRESENT PROCEDURE AND
THE TYPE CURVE METHOD, WELL 3, MILTON

DETAILS	PRESENT PROCEDURE (TRIAL 3)	TYPE CURVE METHOD
Storage Coefficient	0.012	0.0026
Transmissivity (sft/day)	473.4	527.4

b) Gridley, Illinois

A group of three wells located within the corporate limits of the village of Gridley (McLean County, Illinois) were used for a pumping test on July 2, 1953. The effects of pumping well 3 were measured in observation wells 1 and 2. Pumping started at 9:45 A.M. on July 2, 1953 and was continued at a constant rate of 220 gpm until 6:02 P.M. The generalized graphic logs of these wells and the time-drawdown data are given in Walton (P.226-229, 1970).

In the present study, only the first 100 minutes of time-drawdown data measured at the observation well 1 are considered for analysis. The generalized graphic log of well 1 is shown in Fig. B.1, Appendix B. The time-drawdown data are listed in Table B.3. The distance between the pumping well (well 3) and the observation well (well 1) is 824 ft. A time increment of 5 minutes is used in this analysis and this resulted in 20 observations. The pumping rates and the drawdowns corresponding to all these 20 observations are used for analysis.

The different storage coefficient values assumed for different trials and the average transmissivities resulting at the end of calibration are given in Table 3.13. The computed transmissivity values from each of the trials are plotted in Fig. 3.17. These plots indicate that trial 3 ($S=0.000025$) yields transmissivity values which are fairly constant throughout the calibration period. Therefore, the aquifer transmissivity and the storage coefficient are respectively 1347 sft/day and 0.000025. A type curve solution for this time-drawdown data is given in Walton (p.228, 1970) and the results are shown in Table 3.13. The aquifer transmissivity and the storage coefficient values computed from the present procedure are in close agreement to the results obtained from the type curve method. The computed drawdowns resulting from the various trials are compared with the observed values and these are plotted in Fig. 3.18.

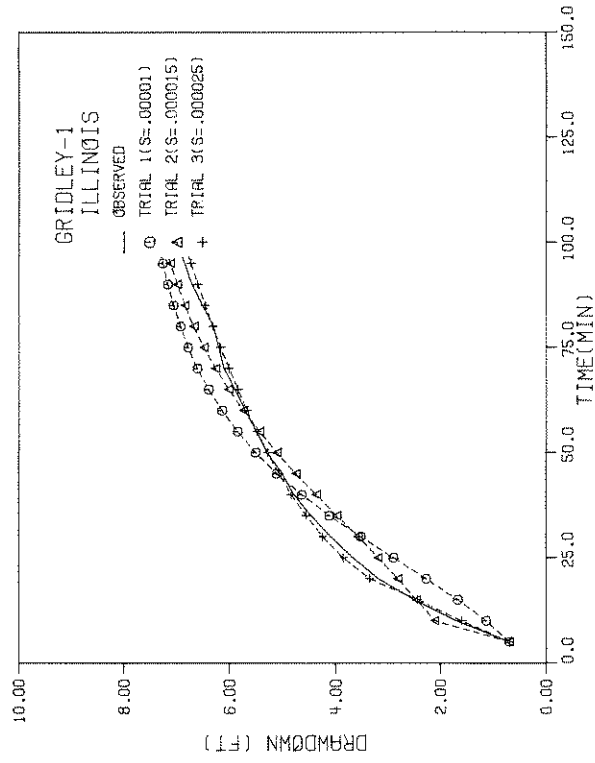


FIGURE 3.17 COMPUTED TRANSMISSIVITY VALUES,
GRIDLEY, JULY 1953

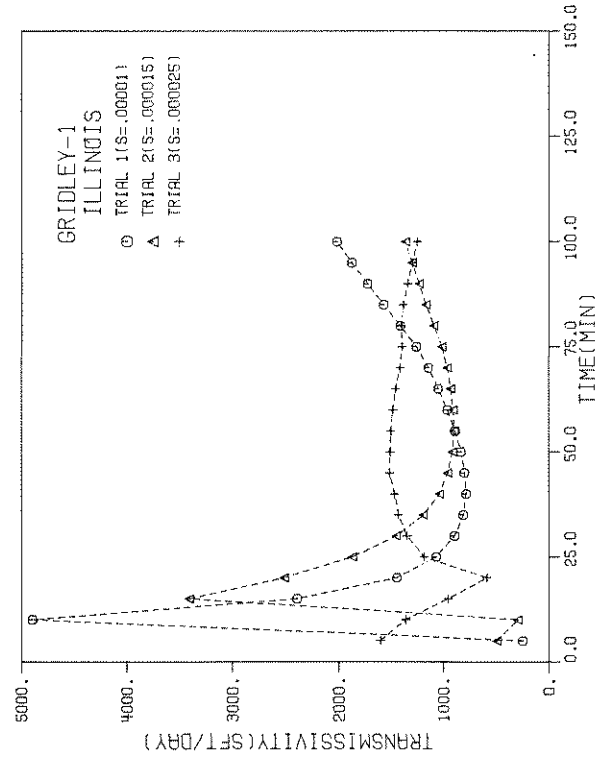


FIGURE 3.18 COMPARISON OF OBSERVED AND
COMPUTED DRAWDOWNS, GRIDLEY,
JULY 1953

TABLE 3.13

STORAGE COEFFICIENTS AND COMPUTED AVERAGE TRANSMISSIVITIES
FROM DIFFERENT TRIALS, GRIDLEY, ILLINOIS

DETAILS	TRIAL 1	TRIAL 2	TRIAL 3	TYPE-CURVE METHOD
Storage Coefficient	0.00001	0.000015	0.000025	0.00002
Transmissivity (sft/day)	1404	1250	1347	1350

c) Grand Island, Nebraska

Two classical pumping tests were conducted near Grand Island, Nebraska, during the summer of 1931 and the results of these tests were reported by Wenzel (1936). In each test a single well was pumped and the resulting drawdowns were measured in several observation wells drilled along lines radiating from the pumped well. In the present study, a part of the time-drawdown data measured at an observation well during the first pumping test is considered for analysis.

Pumping test 1 was conducted on well 83 from 6:05 A.M. July 29 to 6:04 A.M. July 31, 1931. Pumping was continued at a constant rate of 540 gpm. The resulting drawdowns were measured at several observation wells during the above test and were presented as time-drawdown graphs in Wenzel (1936). A part of the time-drawdown data for observation well 5 are obtained from these graphs at hourly intervals and are listed in Table B.4, Appendix B. Observation well 5 is located at a distance of 229 ft. from pumping well 83. A generalized graphic log of a well located in the vicinity of the test site is shown in Fig. B.1, Appendix B.

The time-drawdown data are analysed by making different trials as shown in Table 3.14. The transmissivity values computed for different observations during calibration are plotted in Fig. 3.19. The

TABLE 3.14

STORAGE COEFFICIENTS AND COMPUTED AVERAGE TRANSMISSIVITIES
FROM DIFFERENT TRIALS, GRAND ISLAND, NEBRASKA

DETAILS	TRIAL 1	TRIAL 2	TRIAL 3 ^{**}	TYPE-CURVE METHOD
Storage Coefficient	0.001	0.01	0.08	0.084
Transmissivity (sft/day)	64,152	43,835	24,461	23,638

** the best matching solution

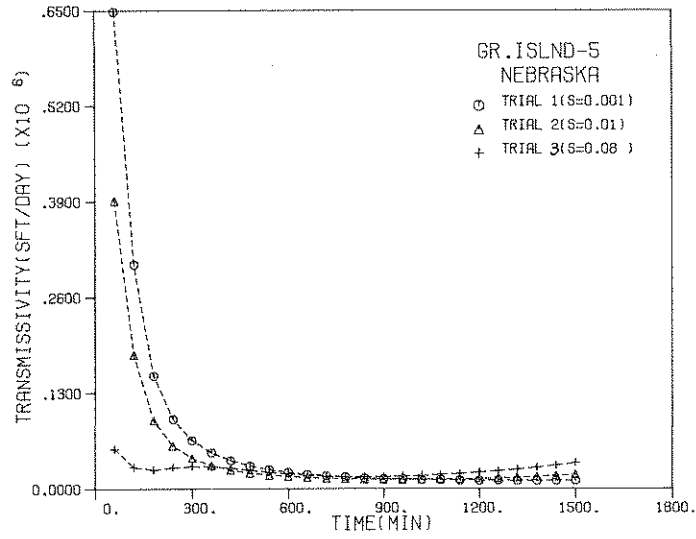


FIGURE 3.19 COMPUTED TRANSMISSIVITY VALUES, GRAND ISLAND, JULY 1931

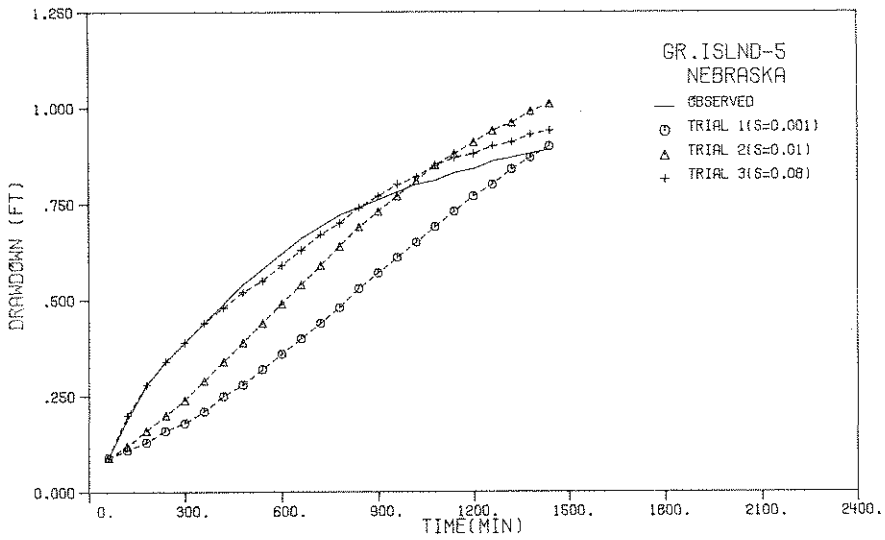


FIGURE 3.20 COMPARISON OF OBSERVED AND COMPUTED DRAWDOWNS, GRAND ISLAND, JULY 1931

transmissivity plot resulting from trial 3 is fairly constant for all observations. The average transmissivities computed at the end of calibration for different trials are depicted in Table 3.14. From the above results it can be concluded that the aquifer transmissivity is 24,461 sft/day and the storage coefficient is 0.08. The results obtained from the type curve method are shown in the last column of Table 3.14. These results are comparable to those computed from trial 3. A comparison between the observed and the computed drawdowns for the different trials is shown in Fig. 3.20. For most of the observations, the computed drawdowns resulting from trial 3 are closer to the observed drawdowns.

3.4 Stream - Aquifer Interaction Without Pumping

3.4.1 Introduction

The response of an aquifer to fluctuations in stream stages have been analysed by several investigators (Sec. 1.1.1 and 2.1.1). The linear systems approach has been used in most of these investigations and the solutions have been concerned mainly with the determination of aquifer diffusivity. This approach is repeated again for completeness and the procedure used for predicting the aquifer response due to fluctuations in river stage is not much different from that given by Pinder et al (1969).

The relationship governing the groundwater level fluctuations due to change in river stage is given in Eq. 2.30.

$$s(x,N) = \sum_{i=1}^N \Delta h(N-i+1) \beta_R(x,i) . \quad (2.30)$$

The β_R coefficients are given by Eq. 2.26 and can be written in the present notation as

$$\beta_R(x,i) = \text{erfc}[x/\sqrt{4vt_i}] \quad (3.16)$$

After substituting Eq. 3.16 into Eq. 2.30 we have in the present notation

$$h(x,N) = \sum_{i=1}^N \Delta h(N-i+1) \text{erfc} \frac{x}{\sqrt{4vt_i}} \quad (3.17)$$

where, $h(x,N)$ is the groundwater level at a distance x from the river at the N^{th} observation, $\Delta h(i)$ is the change in the stream stage at the i^{th} observation, v is the aquifer diffusivity and t_i is the time at the i^{th} observation. The time series of fluctuations in groundwater levels and river stage, and the distance from the river bank to the point of observation are known in advance. The aquifer diffusivity value is not usually known. However, Eq. 3.17 can be solved for v at each observation by using observed groundwater levels and river stages and the procedure illustrated in Sec. 3.1.1. The diffusivity value computed at a given observation is substituted in Eq. 3.16 and the β_R - coefficient is calculated. This procedure is repeated until the end of the calibration period. An average value is computed by using the diffusivity values determined at each observation during calibration.

The β_R - coefficients corresponding to the prediction period are computed by using Eq. 3.16, the average diffusivity, the distance between the river bank and the point of observation and the appropriate time of observation. The variations in stream stages corresponding to the prediction period can be computed using stochastic modeling techniques (Secs. 4.2 and 4.3.3). The β_R - coefficients are then convolved with the change in the predicted stream stage using Eq. 2.30 to compute future groundwater levels.

The above procedure is illustrated in the following case study.

3.4.2 Case Study: Dunns Bridge, Kankakee River Basin

Groundwater level data were measured at three different locations, namely Davis Bridge, Dunns Bridge and Shelby Bridge near the river in the Kankakee River Basin System of the State of Indiana. In this study, the water levels measured in the well N-1, near Dunns Bridge, and the related river stages are used for analysis.

Dunns Bridge is located about 1500 ft. north of the southwestern corner of Sec. 14, T.32N., R.5W. as shown in Fig. 3.21. Well N-1 is drilled about 90 ft. away from the north bank of the river, and the river gage is located 750 ft. downstream. Daily river stages and groundwater levels measured at this location from October 24 to November 7, 1972 are tabulated in Table B.5, Appendix B.

Groundwater levels and river stage shown in Table B.5 are used to compute β_R - coefficients as explained in Sec. 3.4.1. The average aquifer diffusivity value computed from calibration is 3690 sft/day. The storage coefficient of the aquifer in the vicinity of the test site is estimated to be 0.2. Therefore, the transmissivity of the aquifer is 738 sft/day.

The values of β_R - coefficients computed for each observation during calibration are plotted in Fig. 3.22. These values increase with increasing time. A comparison between the observed and the computed water levels in well N-1 is shown in Fig. 3.23. There is good agreement between the observed and the computed water levels.

β_R - coefficients and groundwater levels in well N-1 can be computed for further observations of the Kankakee River Stage using the average transmissivity, the estimated storage coefficient and the relationships given in Eqs 3.16 and 3.17.

3.5 Application of the Present Procedure to a Hypothetical Regional Aquifer Problem

3.5.1 Introduction

Several types of groundwater flow problems have been analysed in the previous sections by using the procedure developed in the present study for prediction of aquifer response. The primary objective of this study is to extend this procedure to the analysis of regional aquifer flow problems. The utility of this method for regional aquifer flow problems is demonstrated by using hypothetical data.

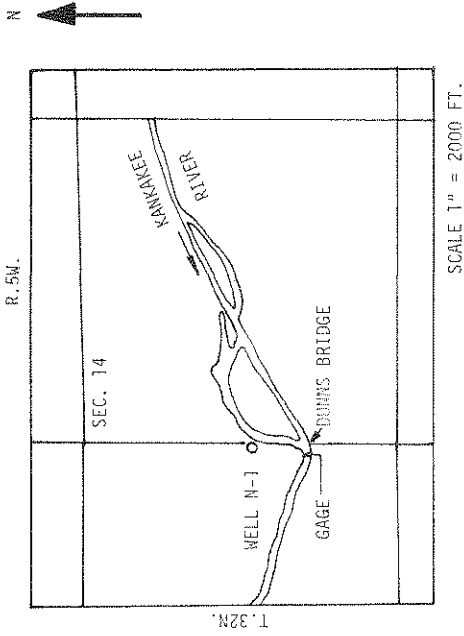


FIGURE 3.21 LOCATION MAP OF DUNNS BRIDGE

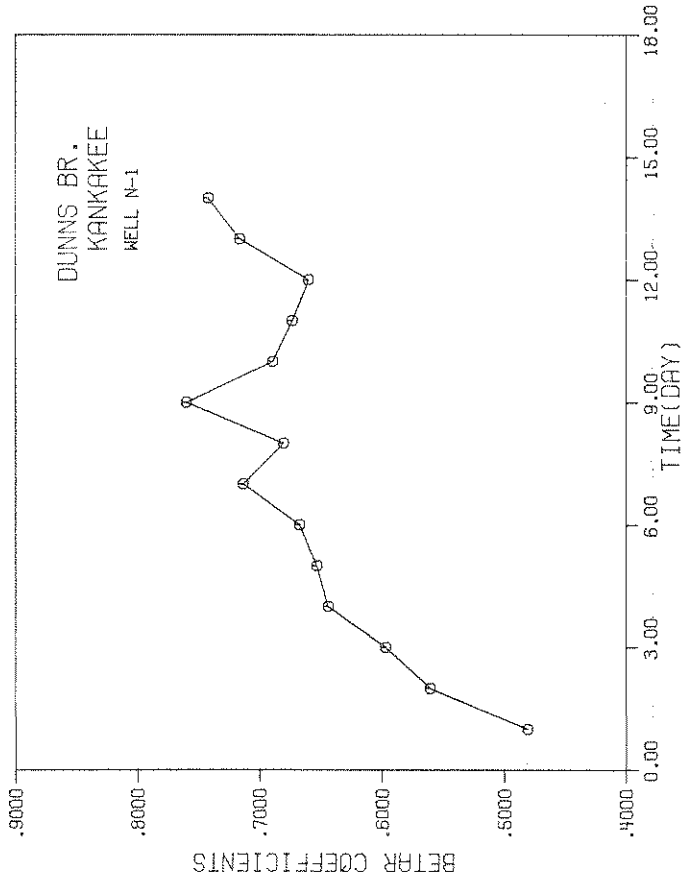


FIGURE 3.22 COMPUTED β_R -COEFFICIENTS, DUNNS BRIDGE

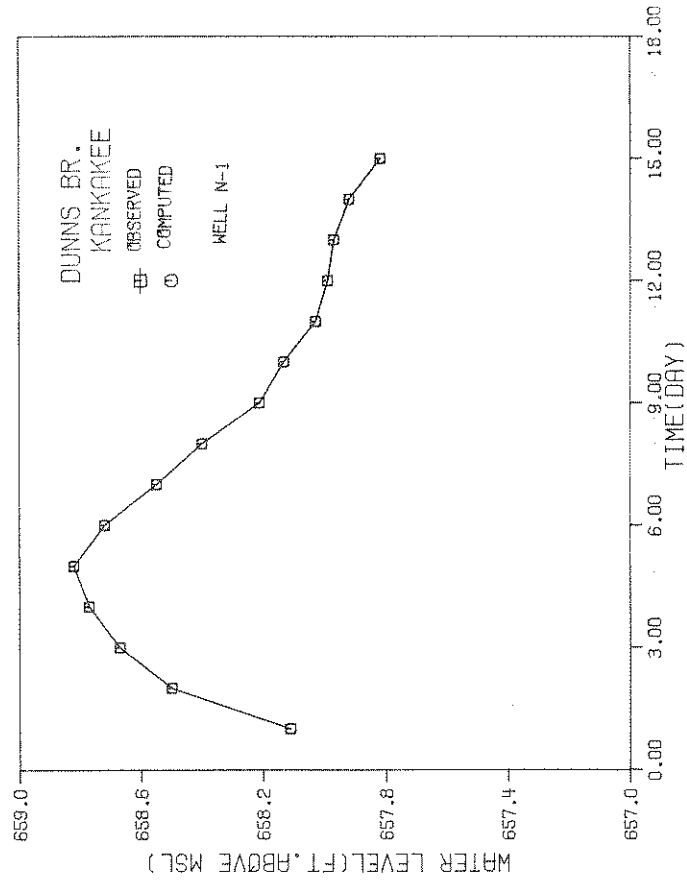


FIGURE 3.23 COMPARISON OF OBSERVED AND COMPUTED GROUNDWATER LEVELS, WELL N-1, DUNNS BRIDGE

3.5.2 Illustrative Example No. 2

Consider a nonhomogeneous aquifer region intersected by a hydraulically connected stream as shown in Fig. 3.24. The aquifer region is subdivided into five homogeneous zones based on the geology of the area. Zone I is the river valley portion and is mostly composed of alluvium. Zones II-V form the terraces and consist of different grades of sands, gravels and clay lenses. The aquifers underlying the zones III, IV and V are of a confined nature and those in Zones I and II may be considered as unconfined.

It is assumed that six pumping wells are already existing in this area and it is proposed to drill four more wells to meet future water demands. The location of these wells is shown in Fig. 3.24. The relative positions of the wells are measured with references to an arbitrary origin and are given in Table 3.15. Other particulars such as well radii, distances of the wells from the river, the ground elevation and the static water levels at each well are tabulated in Table 3.15.

TABLE 3.15
INITIAL DATA FOR THE ILLUSTRATIVE EXAMPLE NO. 2

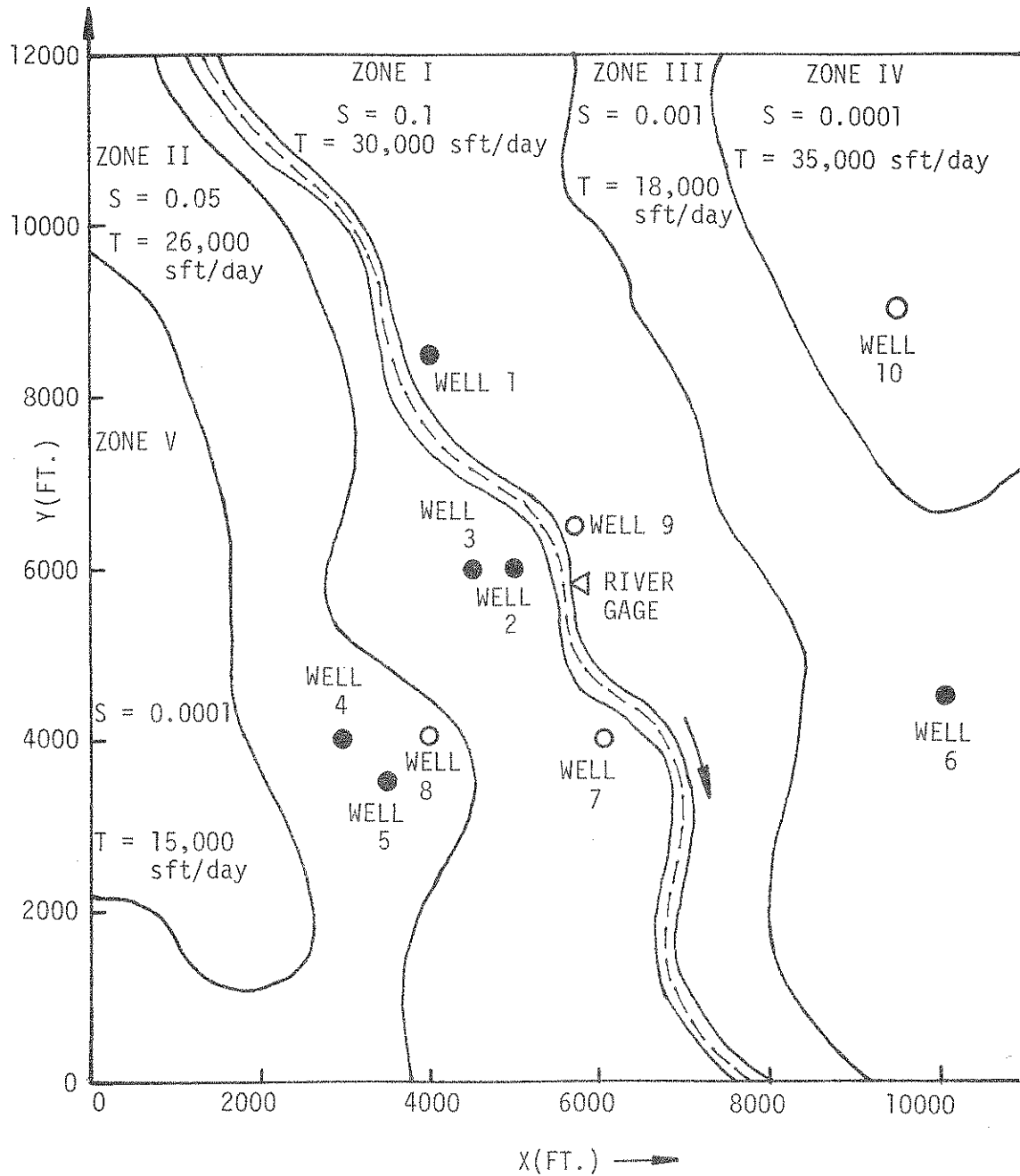
AQUIFER ZONE	WELL NO.	COORDINATES w.r.t. ARBITRARY ORIGIN		DISTANCE FROM RIVER L (ft.)	WELL RADIUS (inches)	GROUND LEVEL (ft. above MSL)	STATIC WATER LEVEL (ft. above MSL)	REMARKS
		X(ft)	Y(ft)					
I	1	4,000	8,500	300	6.0	520.34	513.21	Existing
I	2	5,000	6,000	400	4.0	521.65	512.90	Existing
I	3	4,500	6,000	800	3.0	521.90	512.92	Existing
II	4	3,000	4,000	2,700	6.0	546.84	521.50	Existing
II	5	3,500	3,500	2,500	5.0	545.25	522.61	Existing
III	6	10,000	4,500	3,100	8.0	584.67	527.81	Existing
I	7	6,000	4,000	350	5.0	522.16		Proposed
II	8	4,000	4,000	1,800	4.0	548.59	522.59	Proposed
I	9	5,700	6,500	200	4.0	519.78	512.87	Proposed
IV	10	9,500	9,000	4,750	4.0	587.81	531.23	Proposed

Datum of River Bed Level = 504.14 ft. above MSL

Assumptions: The following assumptions are made in addition to those already stated in Sec. 3.1.

- 1) The river bank is pervious and semi infinite. The river stage is constant within the reach considered for study.
- 2) The two major sources of recharge to the aquifer are the river and the occasional artificial recharge through the wells.

Procedure: Based on the above assumptions, the theoretical relationship given in Eq. 2.22 can be used to analyse this aquifer flow problem. As the vertical leakage is assumed to be insignificant, the β - coefficients are given by Eqs. 2.23a and 2.28. The expression for β_R - coefficients is the same as in



- EXISTING WELLS
- PROPOSED WELLS

SCALE 1" = 2000 FT.

FIGURE 3.24 GENERALIZED AQUIFER REGION (I.E. NO. 2)

Eq. 2.26. The procedure explained in Secs. 3.1.1 and 3.1.2 for the prediction of aquifer response can be used after incorporating suitable terms for the stream-aquifer interaction.

A monthly time increment is used in the analysis and a pumping period of 60 months is considered for the study. The data corresponding to the first 25 months are used for calibration. The later part of the data is used for prediction. Only wells 1-6 are assumed to be existing during the calibration period and all the ten wells are in operation during the prediction period.

Hypothetical Input Data: The input data required for analysing this problem are the pumping rates and drawdowns in all the wells, and river stages measured at the gaging station (Fig. 3.24). The monthly pumping rates and river stages for the 5 year period considered in the study are assumed after examining the data used in a few case studies of regional aquifer flow problems. The monthly drawdowns that would result due to these assumed pumpages and river stages are computed using the appropriate theoretical relationships presented in Chapter 2.

The time series of pumping rates assumed for all the wells are plotted in Fig. 3.25. These records show a seasonal trend with increasing pumping rates from year to year. The negative values in these plots indicate that the wells are occasionally used for recharging the aquifer. The zero discharges can be the result of malfunctioning of the wells. The monthly river stages assumed for the 60 months period are shown in Fig. 3.26. These river stages do not show any pronounced seasonality. These assumed pumping rates (Fig. 3.25) and river stages (Fig. 3.26) are hereinafter referred to as "observed pumping rates" and "observed river stages" respectively.

Drawdowns that would result in all the wells due to the observed pumpages and fluctuations in river stage are calculated using the Theis equation (Eq. 2.10), the relationship for stream-aquifer interaction (Eq. 2.4) and the method of superposition. The aquifer transmissivity and storage coefficient values used in these calculations are shown in Table 3.16. These values are designated "observed drawdowns" and are plotted in Fig. 3.27.

TABLE 3.16

TRANSMISSIVITY AND STORAGE COEFFICIENT VALUES USED IN THE ANALYSIS (I.E. NO. 2)

ZONE	Used To Generate Hypothetical Data		Used For Calibration And Prediction	
	Transmissivity T_H (sft/day)	Storage Coefficient (S_H)	Storage Coefficient (S_C)	ABS. PER ERROR
I	30,000	0.2	0.1	50
II	25,000	0.05	0.05	0
III	18,000	0.01	0.001	90
IV	35,000	0.0005	0.0001	80

$$\text{PERCENT ERROR} = (S_H - S) \times 100 / S_H$$

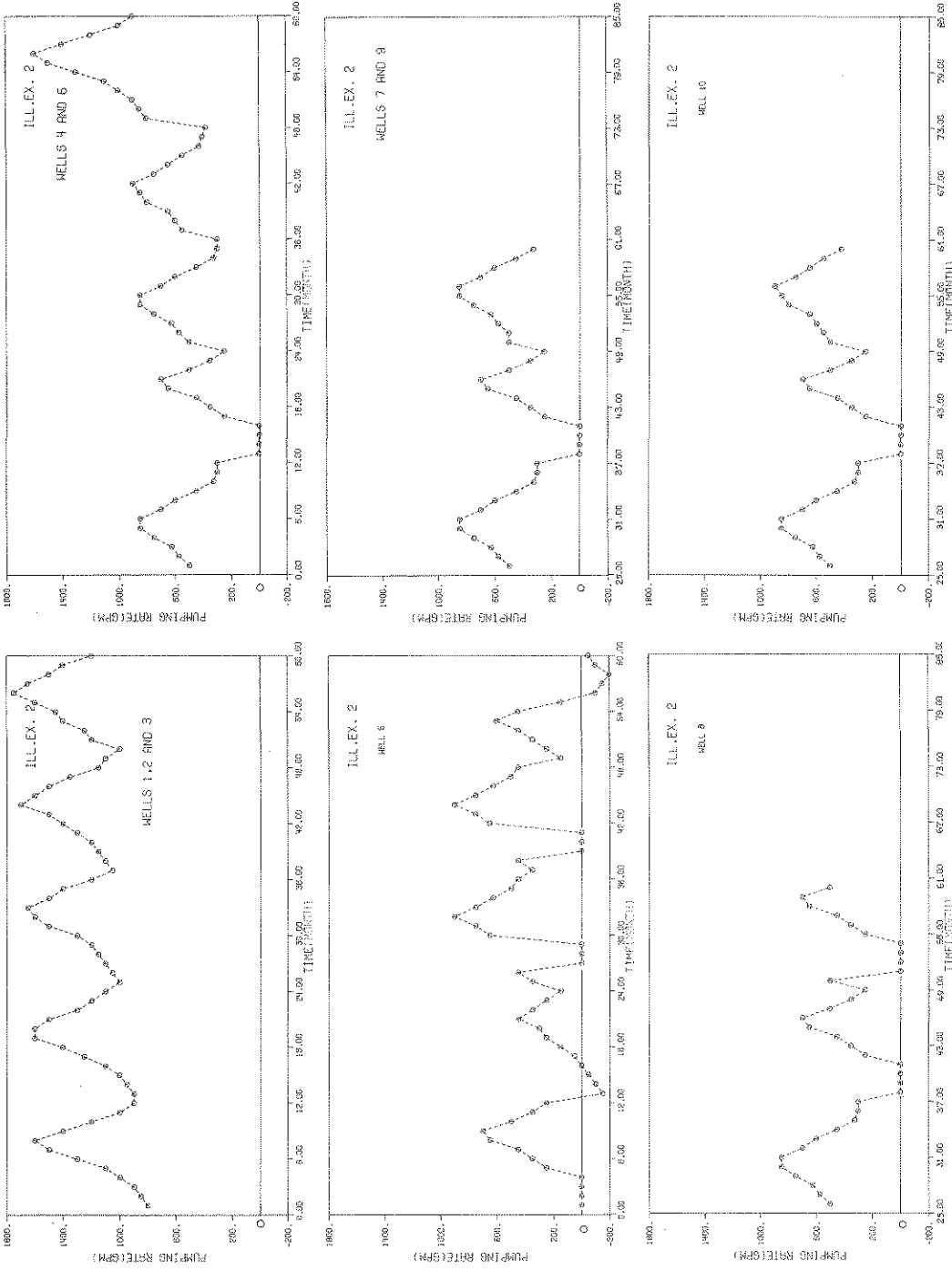


FIGURE 3.25 PUMPING DEMAND (I.E. NO. 2)

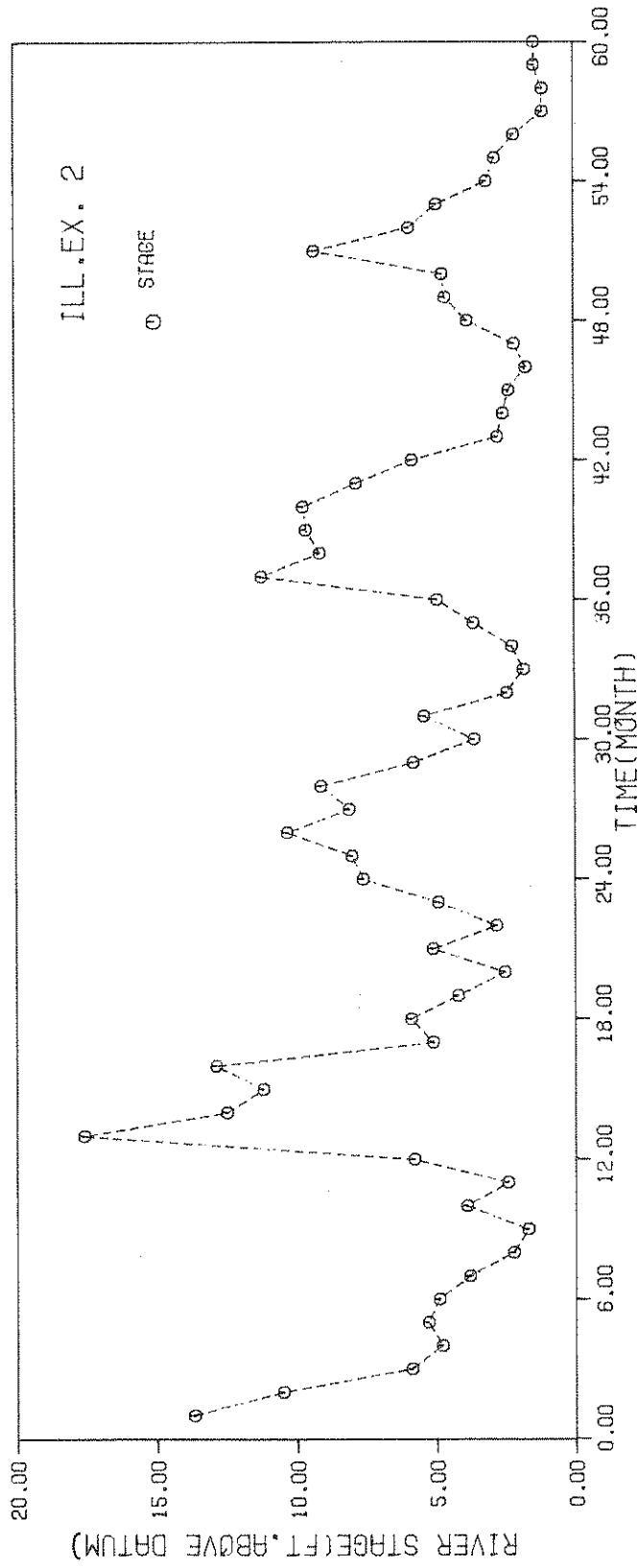


FIGURE 3.26 RIVER STAGES (I.E. NO. 2)

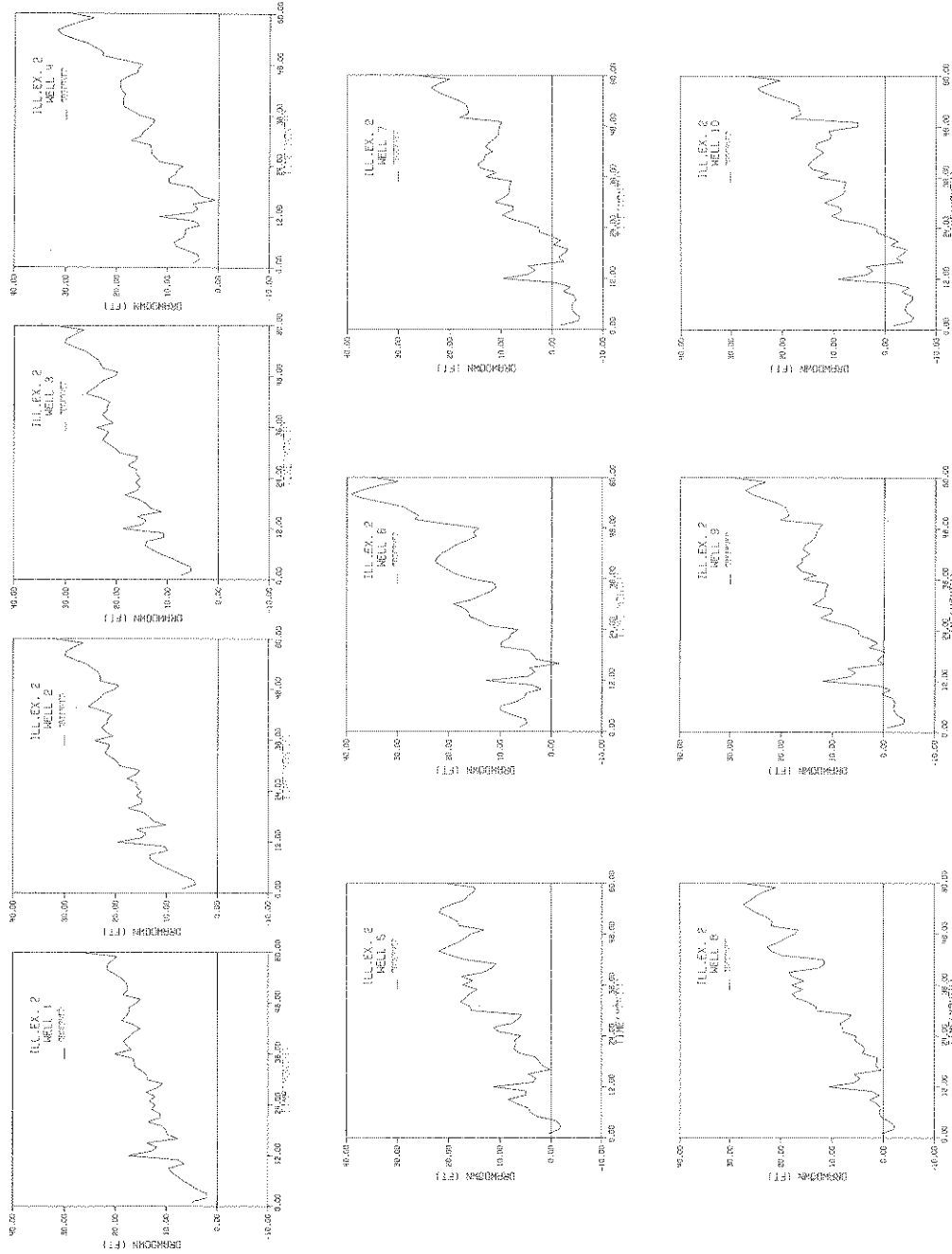


FIGURE 3.27 OBSERVED DRAWDOWNS (I.E. NO. 2)

Calibration and Prediction: The observed pumping rates, river stages and drawdowns (Figs. 3.25 - 3.27) corresponding to the first 25 month period are considered for calibration. The storage coefficients used during the calibration and prediction periods are shown in Table 3.16. These values are different from those used to compute the hypothetical data because in a field situation, the estimated storage coefficients are not likely to be the same as the true values. The absolute errors between the storage coefficients used to generate the hypothetical data and those used for calibration and prediction vary from zero percent to 90 percent as given in Table 3.16.

Typical values of β - coefficients and β_R - coefficients computed during the calibration period are plotted in Figs. 3.28 and 3.29 respectively. The average transmissivity values computed at the end of calibration for the different aquifer zones are given in Table 3.17 along with the percentage error with reference to the transmissivity values assumed to generate the hypothetical data. The average transmissivity value computed for Zone I is close to the assumed value. The absolute percentage errors between the assumed and the computed transmissivities for the other three zones are considerably large.

TABLE 3.17
AVERAGE TRANSMISSIVITIES COMPUTED FROM CALIBRATION (I.E. NO. 2)

AQUIFER ZONE	I	II	III	IV
Avg. Trans. (sft/day) T_A	31,200	37,980	39,650	59,790
Abs. Per. Error	4.0	51.9	120.3	70.8

$$\text{Percent Error} = (T_H - T_A) \times 100 / T_H$$

The β - coefficients and the β_R - coefficients resulting from calibration are used to compute the drawdowns for the first 25 months. These drawdowns are compared with the observed values as shown in Fig. 3.30. The computed drawdowns for all the wells are close to their observed counterparts. Some of the elementary statistics of the error between the observed and the computed drawdowns for a few wells are shown in Table 3.18. The statistics of the observed and computed drawdowns corresponding to the first 25 months are also given in Table 3.18 for comparison. The mean, variance and the mean square of the observed drawdowns are reproduced by the computed values during the calibration period. For example, at well 4, the mean and the mean square of the computed drawdowns are 6.33 ft. and 46.4 ft² as compared to 6.31 ft. and 46.8 ft² respectively of the observed drawdowns. The statistics of the computed drawdowns from the other wells not shown in Table 3.18 are also close to the corresponding statistics of the observed

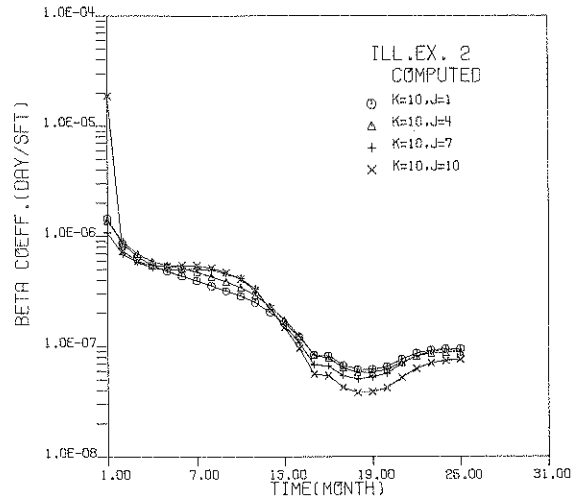
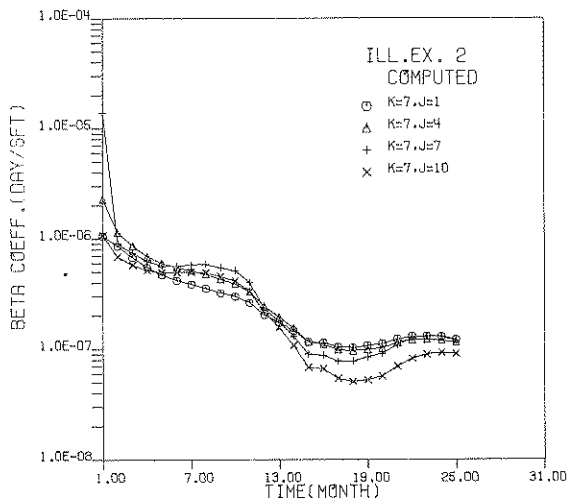
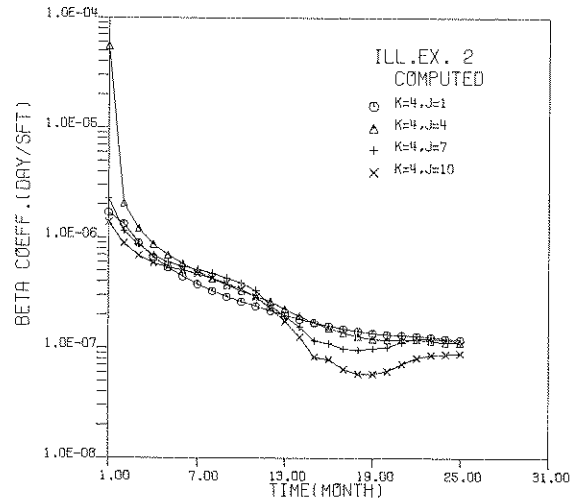
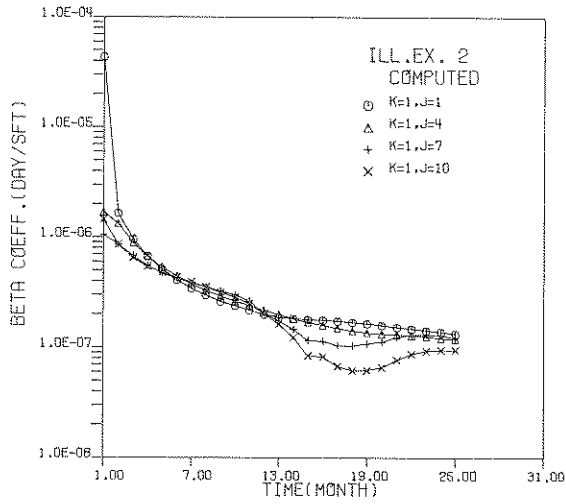


FIGURE 3.28 TYPICAL BETA COEFFICIENTS COMPUTED FROM CALIBRATION
(I.E. NO. 2)

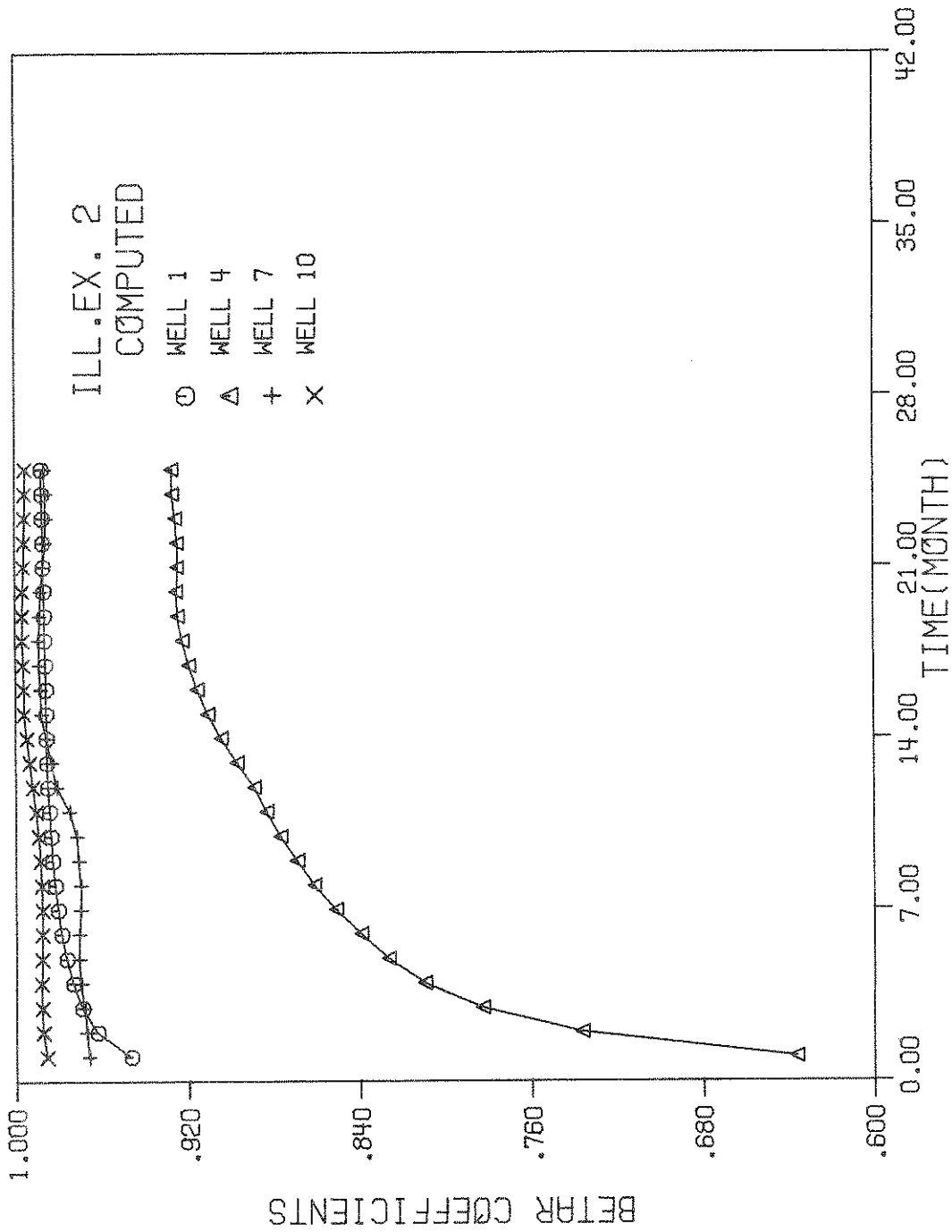


FIGURE 3.29 TYPICAL β_R -COEFFICIENTS COMPUTED FROM CALIBRATION (I.E. NO. 2)

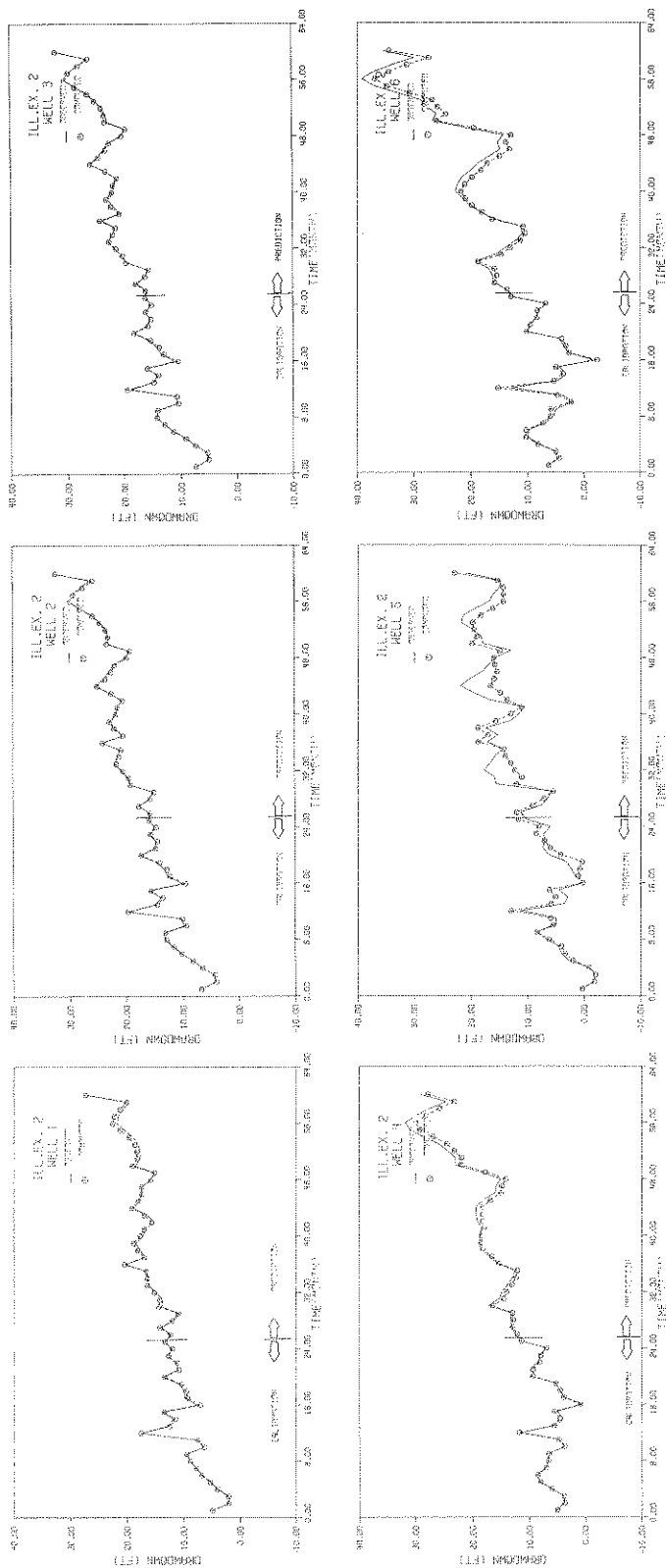


FIGURE 3.30 OBSERVED AND COMPUTED DRAWDOWNS (CALIBRATION AND PREDICTION, I.E. NO. 2)

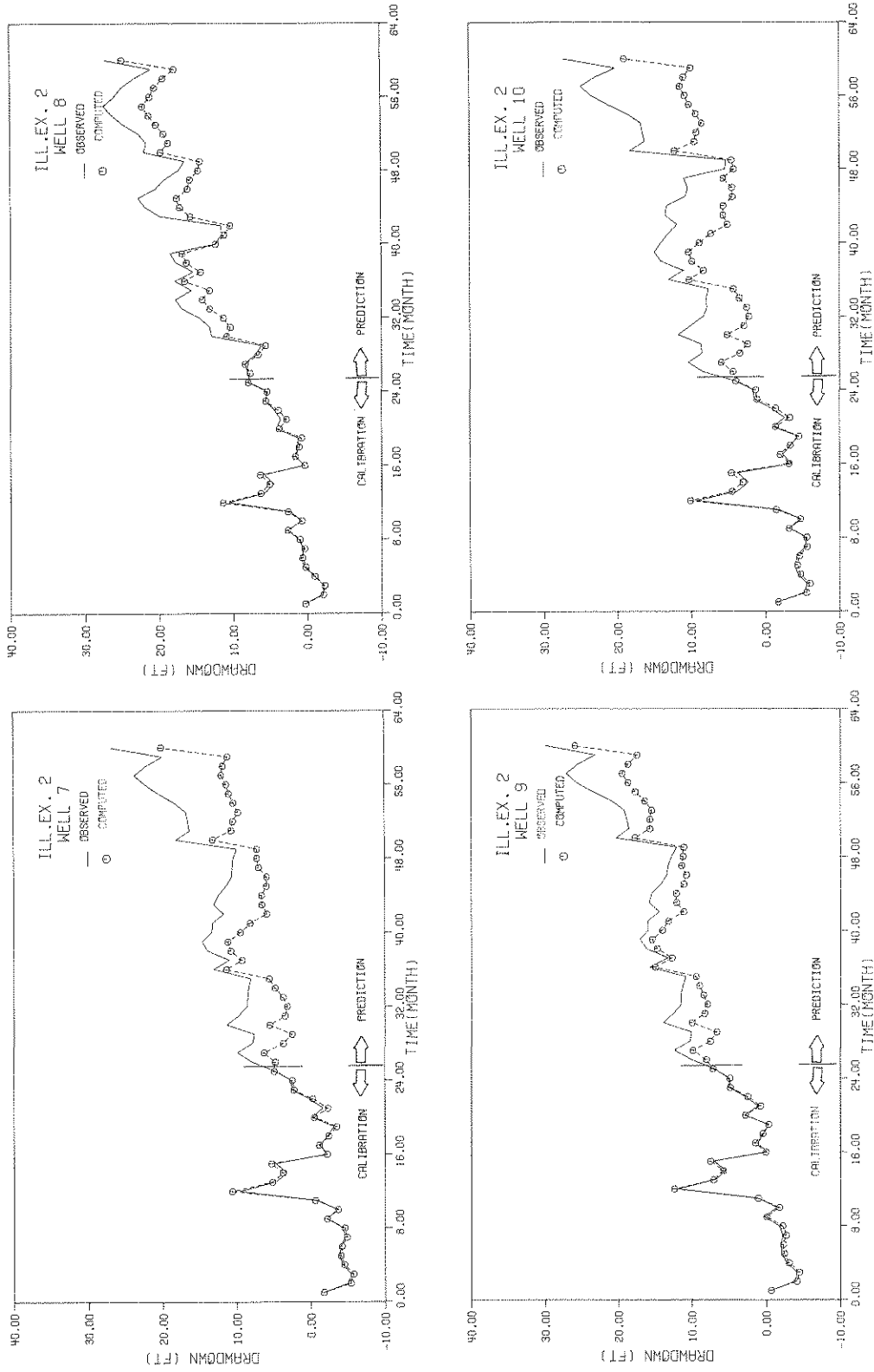


FIGURE 3.30 OBSERVED AND COMPUTED DRAWDOWNS (CALIBRATION AND PREDICTION, I.E. NO. 2) (contd.)

TABLE 3.18

STATISTICS OF OBSERVED AND COMPUTED DRAWDOWNS AND ERROR SERIES

STEP	STATISTIC	WELL 1			WELL 4			WELL 7			WELL 10		
		Obs.	Comp.	Error	Obs.	Comp.	Error	Obs.	Comp.	Error	Obs.	Comp.	Error
CALIBRATION	Mean	9.30	9.18	0.13	6.31	6.33	-0.02	-0.76	-0.81	0.37	-1.51	-1.51	0.0
	Variance	15.24	14.74	0.04	7.36	6.64	0.07	15.06	17.30	0.14	14.42	16.59	0.20
	Mean Sq.	101.2	98.4	0.05	46.8	46.4	0.06	15.0	17.27	0.13	16.12	18.21	0.19
PREDICTION	Mean	17.17	17.54	-0.37	19.63	18.72	0.91	13.68	8.21	5.47	13.63	7.19	6.44
	Variance	9.77	10.45	0.05	33.63	29.18	0.24	26.13	13.39	6.28	31.74	13.49	8.70
	Mean Sq.	304.4	317.9	0.19	418.1	378.9	1.06	212.5	80.5	36.0	216.6	64.80	49.9

Error = Observed Drawdown - Computed Drawdown

Negative drawdowns indicate that the water levels are above the datum

drawdowns. The mean, mean square and variance of the error series are very small in comparison to those of either the observed or the computed drawdowns. It is evident from these results that large discrepancies between the assumed and the computed transmissivities cause comparatively small errors between the observed and the computed drawdowns during the calibration period. As the discrepancies between the observed and the computed drawdowns are small, the calibration can be considered to be satisfactory. However, if there are large discrepancies, the calibration trials should be repeated by using refined estimates of storage coefficients until there is close agreement between the observed and the computed drawdowns.

The estimated storage coefficients (Table 3.16) and the average transmissivities (Table 3.17) computed from calibration are used to predict drawdowns for the observations 26 through 60.

Typical values of β - coefficients and β_R - coefficients computed during the prediction period are shown in Figs. 3.31 and 3.32 respectively. These coefficients are convolved with the pumping rates and river stages during the prediction period for calculating the predicted drawdowns at different wells. These predicted drawdowns are plotted in Fig. 3.30 along with the respective observed values. The predicted drawdowns of wells 1-6, 8 and 9 are close to the observed values. The discrepancies between the observed and the predicted drawdowns of wells 7 and 10 are slightly large. However, the predicted drawdowns from these two wells follow the general trend as their observed counterparts. A comparison between the statistics of the observed and the computed drawdowns, and of the error series corresponding to the prediction period for wells 1, 4, 7 and 10 are shown in Table 3.18. These results show that the mean, the variance and the mean square values of the observed and the predicted drawdowns from wells 1 and 4 are very

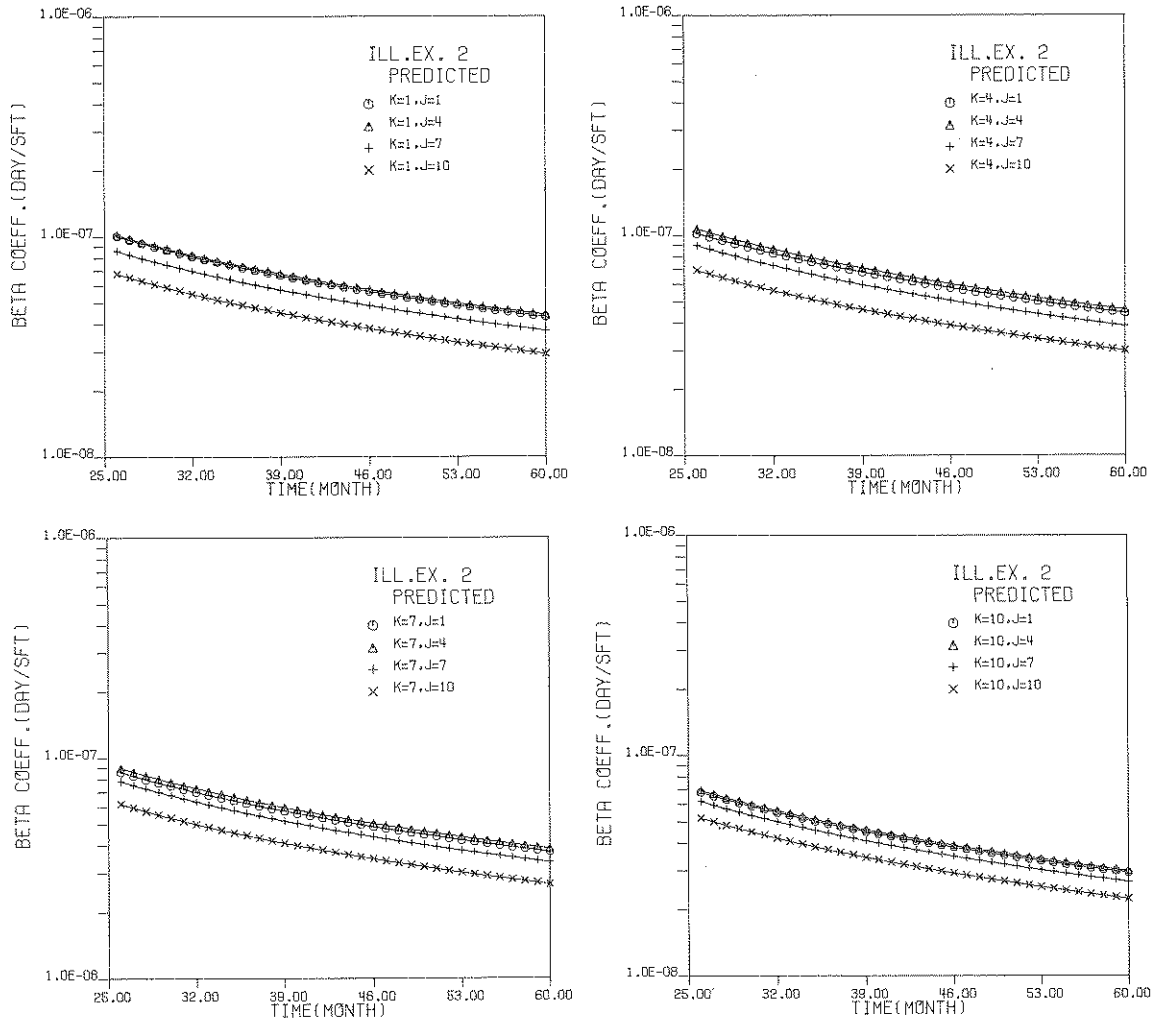


FIGURE 3.31 TYPICAL BETA COEFFICIENTS COMPUTED FROM PREDICTION
(I.E. NO. 2)

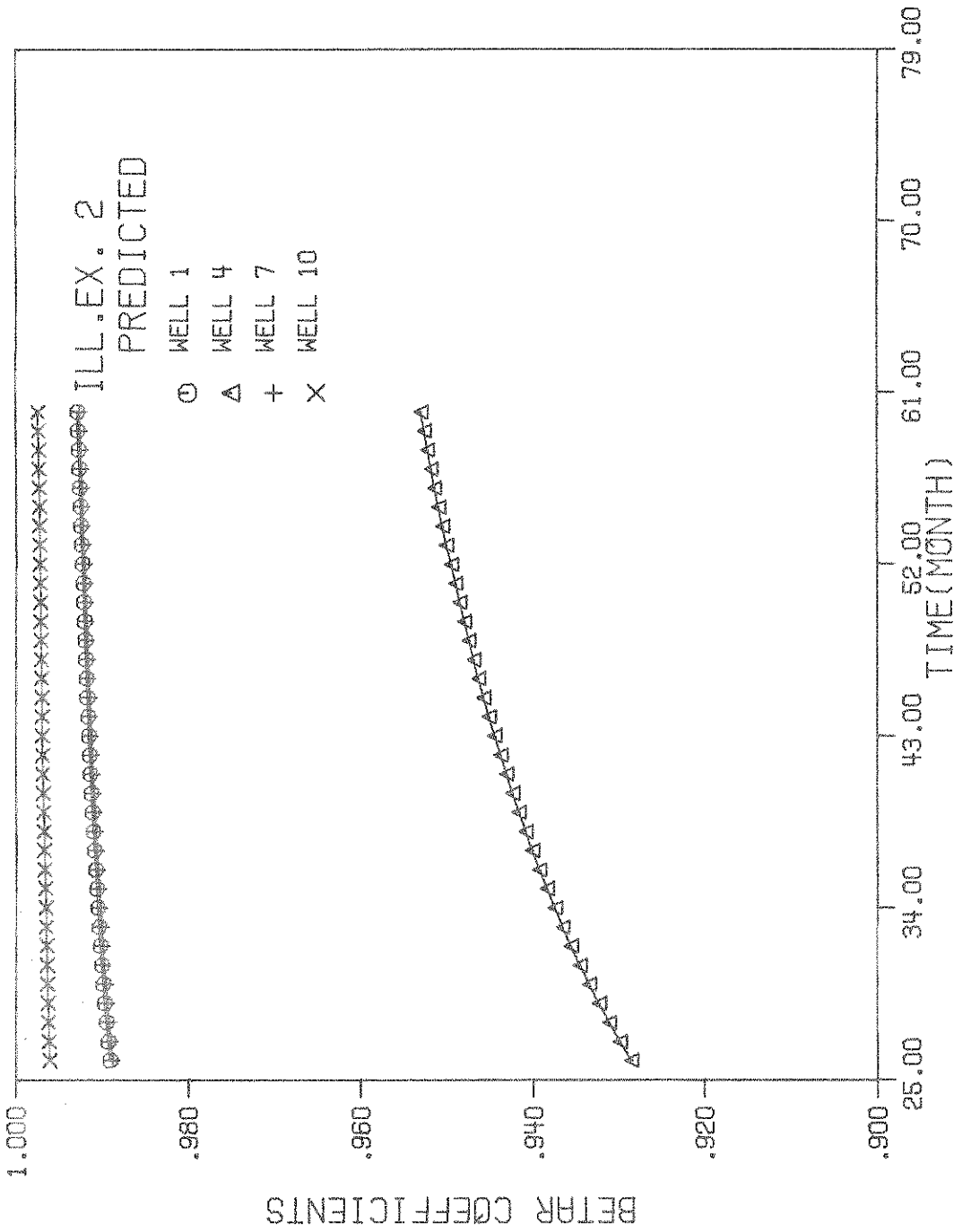


FIGURE 3.32 TYPICAL β_R -COEFFICIENTS COMPUTED FROM PREDICTION (I.E. NO. 2)

close. The statistics of the predicted drawdowns from the other wells except those of wells 7 and 10 are also close to the statistics of the respective observed drawdowns. However, there are large discrepancies between the statistics of the observed and the predicted drawdowns of wells 7 and 10 as can be seen from Table 3.18. These large discrepancies can be attributed to the errors between the assumed and the estimated storage coefficients (Table 3.16) and those between the assumed and the computed average transmissivity values (Table 3.17). For example, in zones III and IV, the error between the assumed and the computed aquifer properties (T and S values) are as high as 70 or 90 percent. It is obvious that these errors are causing large discrepancies between the observed and the predicted drawdowns of well 10. However, it is interesting to note that these large discrepancies in the aquifer properties in zones III and IV are not affecting the predicted drawdowns of wells such as 1, 2, 3 and 5 which are located away from well 10. Consequently, it can be concluded that the prediction performance of the present approach is satisfactory and this procedure can be used successfully for analysing regional aquifer flow problems.

CHAPTER 4
CAUSALITY AND THE CONSTRUCTION OF
STOCHASTIC MODELS FOR GROUNDWATER LEVELS

Groundwater levels are affected by hydrologic processes such as precipitation, evapotranspiration and river stage. Therefore, these variables are necessary as inputs in formulating models for the evaluation of groundwater resources. A preliminary investigation of the nature of the relationship between groundwater levels and these causal variables will be of considerable help in introducing them appropriately into groundwater models. Usually these causal relationships are investigated by examining time series plots, by gross water budget analysis or by cross correlation studies. However, these methods may not yield reliable information under certain circumstances such as when water levels are at a great depth below the ground surface. In this chapter, some statistical methods are used to investigate these causal relationships. Stochastic models are also developed for the prediction of groundwater levels using past groundwater levels, precipitation and river stage data.

4.1 The Concept of Causality

The concept of causality is commonly used in experimental sciences where it is possible to verify whether change in one variable is the cause for change in another. This is usually investigated by varying one of the variables of the experimental process while keeping the others at a constant value and observing the changes in the process. However, in dealing with the techniques of model construction based on hydrologic variables that are the end products of complex atmospheric processes, this experimental procedure cannot be adopted. Therefore, the pattern of influence among the different hydrologic processes cannot be completely explained by the conventional concept of causality. However, a definition of causality which is weaker than that employed in the experimental sciences can be introduced to investigate the causal relationship among the different hydrologic variables. One such definition has been given by Kashyap and Rao (1976) and is presented below.

" y_2 will be said to be causal for y_1 (and denoted by $y_2 \rightarrow y_1$) if the accuracy of the forecast of $y_1(t)$ obtained by using the history $y_1(j)$, $j < t$, and $y_2(j)$, $j < t$, is greater than that obtained using only the past history of y_1 ."

The above definition can be formalized as explained (Granger, 1963) below.

A variable y_2 is called causal for a variable y_1 and denoted by the relation $y_2 \rightarrow y_1$ if the following inequality is satisfied:

$$\text{cov}[y_1(t)|y_1(t-j), y_2(t-j), j > 1] < \text{cov}[y_1(t)|y_1(y-j), j > 1] \quad (4.1)$$

The implication of the above explanation and the inequality 4.1 for modeling is given by the following theorem (Kashyap and Rao, 1976). Theorem: " $y_2 \rightarrow y_1$ ~~iff~~ the coefficient $a_{1,2}(D)$ in the minimum forecast

error equation for $y_1(t)$ in a family of models involving at most two variables y_1 and y_2 is nonzero."

A general form of the minimum forecast error equation can be expressed as,

$$y_1(t) = \sum \alpha_j y_1(k-j) + \sum \beta_k y_2(k-k) \quad (4.2)$$

where, α_j and β_k correspond to the coefficients $a_{1,2}(D)$, and j and k are the lags at which $y_1(\cdot)$ and $y_2(\cdot)$ are significant.

Thus, when there are only two variables say $y_1(t)$ and $y_2(t)$, it is relatively easy to check for causality. The variable $y_1(t)$ is first modeled by using only its past values. Next we model it using both its past values and the past values of $y_2(t)$. If the coefficients of the $y_2(\cdot)$ terms in the second model are statistically significant, we deduce $y_2 \rightarrow y_1$ in the sense of Granger (1963). However, the procedure for checking the causality of more than two variables will be more complex. Therefore, we will deal with only pairs of variables in the present study.

4.1.1 Tests for Causality with Two Variables

Let y_1 and y_2 be the two variables of a complex process. It is required to forecast y_1 and hence to test if $y_2 \rightarrow y_1$. This could be accomplished in several ways. A possible approach is to fit two different autoregressive models for $y_1(t)$, one of the models having the past values of y_1 only and the other model having the past values of both y_1 and y_2 . The residual variances of these two models are compared by using regression theory, and tested to examine if the addition of the $y_2(\cdot)$ terms in the second model significantly affects the residual variance. This method is not general enough for the following reasons. (1) The autoregressive model in the observed variables may not always be the most appropriate model. A log transformed model or an integrated autoregressive (IAR) model could be more appropriate. (2) When the $y_2(\cdot)$ terms are added in the second model, the terms such as $y_2(t-1)$ or $\ln[y_2(t-1)]$ can be considered without any definite rule. Results based on a model with incorrect structure are not valid in general. (3) The regression theory and the associated statistics are valid only if independent and identically distributed (IID) observations are used for both regressed and regressor variables. Therefore, one should work with the whitened series derived from y_1 and y_2 processes.

Based on the above argument, let us consider the validated univariate models for both y_1 and y_2 as shown in Eqs. 4.3.

$$y_1(t) = (\theta_1)^T \underline{y}_1(t-1) + w_1(t) \quad (4.3a)$$

$$y_2(t) = (\theta_2)^T \underline{y}_2(t-1) + w_2(t) \quad (4.3b)$$

where, $(\theta_i)^T = [\alpha_{i,1}, \alpha_{i,2}, \dots]$

$\underline{y}_i^T(t-1) = [y_i(t-1), y_i(t-2), \dots]^T$

T = symbolical representation for transpose

$i = 1, 2.$

In Eqs. 4.3, $w_1(\cdot)$ and $w_2(\cdot)$ are the two "Whitened processes" to be used for testing the causality. It is necessary that the models shown above (Eqs. 4.3) be formulated by using the data observed during the concurrent periods only.

If $y_2 \rightarrow y_1$, then there must exist at least a j and $\alpha_j \neq 0$ so as to satisfy

$$w_1(t) = \alpha_j w_2(t-j) + n(t) \quad (4.4)$$

where, $n(\cdot)$ is an IID sequence with zero mean. If the coefficients α_j in Eq. 4.4 can be shown to be significantly different from zero for any j , then we can say that $y_2 \rightarrow y_1$. This can be done by using any of the tests given below (Kashyap and Rao, 1976).

Test 1: Based on Hypothesis Testing (Regression Theory)

Suppose there are N observation pairs $[w_1(t), w_2(t), t = 1, 2, \dots, N]$. Let r_j represent the cross-correlations between $w_1(\cdot)$ and $w_2(\cdot)$ at any lag j . The relationship for r_j is given in Eq. 4.5.

$$r_j = \frac{\left[\frac{1}{N-j} \sum_{t=j+1}^N w_1(t) w_2(t-j) \right]}{\left[\frac{1}{N-j} \sum_{t=j+1}^N w_1^2(t) \right] \left[\frac{1}{N-j} \sum_{t=j+1}^N w_2^2(t) \right]} \quad (4.5)$$

If $\alpha_j = 0$, then

$$(N-j-1) \left[\frac{r_j^2}{1-r_j^2} \right] \sim F_{\epsilon}(1, \nu) \quad (4.6)$$

where, $F_{\epsilon}(1, \nu)$ is the critical statistic of the F-distribution at ν degrees of freedom and ϵ level of significance. If we fix a suitable probability of Type I error such as $(1-\epsilon)$, where $\epsilon = 0.05$ or 0.01 , then we get the corresponding threshold d from the table of F-distributions. The decision rule can be written in terms of r_j^2 as given below:

$$\left. \begin{array}{l} r_j^2 \leq d/(N-j-1+d) \text{ accept hypothesis } (\alpha_j=0) \\ r_j^2 > d/(N-j-1+d) \text{ reject hypothesis } (\alpha_j \neq 0) \end{array} \right\} \quad (4.7)$$

Test 2: Based on the Likelihood Approach

The modified likelihood values J_i , $i = 1, 2$, for class 1 ($\alpha_j=0$) and class 2 ($\alpha_j \neq 0$) are computed as shown in Eqs. 4.8.

$$J_1 = -\frac{N}{2} \ln \left[\frac{1}{N} \sum_{t=1}^N w_1^2(t) \right] \quad (4.8)$$

$$J_2 = -\frac{N}{2} \ln \left[\frac{1}{N} \sum_{t=1}^N w_1^2(t) (1-r_j^2) \right] - 1$$

The hypothesis that $\alpha_j=0$ is accepted if $J_1 > J_2$. The alternate is accepted if $J_2 > J_1$. Further details on this test may be found in Kashyap and Rao (1976).

4.2 Construction of Stochastic Models

In the present study, the stochastic difference equation models of the hydrologic or the meteorologic processes such as precipitation, temperature, streamflow and stream stages are considered. The general

form of the stochastic difference equation which can be used to model the above processes is discussed below.

Let $Y(k)$ represent the monthly value of the variate Y in the k^{th} instant, $k = 1, 2, 3, \dots, N$. Let the variate Y be significantly correlated with the other variates, say X and Z . In a physical sense, we may consider that the variate Y represents the mean monthly stages in a river, whereas the variates X and Z stand respectively for the mean rainfall and the mean monthly groundwater levels in the vicinity of the stream gaging station. A general representation for $Y(k)$ is a stochastic difference equation which relates $Y(k)$ to its past values, $Y(k-1)$, $Y(k-2)$, ... and the past values of the variates X and Z as shown in Eq. 4.9.

$$Y(k) = \alpha_0 + \sum_{j=1}^{n_0} \alpha_j Y(k-j) + \sum_{j_1=1}^{n_1} \alpha_{j_1} X(k-j_1) + \sum_{j_2=1}^{n_2} \alpha_{j_2} Z(k-j_2) + \zeta(k) \quad (4.9)$$

In Eq. 4.9, $\zeta(k)$ is the random input and may be represented as shown in Eq. 4.10 if it is correlated,

$$\zeta(k) = \sum_{j_3=1}^{n_3} \alpha_{j_3} W(k-j_3) + W(k) \quad (4.10)$$

where, $n = n_0 + n_1 + n_2 + n_3 + 1 =$ the total number of parameters, and $W(\cdot) =$ independently and identically distributed random variables with zero mean.

The integers n_i , $i=0,1,\dots$, and the coefficients α_j in Eq. 4.9 are unknown and may be slowly varying functions of time k . The random input $\zeta(k)$ may be attributed to that part of the variate Y which is not accounted for by the variates X , Y or Z . Once again, in a physical sense, $\zeta(k)$ could stand for the unexplained components of the physical process such as evaporation and induced infiltration, which also influence the stages in a river to some extent. Since the random input $\zeta(k)$ may be subsequently correlated, at least to a lesser degree, with $Y(k)$, it is customary to represent it as in Eq. 4.10. In Eq. 4.10 the sequence $W(\cdot)$ consists of independently and identically distributed random variables with zero mean. Usually the probability distribution of $W(\cdot)$ is not normal. The coefficients α_j and the integers n_i , $i = 0, 1, \dots$ have to be estimated with the aid of the observed values of the variates, Y , X and Z .

If the variate Y exhibits significant periodicities, then it is customary to include the sinusoidal trend functions in the stochastic difference equation 4.9 as

$$Y(k) = \alpha_0 + \sum_{j=1}^{n_0} \alpha_j Y(k-j) + \sum_{j_1=1}^{n_1} \alpha_{j_1} X(k-j_1) + \sum_{j_2=1}^{n_2} \alpha_{j_2} Z(k-j_2) + \sum_{j_3=1}^{n_3} \alpha_{j_3} W(k-j_3) + \sum_{j_4=1}^{n_4} \left[\beta_{j_4} \sin\left(\frac{2\pi j_4 k}{12}\right) + \gamma_{j_4} \cos\left(\frac{2\pi j_4 k}{12}\right) \right] + W(k). \quad (4.11)$$

The relationship shown in Eq. 4.11 is a general stochastic difference equation that can be used to represent most of the hydrologic and meteorologic processes. The commonly used autoregressive (AR), moving

average (MA), and the autoregressive moving average (ARMA) models are all special forms of the general stochastic difference equation, 4.11.

An autoregressive model for $y(k)$ which is related to three of its past values is written as

$$y(k) = \alpha_0 + \alpha_1 y(k-1) + \alpha_2 y(k-2) + \alpha_3 y(k-3) + w(k) \quad (4.12)$$

where, $w(k)$ is the ideal one step-ahead prediction error encountered in predicting $y(k)$. The $w(k)$ series is called the "whitened process" derived from y after the model is validated as explained in Sec. 4.2.2.

4.2.1 Parameter Estimation

The unknown coefficients α_j , β_j and γ_j , $j = 1, 2, \dots$ and the integers n_i , $i = 0, 1, 2, \dots$ (Eq. 4.11) can be estimated from the given observations $y(k)$, $k = 1, 2, \dots, N$ using a suitable criterion of performance. In the present study the least square criterion is selected. The method used for parameter estimation is discussed in Kashyap and Rao (1973, 1976).

For modeling a given process, a number of models are analyzed with different values of the integers n_i , $i = 0, 1, 2, \dots$ in the general stochastic difference equation, 4.11. Appropriate sinusoidal trend functions are included on the basis of the results obtained from the autocovariance and the power spectral analysis of the observed values $y(k)$, $k = 1, 2, 3, \dots, N$. The coefficients α_j , β_j , and γ_j , $j = 1, 2, \dots$ for each model are estimated by using the real time recursive prediction algorithm discussed by Kashyap and Rao (1973, 1976). The residuals and the estimated parameters from the different models are then tested by using several validation tests. The general criteria for validating the models is explained next.

4.2.2 Validation of Models and Selection Criteria

A model can be considered as validated if it adequately represents the purpose such as forecasting, for which it is designed. However, the validity of a model can be specified only in relative terms and in comparison with other models considered for the process. We can envision two different approaches to the problem of validation. The first of these has analytical basis behind it whereas the second approach is based on simulation results.

In the first approach, the validity of the assumptions underlying the model is tested by using the usual theory of hypothesis testing. In many cases, the only important assumption is that the disturbance sequence $W(.)$ be of zero mean and uncorrelated sequence. The estimates of the disturbances or equivalently the residuals are obtained by using the given model and the available observations. The assumption that the residuals are uncorrelated is checked after reformulating the problem as a choice between two hypotheses H_0 and H_1 . The hypothesis H_0 , usually called the null hypothesis, declares the residuals to be independent and of zero mean. The hypothesis H_1 , usually called the alternate, declares the successive residuals to be dependent and obey an autoregressive process. If the hypothesis H_0 is accepted at a suitable prespecified

Level of significance, then the corresponding model is accepted. On the other hand, if H_1 is accepted, the model is considered to be unsatisfactory. The residuals are also analyzed to discover the nature of the serial dependence among them. If there is a sinusoidal trend component in the residuals, then this information can be used to modify the model, by including additional sinusoidal trend functions. The details of the specific methods of hypothesis testing used in the present study are explained in Sec. 4.3.4.

In the second approach used to validate a model, we can compare the characteristics of the model output, such as correlograms, spectral densities and extreme value characteristics, with the corresponding characteristics of the observed data. The various statistical characteristics of the model output can be obtained either by analysis or by simulation. The model is accepted if the discrepancy between the characteristics of the simulated and the observed data is within one or two standard deviations of the corresponding characteristics.

For a given process, there may be more than one model that satisfies all the validation tests. Under such circumstances some criteria are needed for the model choice. In the present study, the final models were selected on the basis of the following criteria. (i) The number of parameters in the model should be as few as possible, but at the same time the residuals and the estimated parameters should satisfy all the validation tests. (ii) If $\hat{\sigma}_w^2 = \frac{1}{N} \sum_{k=1}^N (w(k))^2$ is the residual variance and $\hat{\sigma}_s^2 = \frac{1}{N} \sum_{k=1}^N (y(k) - \bar{y})^2$ is the variance of the signal, then the ratio $\hat{\sigma}_w^2 / \hat{\sigma}_s^2$ should be as small as possible.

4.3 Investigation of the Causal Relationship between Groundwater Levels, Precipitation and River Stages

In this section, the causal relationships between precipitation, river stages and groundwater levels are investigated by using the tests for causality explained in Sec. 4.1.1. Only pairs of variables, i.e. either precipitation and groundwater levels or river stages and groundwater levels are included at a time for checking the causality. The general procedure explained in Sec. 4.2 for the construction of stochastic models is used for the development of models for rainfall, river stages and groundwater level data individually. These models are validated and the residuals (whitened process) are used to check for the causality as explained in Sec. 4.1.1. The final models for the groundwater level processes are then formulated using the individual stochastic models and the causal relationship either with precipitation or with river stage data.

4.3.1 Data Used in the Study

Monthly values of rainfall, river stages and groundwater levels observed at Lafayette and West Lafayette, Indiana were used in the present study.

Rainfall data are recorded at several gaging stations in Lafayette and West Lafayette. In the present study, the rainfall data measured only at two gaging stations are considered for analysis. These stations are, (i) the Purdue Agronomy Farm, West Lafayette and (ii) the O'Neal Farm, Lafayette. The location of

these two gaging stations are shown in Fig. 4.1. The rainfall data from the Agronomy Farm are available since 1954 and that at the O'Neall Farm dates back to 1918. The monthly rainfall data from these stations were obtained from the publication, "Climatological Data," of the U.S. Department of Commerce.

The river stage data used in this study were those observed at the Wabash River which separates the twin cities, Lafayette and West Lafayette as shown in Fig. 4.1. The stage gage is located in Lafayette (Fig. 4.1) with the datum of the gage at 504.14 ft. above mean sea level. The mean monthly stages of the Wabash River were collected from the "Daily River Stages" (Weather Bureau, U.S. Dept. of Commerce) and the data dates back to 1914.

Several observation wells are used in Lafayette and West Lafayette by the U.S. Geological Survey to measure groundwater levels. Although these wells are never used for pumping, the static water levels measured from these wells are significantly affected by pumping in neighboring wells. The water levels from these wells are measured with reference to the land surface datum at irregular time intervals and are published in Water-Supply Papers (U.S. Geological Survey). These water levels were averaged over a month to obtain monthly values. In this study, the monthly average values of groundwater levels measured only at three observation wells are considered for analysis. The location of these wells are shown in Fig. 4.1 and are designated Tc-4, Tc-7 and Tc-9. Observation well Tc-4 is located in Lafayette and is very close to the Wabash River. Wells Tc-7 and Tc-9 are respectively situated in West Lafayette and Lafayette and both are away from the Wabash River. Details of these observation wells, the values of the land surface datum and the period of available data are given in Table 4.1.

As mentioned earlier (Sec. 4.2) only concurrent data are used to investigate the causality between any two variables. Due to this, all the available data could not be used in the analysis. Details of the specific length of data used for modeling different hydrologic processes are given in Table 4.1 along with the other particulars. Plots of these data for the periods shown in col. 7 of Table 4.1 are presented in Fig. 4.2.

4.3.2 Statistical Characteristics of the Data

Some of the elementary statistics of the hydrologic data used in this analysis are presented in Table 4.2. The mean of the precipitation values observed at the Purdue Agronomy Farm is slightly lower than that of the precipitation from the O'Neall Farm. However, the variances of the data from both these stations are approximately the same which indicates that there is not much variability in monthly rainfall between West Lafayette and Lafayette. The monthly Wabash River stages show large fluctuations as the variance of this series is very high in comparison to its mean. The water levels in well Tc-4 are very near the ground surface as compared to those of well Tc-7 or well Tc-9. At well Tc-4 the average depth of water from the land surface is 16.61 ft. as compared to 73.96 ft. at well Tc-9 and 168.06 ft. at well Tc-7. The variance of the water levels measured at well Tc-4 is approximately six times as great as that of the water levels

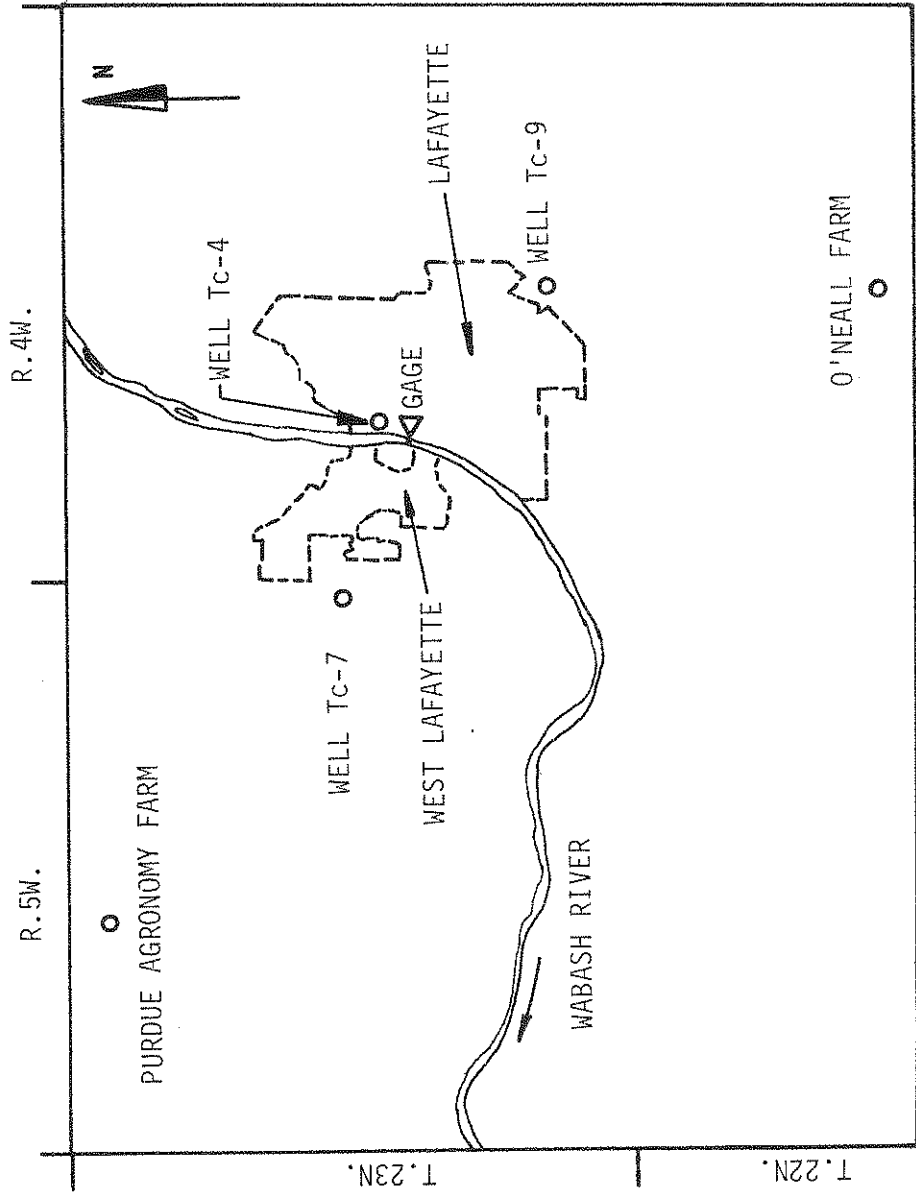


FIGURE 4.1 LOCATION OF STATIONS

TABLE 4.1

DETAILS OF HYDROLOGIC DATA

DATA	Measured at	Location Details	Symbol Used in the Text	Datum (Ft. above M.S.L.)	Duration of Data Used in the study		Source of Data and Remarks
					Available	study	
1	2	3	4	5	6	7	8
Rainfall	Purdue Ag. Farm W. Lafayette, IN	Lat: 40°28'N. Long: 87°00'W.	AGF		1954-present	1954-'73	Climatological Data U.S. Dept. of Commerce
Rainfall	O'Neal Farm Lafayette, IN	Lat: 40°21'N.	ONF		1918-present	1947-'62	Climatological Data U.S. Dept. of Commerce
River Stages	Wabash River, Lafayette, IN	Gage at Brown St. Levee, Laf.	WAB	504.14	1914-present	1954-'73	Daily River Stages U.S. Weather Bureau stage measured above datum.
Groundwater Levels	Well Tc-4 Lafayette Water Works, Lafayette Unused drilled well, dia. 12", depth 127 ft.	T23N, R4W, Sec. 20 NE¼ SW¼ NE¼ East bank of Wabash River near Canal St. Well 7 at City Well Field	H1	520.87	1944-present	1954-'73	U.S.G.S. Water Supply Papers "Groundwater Levels in Northeastern States". Water levels reported as depths below land surface datum.
Groundwater Levels	Well Tc-7 Purdue Univ. W. Lafayette Abandoned drilled well, dia. 8", depth 206.5 ft.	T23N, R5W, Sec. 13 SE¼ SE¼ Research Housing pumphouse.	H2	679.00	1945-present	1954-'73	
Groundwater Levels	Well Tc-9 Aluminum Co. of America, Laf. Drilled unused well, dia. 16", depth 160 ft.	T23N, R4W, Sec. 34 NW¼ NW¼ Earl Ave & U.S. Highway 52	H3	662.00	1947-1962	1947-'62	

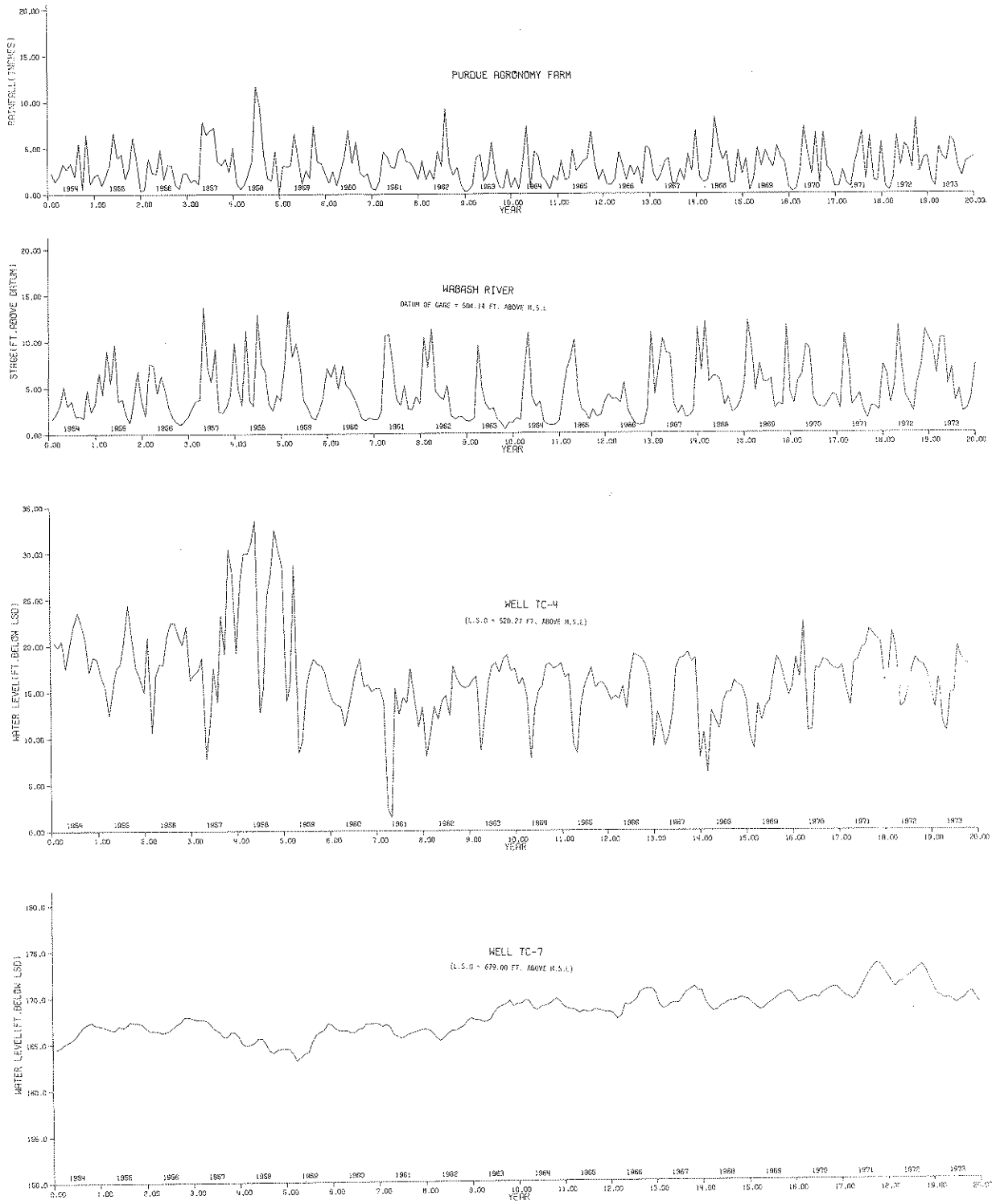


FIGURE 4.2 HYDROLOGIC DATA

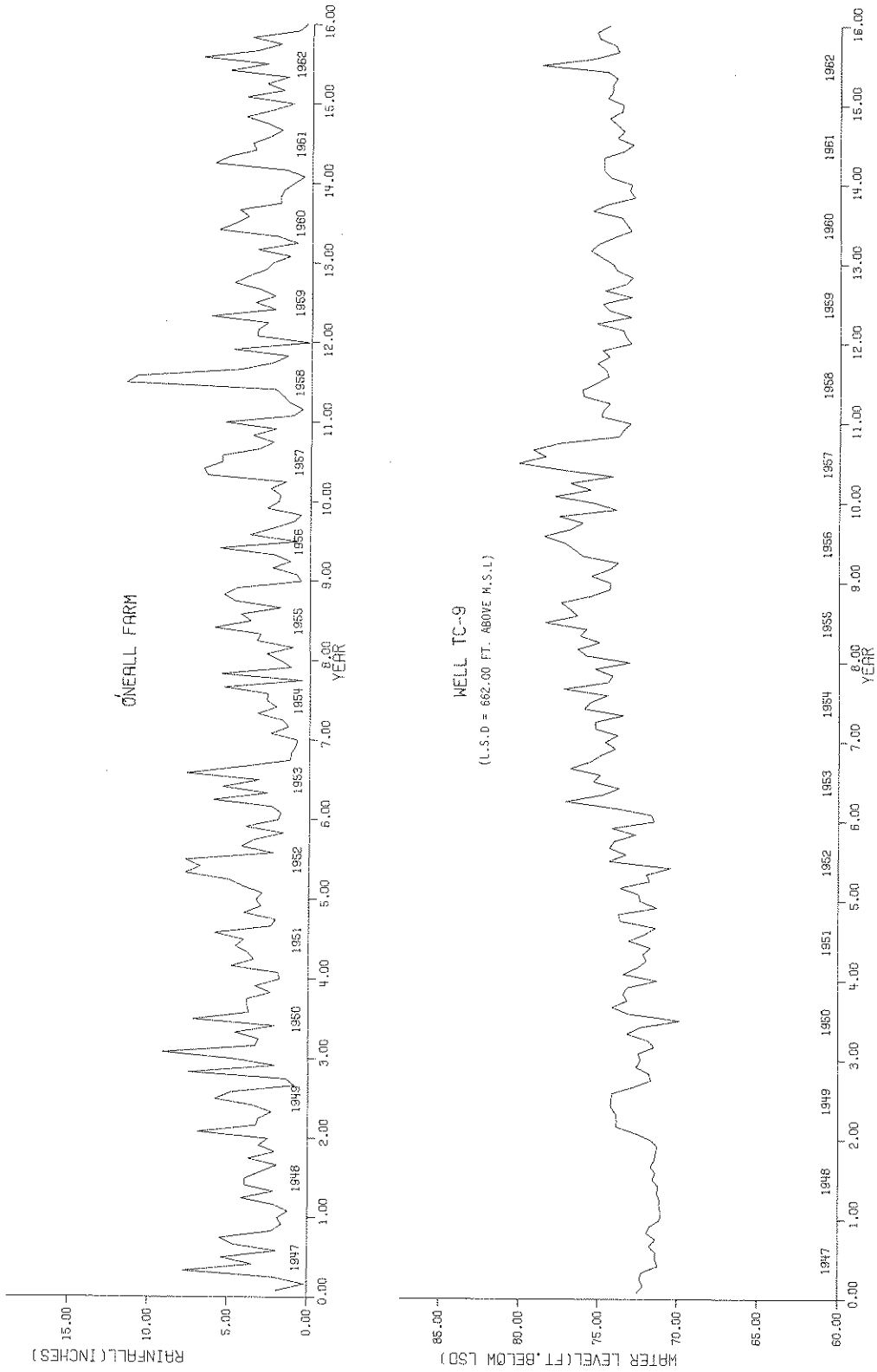


FIGURE 4.2 HYDROLOGIC DATA (contd.)

TABLE 4.2
STATISTICS OF DATA USED IN STOCHASTIC MODELS

STATISTIC	PRECIPITATION (IN)		WABASH RIVER STAGES (Ft. above datum)	GROUNDWATER LEVELS (Ft. below Land Surface Datum)		
	PURDUE AG. FARM	O'NEALL FARM		Well Tc-4	Well Tc-7	Well Tc-9
Period of Data	1954-'73	1947-'62	1954-'73	1954-'73	1954-'73	1947-'62
Mean	3.04	3.28	4.64	16.61	168.06	73.96
Variance	4.04	3.88	9.21	22.26	4.28	3.46
Skew. Coeff.	1.05	1.16	0.98	0.64	0.13	0.51
Coeff. of Kurtosis	4.23	4.87	3.04	5.20	2.58	3.18
Minimum	0.08	0.12	0.40	1.40	168.23	69.85
Maximum	11.70	11.60	13.80	33.60	173.25	80.08
Median	2.72	2.91	3.60	16.50	168.23	73.90

observed in well Tc-7 or Tc-9. This shows the general effect of the Wabash River stage on increasing the fluctuations in well Tc-4. The Wabash River stages and the rainfall data from the Agronomy Farm and the O'Neall Farm are highly skewed, whereas the water levels in wells Tc-4, Tc-7 and Tc-9 are not as highly skewed as indicated by the skewness coefficients given in Table 4.2.

The means and standard deviations of the observed data in individual months are plotted in Fig. 4.3. In these plots, the first month is January and the last month is December. The monthly means of the precipitation data, the Wabash River stages and the water levels in well Tc-4 can be seen to change over the year. Consequently, a seasonal pattern exists in the above processes. However, the monthly means of water level data from wells Tc-7 and Tc-9 are fairly constant over the year and do not exhibit any pronounced seasonality. The monthly standard deviations of the Wabash River stages and of the water levels in well Tc-4, Tc-7 and Tc-9 exhibit pronounced seasonal patterns. The seasonal patterns of the monthly standard deviations of the precipitation data are not clearly perceptible.

The histograms of the precipitation data, the river stages and of the water levels in the different wells are shown in Fig. 4.4. These plots indicate that the histograms of precipitation data from the Purdue Agronomy Farm and the O'Neall Farm are approximately the same and both are highly skewed. The histogram of the Wabash River stages is also highly skewed whereas those of water levels from Wells Tc-4, Tc-7 and Tc-9 are approximately symmetrical. There is a predominance of months when the precipitation is less than about 4 inches. Similarly, the frequencies of Wabash River stages being less than about 5 ft. are high. The histogram of well Tc-4 shows a predominance of small fluctuations in water levels. The water levels in wells Tc-7 and Tc-9 do not fluctuate as frequently as those of well Tc-4.

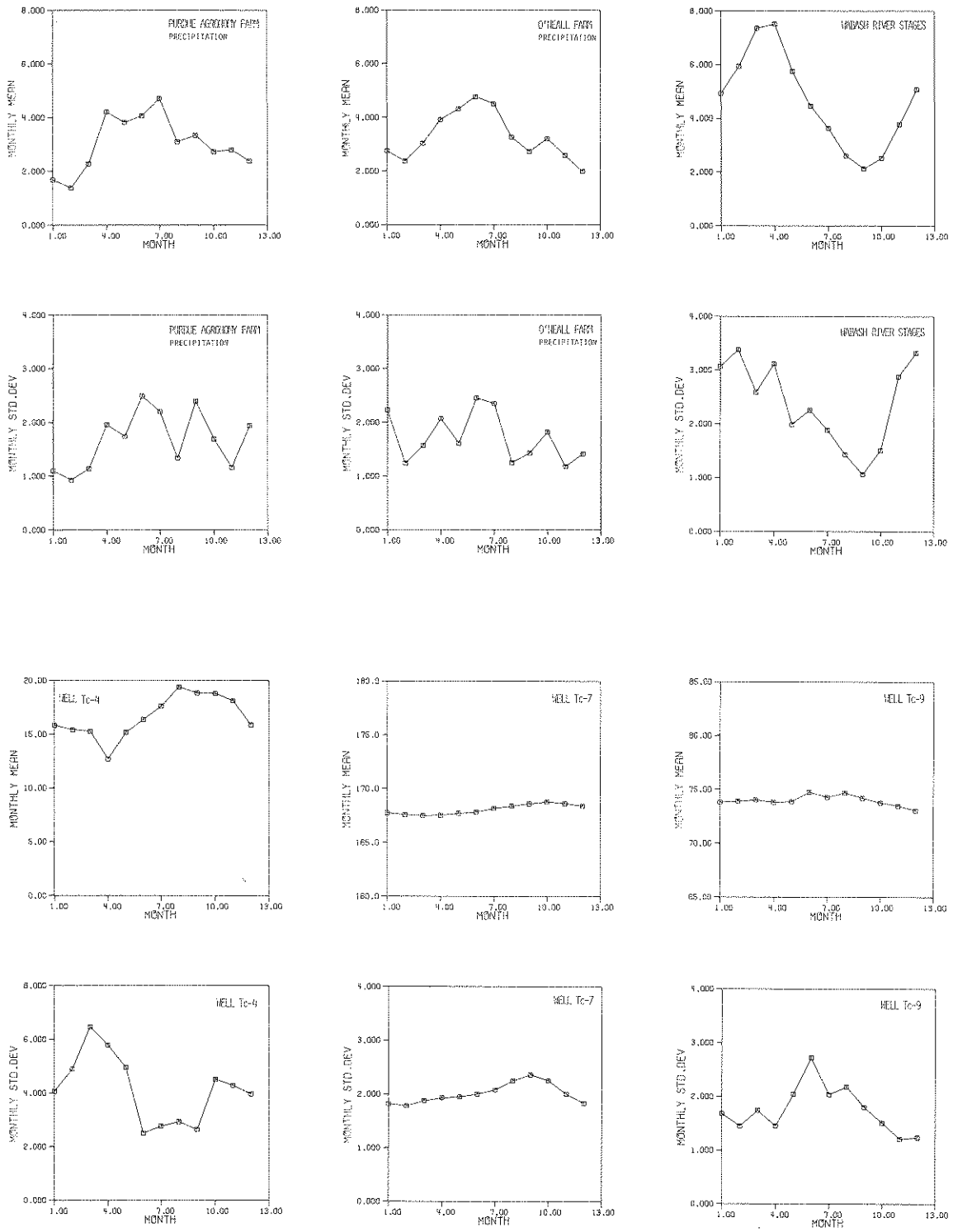


FIGURE 4.3 MONTHLY MEANS AND STANDARD DEVIATIONS OF OBSERVED DATA

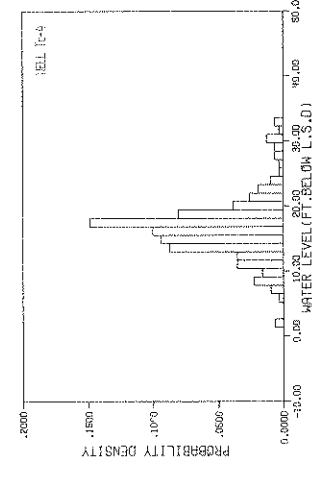
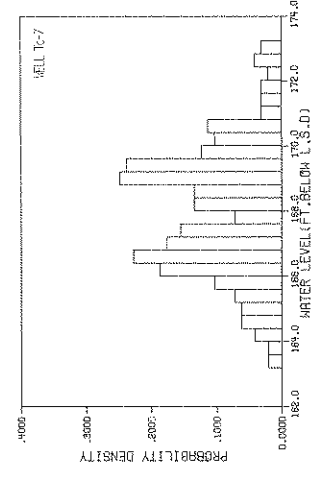
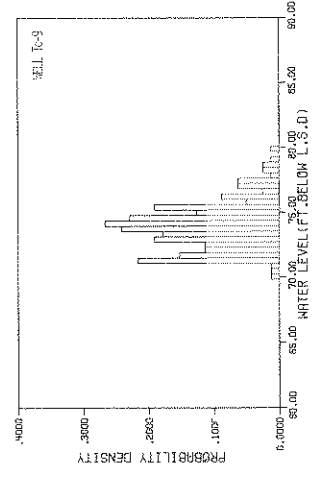
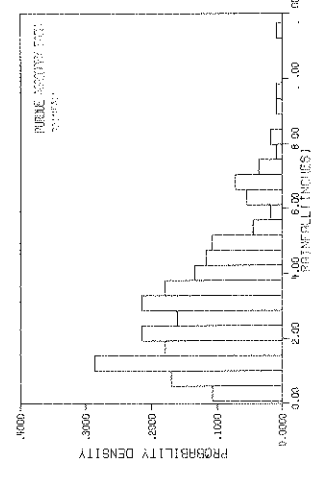
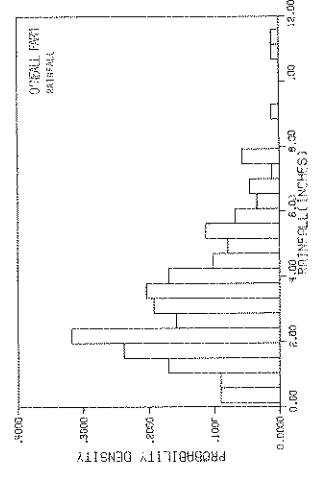
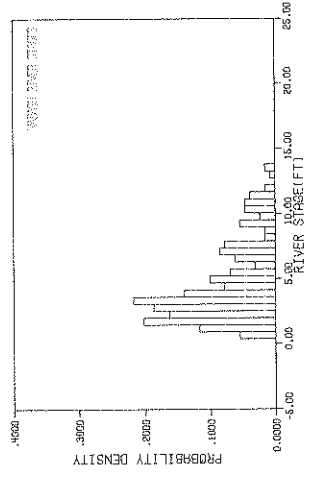


FIGURE 4.4 HISTOGRAMS OF OBSERVED DATA

The autocovariances and the power spectra of the data used in the study were also examined. The computational details of the estimation of autocovariances and power spectral densities are found in Jenkins and Watts (1968), and are also discussed by Dixon (1971). The autocovariances and power spectral estimates are normalized by dividing each of the values by the variance of the appropriate series. The resulting correlograms and power spectral densities are shown in Fig. 4.5. The correlograms of observed precipitation data from both the stations indicate the presence of an annual cycle. The prominence of the annual cycle is also apparent in the power spectral density plots of the precipitation data. The correlograms and power spectral densities of the Wabash River stages and of the water levels in well Tc-4 indicate the existence of strong annual periodicity and some concentration of power at low frequencies. The water level data observed from wells Tc-7 and Tc-9 do not show any significant annual periodicities as evident from their correlograms and power spectral density plots in Fig. 4.5. The comparatively strong annual cycle in well Tc-4 may be attributed to its proximity to the Wabash River. The correlograms of the observed water levels in wells Tc-7 and Tc-9 indicate the highly correlated nature of the respective water levels.

The above results regarding the correlograms and the power spectral densities of the observed data clearly indicate that the models fitted to the observed data must account for the annual periodicities and the low frequency effects.

The cross correlation among the time series of the groundwater levels, precipitation and the Wabash River stages are examined by computing cross covariances as explained in Jenkins and Watts (1968). The computational details of cross covariances are found in Dixon (1970) and a discussion of the hydrological applications is given in Kisiel (1969). Plots of cross correlograms of water levels in the different wells and the precipitation data are shown in Fig. 4.6. In these plots the 95% confidence limits (Box and Jenkins, 1970) are indicated as 2-standard error limits and are given by $\pm 2/\sqrt{N}$, where N is the number of months of the data used in the computation. These cross correlograms indicate that the groundwater levels in the Lafayette-West Lafayette area are significantly correlated with the precipitation series, in the sense that these cross correlation coefficients are higher than the 2-standard error limits at several lags. For example, the water levels in well Tc-7 are significantly correlated with the precipitation at the Agronomy Farm at a positive lag of 20 months and at negative lags of 9 and 21 months. However, the highest cross correlation between these water levels and precipitation is about 0.18 at a lag of about 9 months, which indicates that the present change in groundwater levels is primarily influenced by the rainfall that had occurred about nine months previously.

The cross correlograms of the groundwater levels and the Wabash River stages are plotted in Fig. 4.7. The 95% confidence limits are also shown in these plots. These cross correlograms indicate the highly periodic relationship between the different hydrologic variables considered in the study. The cross correlogram between water levels in well Tc-4 and the Wabash River Stages indicates significant positive

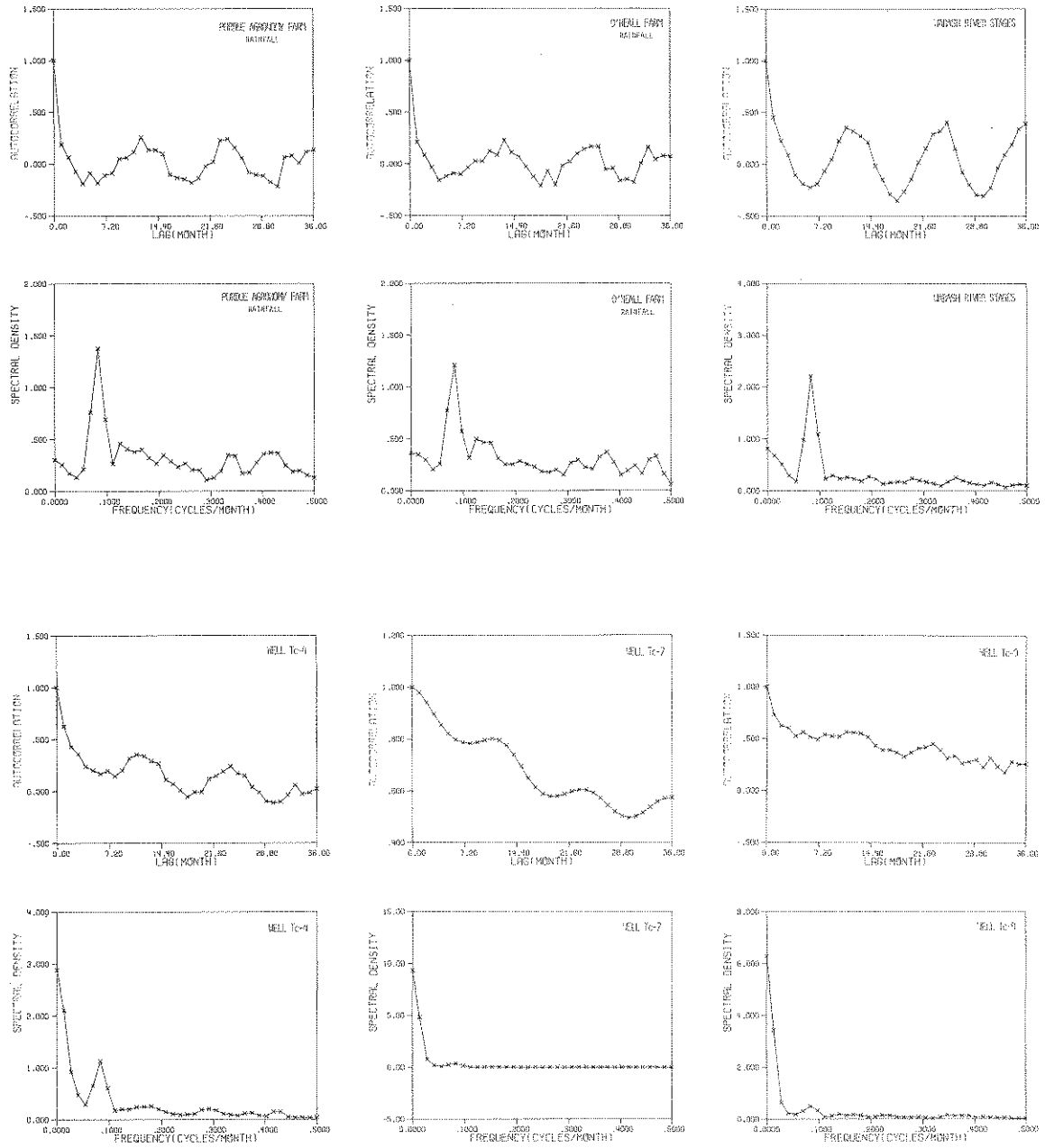


FIGURE 4.5 CORRELOGRAMS AND POWER SPECTRA OF OBSERVED DATA

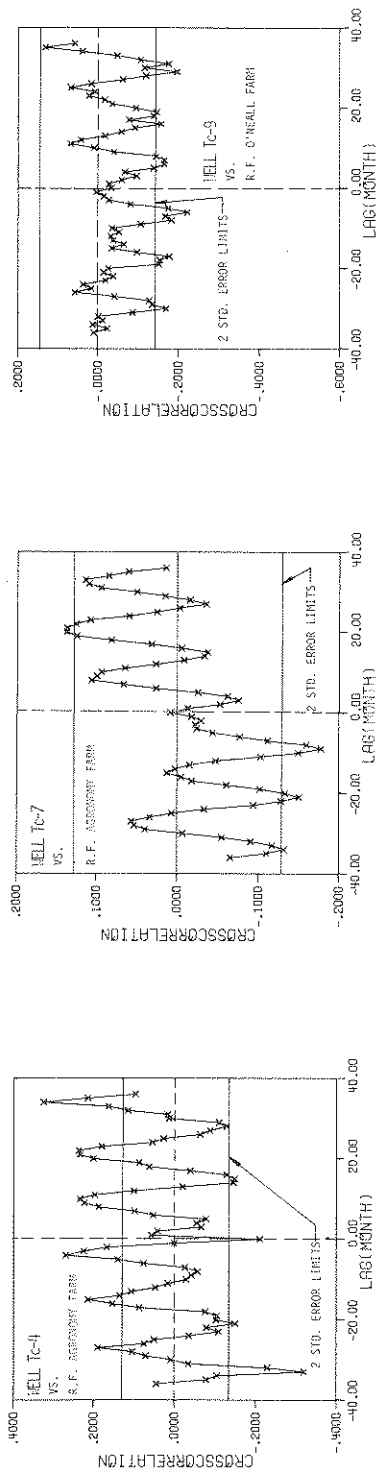


FIGURE 4.6 CROSS CORRELATIONS BETWEEN OBSERVED GROUNDWATER LEVEL AND PRECIPITATION DATA

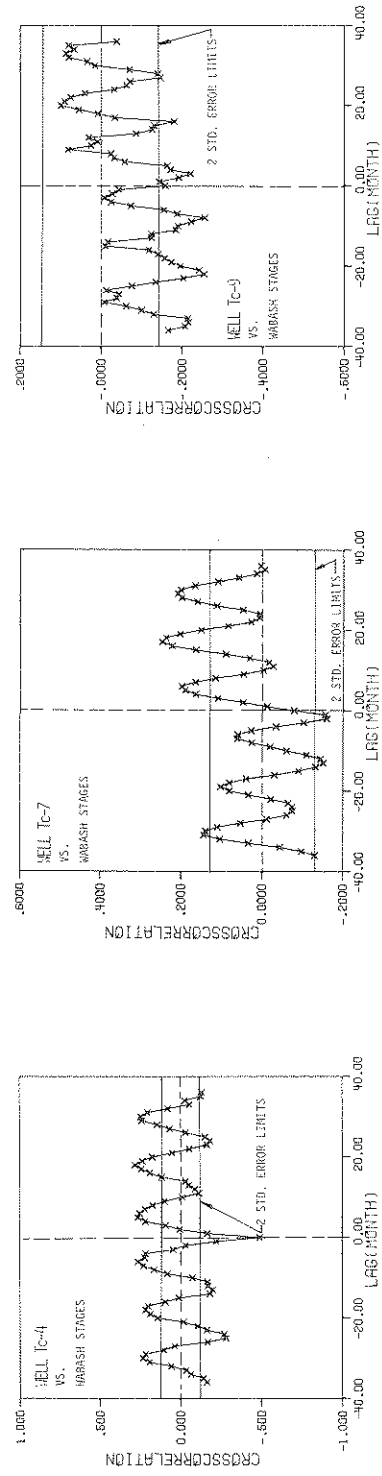


FIGURE 4.7 CROSS CORRELATIONS BETWEEN OBSERVED GROUNDWATER LEVEL AND RIVER STAGES

correlations at lags of 1, 12 and 24 months, and negative correlations at lags of 6, 18 and 30 months. However, the cross correlation at lag zero is the most predominant of all, which indicates that the well Tc-4 responds to the river stages within a few days. The cross correlograms for water levels in well Tc-7 and well Tc-9 also show significant correlations with the Wabash River stages. As these wells are located far away from the Wabash River, these cross correlograms exhibit certain lag period, which indicates that the present change in water levels at these wells is influenced by the Wabash River stages that was observed several months previously.

4.3.3 Univariate Models for Groundwater Levels, Precipitation and River Stages

In this section, univariate models of the form of relationship shown in Eq. 4.3 are fitted to groundwater levels, precipitation and river stages. For example, a univariate model for Wabash River stages is formulated by using its past values and appropriate sinusoidal trend functions representing the predominant periodicities. The general procedure explained in Sec. 4.2 is used for the construction of these stochastic models. Several types of univariate models are tried for water levels in the different wells, precipitation data from the Agronomy Farm and the O'Neal Farm and the Wabash River stages. The parameters in these models are estimated by using the least square criterion as discussed in Kashyap and Rao (1973, 1976). The residuals resulting from these models are tested for "whiteness." The best fitted univariate models for the groundwater levels, precipitation and the river stages are presented in Table 4.3. The parameter estimates and their standard error of the different models are given in Table 4.4. These standard errors are very small in comparison to their corresponding parameters. Consequently all the estimated parameters are considered significant. Models AGF and ONF for monthly precipitation are dependent on the precipitation from the preceding two months and on the sinusoidal trend functions with periodicities of 12 and 6 months. In model WAB for Wabash River stages, the effect of the annual cycle is stronger than that of the semi-annual cycle. The water levels in well Tc-4 (Model H1) at any given month are related to the water levels in the previous two months, and also to those of the seventh preceding month. The sinusoidal trend functions with periodicities of 12 and 6 months are also included in this model. In model H2 for water levels in well Tc-7, the autoregressive parameters are predominant as compared with those of the sinusoidal trend functions. It is interesting to note that the water levels in well Tc-7 are significantly related to those of the tenth preceding month. Model H3 for water levels in well Tc-9 is an autoregressive model with four terms.

4.3.4 Validation Tests on Residuals

The residuals $W_A(k)$, $W_B(k)$, $W_S(k)$, $W_X(k)$, $W_Y(k)$ and $W_Z(k)$ for the different univariate models can be obtained by using the observed data and the corresponding stochastic difference equations shown in Table 4.3. For example, the residuals, $W_Y(\cdot)$ of model H2 can be computed using the relationships shown in Eqs. 4.13,

TABLE 4.3

UNIVARIATE MODELS FITTED TO MONTHLY GROUNDWATER LEVELS,
PRECIPITATION AND RIVER STAGES

SYMBOL	DATA	STATION	MODEL
AGF	Precipitation	Purdue Agromony Farm	$y(k+1) = 3.016 + 0.024 y(k) - 0.016 y(k-1) + 0.232 \sin \omega_1 k - 1.160 \cos \omega_1 k - 0.042 \sin \omega_2 k - 0.202 \cos \omega_2 k + W_A(k)$
ONF	Precipitation	O'Neal Farm	$y(k+1) = 2.944 + 0.086 y(k) + 0.022 y(k-1) + 0.594 \sin \omega_1 k - 0.804 \cos \omega_1 k - 0.297 \sin \omega_2 k - 0.019 \cos \omega_2 k + W_B(k)$
WAB	River Stages	Wabash River at Lafayette	$y(k+1) = 3.270 + 0.253 y(k) + 0.049 y(k-1) + 1.427 \sin \omega_1 k + 1.220 \cos \omega_1 k - 0.022 \sin \omega_2 k - 0.277 \cos \omega_2 k + W_S(k)$
H1	Groundwater Levels	Well Tc-4	$y(k+1) = 5.908 + 0.497 y(k) + 0.104 y(k-1) + 0.038 y(k-7) - 0.975 \sin \omega_1 k - 1.242 \cos \omega_1 k + 0.239 \sin \omega_2 k + 0.449 \cos \omega_2 k + W_X(k)$
H2	Groundwater Levels	Well Tc-7	$y(k+1) = 2.772 + 1.310 y(k) - 0.351 y(k-1) + 0.025 y(k-10) + 0.019 \sin \omega_1 k - 0.187 \cos \omega_1 k + W_Y(k)$
H3	Groundwater Levels	Well Tc-9	$y(k+1) = 10.611 + 0.543 y(k) + 0.028 y(k-1) + 0.182 y(k-2) - 0.135 y(k-3) + 0.239 y(k-4) + W_Z(k)$

$\omega_1 = 2\pi/12$, $\omega_2 = 2\pi/6$ $W_A(k)$, $W_B(k)$, $W_S(k)$, $W_X(k)$, $W_Y(k)$, $W_Z(k)$ are residuals

TABLE 4.4

PARAMETER ESTIMATES AND THEIR STANDARD
ERRORS IN UNIVARIATE MODELS

SYMBOL	1	y(k)	y(k-1)	y(k-2)	y(k-3)	y(k-4)	y(k-7)	y(k-10)	S ₁₂	C ₁₂	S ₆	C ₆
AGF	3.016 (0.019)	0.024 (0.004)	-0.016 (0.004)						0.232 (0.011)	-1.160 (0.012)	-0.42 (0.011)	-0.202 (0.011)
ONF	2.944 (0.025)	0.086 (0.005)	0.022 (0.005)						0.594 (0.014)	-0.804 (0.015)	-0.804 (0.013)	-0.019 (0.014)
WAB	3.270 (0.025)	0.253 (0.004)	0.049 (0.004)						1.427 (0.018)	1.220 (0.015)	-0.022 (0.014)	-0.277 (0.014)
H1	5.908 (0.075)	0.497 (0.004)	0.104 (0.004)				0.038 (0.004)		-0.975 (0.026)	-1.242 (0.024)	0.239 (0.022)	0.449 (0.022)
H2	2.772 (0.124)	1.310 (0.004)	-0.351 (0.004)					0.025 (0.001)	0.019 (0.002)	-0.187 (0.002)		
H3	10.611 (0.300)	0.543 (0.005)	0.028 (0.006)	0.182 (0.006)	-0.135 (0.006)	0.239 (0.005)						

Numbers in parentheses indicate standard errors.

$$S_{12} = \sin \omega_1 k, \quad C_{12} = \cos \omega_1 k, \quad S_6 = \sin \omega_2 k,$$

$$C_6 = \cos \omega_2 k, \quad \omega_1 = 2\pi/12, \quad \omega_2 = 2\pi/6$$

$$W_Y(k+1) = y_0(k+1) - y_c(k+1) \quad (4.13a)$$

where, $y_0(\cdot)$ = observed water levels in well Tc-7,

$y_c(\cdot)$ = water levels in well Tc-7 computed from Eq. 4.13b.

$$y_c(k+1) = 2.772 + 1.310 y_c(k) - 0.351 y_c(k-1) + 0.025 y_c(k-10) + 0.019 \sin \omega_1 k - 0.187 \cos \omega_1 k \quad (4.13b)$$

The "whiteness tests" pertaining to the residuals resulting from the different models discussed below.

(i) - *The Correlogram Test.* We have assumed previously that the sequence $W(\cdot)$ is made up of independent random variables. This aspect is tested by computing the correlation coefficients $d_j(w)$ of the residuals at different lags $j=1,2,\dots,M$.

$$d_j(w) = r_j(w)/r_0(w) \quad (4.14)$$

where,

$$r_j(w) = \frac{1}{n-j} \sum_{k=j+1}^N W(k) W(k-j) \quad (4.15)$$

If $[W(\cdot)]$ is white with zero mean the correlation coefficients $d_j(w)$ should be small in comparison with unity and must lie within the range of $\pm 2/\sqrt{N}$ with 95% probability (Box and Jenkins, 1970). The values of confidence limits for the correlation coefficients of the different processes are listed in Table 4.5. The plots of the correlograms for the residuals of the different models are shown in Fig. 4.8 along with the confidence limits which are shown as 2-standard error limits. The residual correlation coefficients are within the confidence limits. Consequently, we can conclude that the residuals from the different univariate models are uncorrelated.

TABLE 4.5

CONFIDENCE LIMITS FOR CORRELOGRAM TEST AND
CUMULATIVE PERIODOGRAM TEST ON RESIDUALS

SYMBOL	No. of Observations	Correlogram Test		Cum. Periodogram Test		
		α	$2/\sqrt{N}$	α	q	K_α/\sqrt{q}
AGF	238	0.05	0.130	0.25	119	0.094
ONF	190	0.05	0.145	0.25	95	0.105
WAB	238	0.05	0.130	0.25	119	0.094
H1	232	0.05	0.131	0.25	116	0.095
H2	229	0.05	0.132	0.25	114	0.096
H3	187	0.05	0.146	0.25	93	0.106
HWA	214	0.05	0.137	0.25	107	0.099
HWB	214	0.05	0.137	0.25	107	0.099

α = significance level
 $K_\alpha = 1.02$ for $\alpha = 0.25$

q = N/2 if N is even
= (N-1)/2 if N is odd

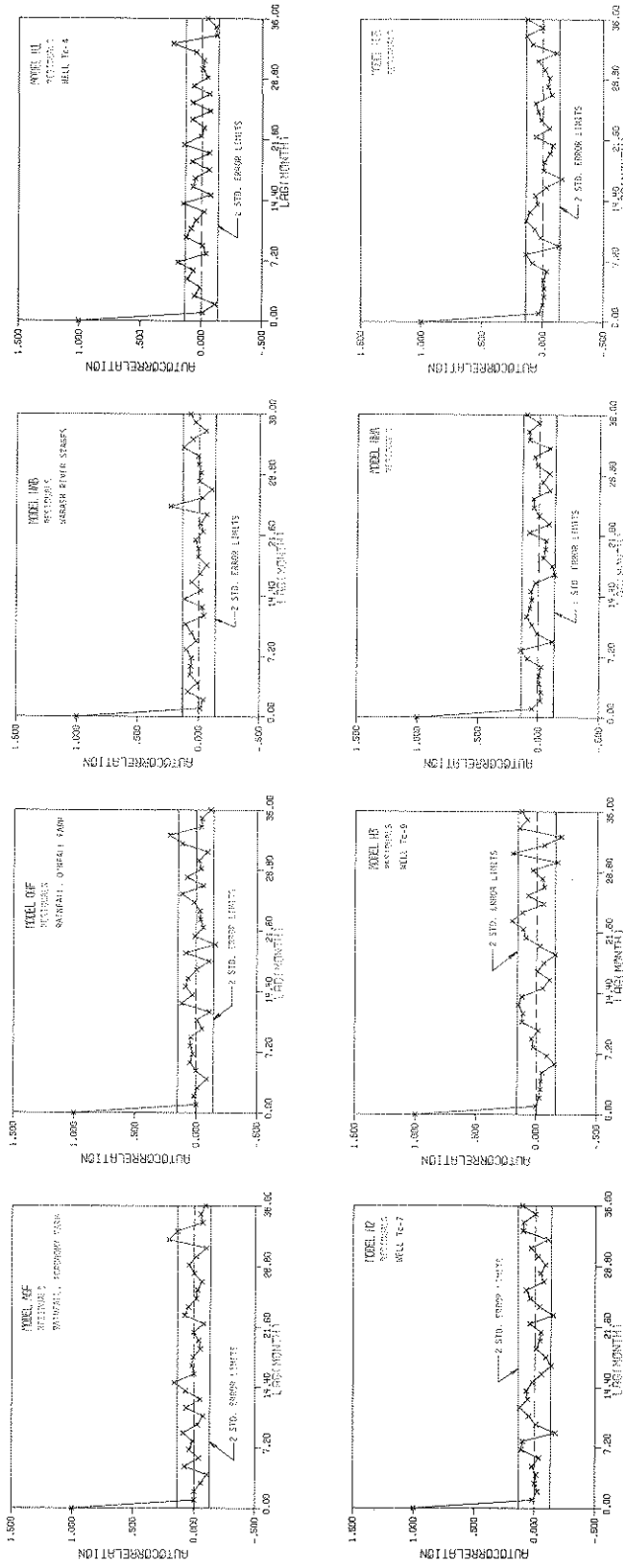


FIGURE 4.8 CORRELOGRAMS OF RESIDUALS

(ii) - *The Cumulative Periodogram Test.* The cumulative periodogram test is performed to detect the presence of any deterministic sinusoidal components in the residuals (Bartlett, 1955). The periodogram $I(f_k)$ of the residuals $[W(\cdot)]$ is defined in Eq. 4.16

$$I(f_k) = \frac{2}{N} \left[\left(\sum_{j=1}^N W(j) \cos 2\pi f_k j \right)^2 + \left(\sum_{j=1}^N W(j) \sin 2\pi f_k j \right)^2 \right] \quad (4.16)$$

where, $f_k = k/N$, $k = 1, 2, \dots, N-1$. The normalized cumulative periodogram C_k is given as

$$C_k = \sum_{j=1}^k \left[I(f_j) / N \times \text{VAR}(W(k)) \right], \quad k=1,2,\dots,N/2 \quad (4.17)$$

where N is an even integer. The plot of C_k against f_k is known as the cumulative periodogram of the data. If the residuals are free from deterministic sinusoidal components, then their normalized cumulative periodogram should be tightly scattered around the straight line from $(0,0)$ to $(0.5,1)$ and should lie within the confidence limits. The values of the confidence limits are shown in Table 4.5. The cumulative periodograms of residuals from the different univariate models are plotted in Fig. 4.9. In all the cases the periodograms lie within the 25% confidence limits and are tightly scattered around the straight line passing through $(0,0)$ and $(0.5,1)$. Consequently, the residuals are free from any deterministic sinusoidal trend terms at the 75% probability level.

(iii) - *The Portmanteau Test.* This is a "goodness of fit" test to detect the whiteness of a sequence of residuals (Box and Pierce, 1970). The test statistic is given as

$$Q = N \sum_{j=1}^K d_j^2(w) \quad (4.18)$$

where N is the number of data points and $d_j(w)$ are the serial correlation coefficients given in Eq. 4.14. The statistic Q is approximately distributed as χ^2 with ν degrees of freedom. The value of ν is given by $\nu = K-p-q$, where K is the number of lags considered and p and q are respectively the number of autoregressive and moving average terms used in the model. The critical values of χ^2 -statistic for different values of ν may be obtained from statistical tables. A few of these critical values corresponding to selected ν values are listed in Table 4.6. The decision rule used in the Portmanteau test is explained next. We accept the hypothesis that the residuals $[W(\cdot)]$ are white if the test statistic Q at any given lag is less than the corresponding critical statistic. The hypothesis is rejected if it is otherwise. The results of the Portmanteau test for the residuals from all the univariate models (Table 4.3) are presented in Table 4.7. The test statistics for the residuals from the models AGF, ONF, WAB, and H2 are less than the respective critical values. Consequently, it can be concluded that the residuals from these models are white. The residuals of model H3 satisfy the Portmanteau test at lags of 6 and 10 months but fail to do so at lags of 15 and 20 months. Consequently, the residuals from this model may be considered to be white for lags less than 15. The test statistics for the residuals from model H1 are greater than the respective critical

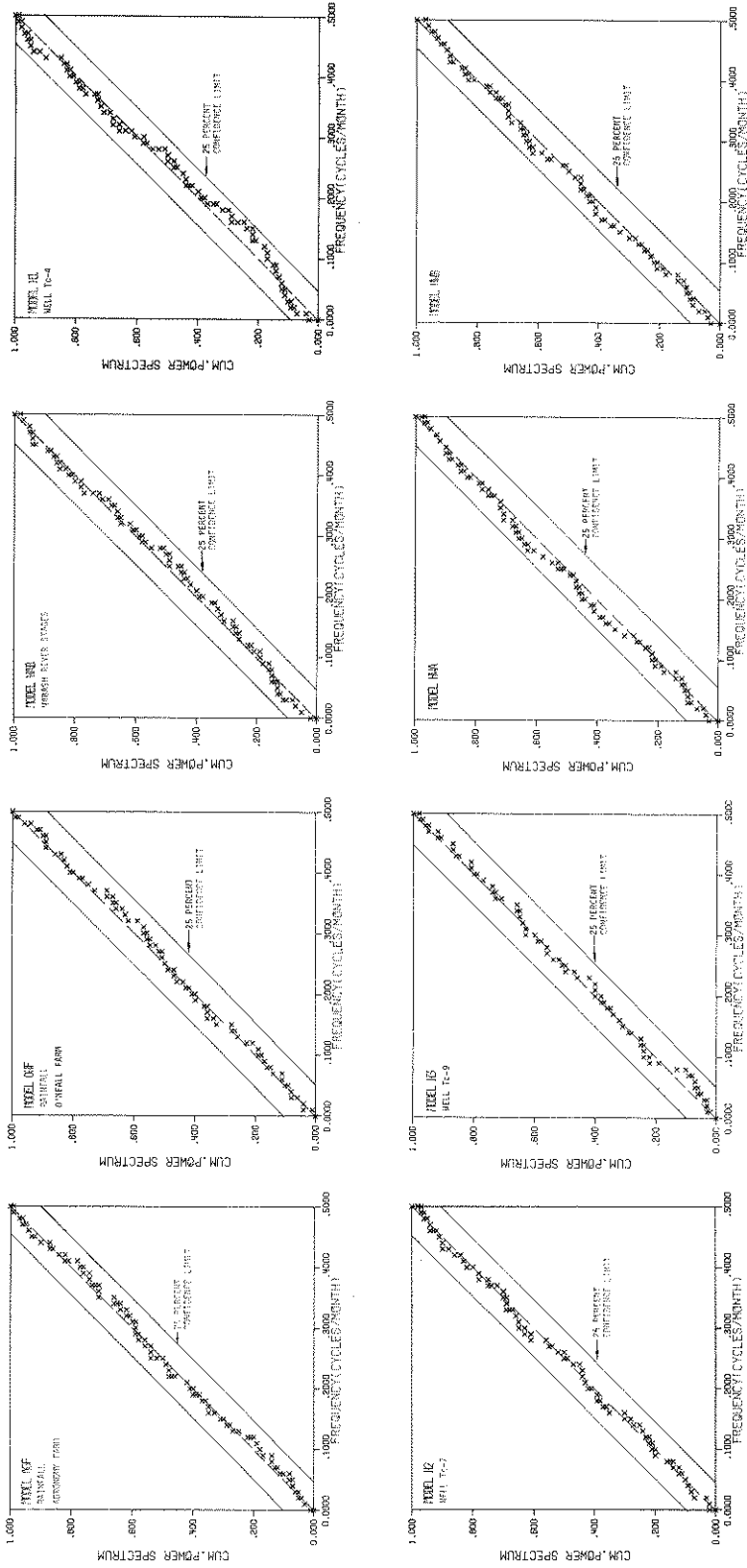


FIGURE 4.9 CUMULATIVE PERIODOGRAMS OF RESIDUALS

TABLE 4.6

CRITICAL VALUES FOR PORTMANTEAU TEST, F-TEST
AND CHI-SQUARE TEST ON RESIDUALS

Lag K	α	PORTMANTEAU TEST						F-Test	CHI-SQ. TEST
		GROUP-A (p+q=5)		GROUP-B (p+q=3)		GROUP-C (p+q=2)			
		ν	CRITICAL STATISTIC	ν	CRITICAL STATISTIC	ν	CRITICAL STATISTIC		
5	0.05	0	-	2	5.99	3	7.82	2.21	11.07
10	0.05	5	11.07	7	14.07	8	15.51	1.83	18.31
15	0.05	10	18.31	12	21.03	13	22.36	1.67	25.00
20	0.05	15	25.00	17	27.59	18	28.87	1.59	31.41

ν = no. of degrees of freedom, p = no. of A.R. terms, q = no. of M.A. terms
 $\nu = K-p-q$

values at all the lags considered. Therefore, the residuals from model H1 for water levels in well Tc-4 are not white but constitute an autoregressive process.

(iv) - *The F-Test and the Chi-Square Test.* The F-test is used to investigate the lack of correlation among the residuals. An alternative form of the F-test is the Chi-Square test (χ^2 -test). The decision rules of these tests are documented in Kashyap and Rao (1976). The critical values of the F-test for different lags are given in Kashyap and Rao (1976) and those of the χ^2 -test are found in statistical tables. A few of these critical values at selected lags are given in Table 4.6. The residuals are considered to be uncorrelated when the test statistic at any lag is less than the corresponding critical value.

The values of the F-test statistic and those of the χ^2 -statistic computed from the residuals of the different univariate models are shown in Table 4.7. The test statistics at different lags are less than the respective critical values. Consequently, the residuals from the different univariate models (Table 4.3) are uncorrelated.

Based on the above results, it can be concluded that the residuals from models AGF, ONF, WAB, H2 and H3 are white. However, the residuals of model H1 for water levels in well Tc-4 satisfy all the tests except the Portmanteau test. Consequently, the model H1 is not valid and the reason is obvious. The water levels in well Tc-4 are highly correlated with the Wabash River stages as explained in Sec. 4.3.2. Any model designed for these water levels should also consider the stage variation in the Wabash River. In the present study, we are interested only in the whitened processes resulting from univariate models. Consequently, the water level process from the well Tc-4 is not considered for investigating the causal relationships.

TABLE 4.7

RESULTS OF PORTMANTEAU TEST, F-TEST AND
CHI-SQUARE TEST ON RESIDUALS

MODEL	LAG K	PORTMANTEAU TEST		F-TEST		CHI-SQ. TEST	
		STATISTIC	DECISION	STATISTIC	DECISION	STATISTIC	DECISION
AGF (p=2, q=0)	5	3.30	A	0.66	A	3.30	A
	10	7.30	A	0.63	A	6.43	A
	15	11.43	A	0.58	A	8.93	A
	20	18.60	A	0.70	A	14.30	A
ONF (p=2, q=0)	5	1.55	A	0.30	A	1.54	A
	10	2.93	A	0.26	A	2.68	A
	15	8.48	A	0.46	A	7.20	A
	20	14.17	A	0.53	A	11.20	A
WAB (p=2, q=0)	5	2.30	A	0.44	A	2.25	A
	10	7.87	A	0.63	A	6.40	A
	15	15.29	A	0.69	A	10.56	A
	20	17.22	A	0.55	A	11.52	A
H1 (p=3, q=0)	5	7.35	R	1.40	A	6.95	A
	10	20.63	R	1.72	A	16.65	A
	15	30.74	R	1.48	A	21.48	A
	20	36.78	R	1.22	A	23.90	A
H2 (p=3, q=0)	5	0.47	A	0.09	A	0.44	A
	10	13.30	A	1.23	A	12.16	A
	15	19.60	A	1.15	A	17.03	A
	20	24.81	A	0.96	A	19.24	A
H3 (p=5, q=0)	6	1.07	A	0.17	A	1.03	A
	10	7.17	A	0.66	A	6.70	A
	15	18.47	R	0.97	A	14.64	A
	20	26.44	R	0.93	A	18.68	A

p = no. of A.R. terms, q = no. of M.A. terms

A = accept the hypothesis that the residuals are uncorrelated at
 $\alpha = 0.05$

R = reject the hypothesis that the residuals are uncorrelated at
 $\alpha = 0.05$

In conclusion, the residual sequences $W_A(\cdot)$, $W_B(\cdot)$, $W_S(\cdot)$, $W_Y(\cdot)$ and $W_Z(\cdot)$ resulting from the valid models for precipitation, river stages, well Tc-7 and well Tc-9 are whitened processes and these are considered for investigating the relationship among the different causal variables.

4.3.5 Checking the Causal Relationships

The whitened processes derived from the valid univariate models (models AGF, ONF, WAB, H2 and H3) are used for checking the causal relationship between precipitation, river stages and groundwater levels. The tests for investigating the causality with pairs of variables are given in Sec. 4.1.1. The different pairs of variables used in the present analysis are shown in Table 4.8. In table 4.8, the series y_1

TABLE 4.8
SETS OF DIFFERENT VARIABLES FOR
INVESTIGATING THE CAUSAL RELATIONSHIPS

SET	Residuals from Univariate Models	
	Series y_2	Series y_1
A	Water levels in well Tc-7 (Model H2, $W_Y(.)$ series)	Precipitation at Ag. Farm (Model AGF, $W_A(.)$ series)
B	Water levels in well Tc-7 (Model H2, $W_Y(.)$ series)	Wabash River stages (Model WAB, $W_S(.)$ series)
C	Water levels in well Tc-9 (Model H3, $W_Z(.)$ series)	Precipitation at O'Neall Farm (Model ONF, $W_B(.)$ series)
D	Water levels in well Tc-9 (Model H3, $W_Z(.)$ series)	Wabash River stages (Model WAB, $W_S(.)$ series)

represents the residuals of the causal variable and the series y_2 corresponds to the residuals from the variable which is the effect. For example, groundwater levels are often affected by precipitation. Obviously precipitation process is the cause and the groundwater level process is the effect. Therefore, in set A the causal relationship between the whitened process of precipitation at the Agronomy Farm ($W_A(.)$ series) and that of water levels in well Tc-7 ($W_Y(.)$ series) is investigated by using the tests given in Sec. 4.1.1. Well Tc-9 is located nearer to the O'Neall Farm than to the Agronomy Farm as can be seen from the location map (Fig. 4.1). Therefore, while investigating the causal relationship between water levels in well Tc-9 and precipitation, the residuals of model ONF are used instead of those from model AGF.

The results of the tests used for checking the causal relationship of pairs of variables in different sets (Table 4.8) are shown in Tables 4.9 and 4.10. The results from Test No. 1 indicate that in set A the residuals of model H2 and those of model AGF are significantly correlated at lags of 1, 8 and 15 months. Test No. 2 shows that the correlations between these two whitened processes are significant at monthly lags of 1, 3, 4, 7, 8, 13, 15, 18 and 20. Considering the results from both these tests, we can conclude that, in set A, the residuals from both the processes are significantly correlated at monthly lags of 1, 8 and 15. These lags appear to bear some physical meaning. The water levels in well Tc-7 are at an average depth of about 168 ft. below the ground surface, thus it might take a considerable time, such as 8 or 15 months, for the precipitation to reach the water table.

For set B, tests 1 and 2 indicate that the residuals from the two variables are significantly correlated at lags 1, 10, 15 and 17 months. The aquifer west of the Wabash River is mainly under unconfined conditions (Maarouf and Melhorn, 1975 and Rosenshein, 1958). However, as well Tc-7 is located about

TABLE 4.9

RESULTS FROM TESTS FOR CHECKING CAUSALITY (SETS A AND B)

LAG j	CRI. VALUE	TEST NO. 1				TEST NO. 2 ($J_1 = 259.94$)			
		SET A		SET B		SET A		SET B	
		TEST STA- TISTIC (r_j)	DECISION	TEST STA- TISTIC (r_j)	DECISION	J_2	DECISION	J_2	DECISION
1	0.0166	0.031	R	0.020	R	262.53	R	261.30	R
2	0.0167	0.002	A	0.006	A	259.20	A	259.68	A
3	0.0168	0.011	A	0.002	A	260.21	R	259.22	A
4	0.0169	0.011	A	0.0	A	260.24	R	258.99	A
5	0.0169	0.007	A	0.0	A	259.76	A	258.98	A
6	0.0170	0.0	A	0.0	A	258.96	A	259.03	A
7	0.0171	0.011	A	0.0	A	260.16	R	258.94	A
8	0.0172	0.027	R	0.016	A	262.13	R	260.82	R
9	0.0172	0.003	A	0.0	A	259.32	A	258.96	A
10	0.0173	0.006	A	0.028	R	259.57	A	262.18	R
11	0.0174	0.002	A	0.0	A	259.12	A	258.98	A
12	0.0175	0.001	A	0.002	A	259.09	A	259.17	A
13	0.0175	0.022	A	0.0	A	260.15	R	259.02	A
14	0.0176	0.001	A	0.0	A	259.10	A	258.98	A
15	0.0177	0.050	R	0.041	R	264.80	R	263.79	R
16	0.0178	0.0	A	0.0	A	259.02	A	258.94	A
17	0.0179	0.003	A	0.020	R	259.24	A	261.21	R
18	0.0180	0.016	A	0.002	A	260.75	R	259.21	A
19	0.0180	0.0	A	0.005	A	258.94	A	259.54	A
20	0.0181	0.011	A	0.0	A	260.20	R	259.05	A

A = Accept the hypothesis that α_j is not significantly different from zero.

R = Reject the hypothesis that α_j is not significantly different from zero.

7800 ft. from the Wabash River, the hydraulic connection between the well and the river is rather weak. Therefore, the large lags seen from these results are meaningful.

As can be seen from Table 4.10, the tests for checking causality do not yield any significant correlations between the residuals of the two variables considered either in set C or in set D. The following reasons explain this occurrence. Well Tc-9 is located about 11,000 ft. away from the east bank of the Wabash River (Fig. 4.1). The aquifer in this region is mainly confined (Maarouf and Melhorn, 1975 and Rosenshein, 1958) and there is no evidence of a hydraulic connection between the river and the aquifer (Bathala et al., 1976). Consequently, the lack of correlation between the residuals of sets C and D can be justified in a physical sense.

The following conclusions can be presented based on the above results. Residuals from the model H2 for water levels in well Tc-7 are significantly correlated at lags of 1, 8 and 15 months with the residuals of model AGF for precipitation at Agronomy Farm. These correlations should be incorporated in model H2 to arrive at a final model for water levels in well Tc-7 in set A. The final model for water levels in well Tc-7 from set B can be formulated by using model H2 and the significant correlations between the

TABLE 4.10
RESULTS FROM TESTS FOR CHECKING CAUSALITY (SETC C AND D)

LAG j	CRITICAL VALUE	TEST NO. 1				TEST NO. 2 ($J_1 = -33.133$)			
		SET C		SET D		SET C		SET D	
		TEST STATISTIC (r_j)	DECISION	TEST STATISTIC (r_j)	DECISION	J_2	DECISION	J_2	DECISION
1	0.0203	0.0	A	0.0	A	-34.13	A	-34.13	A
2	0.0204	0.001	A	0.001	A	-34.01	A	-34.02	A
3	0.0206	0.002	A	0.0	A	-33.93	A	-34.12	A
4	0.0207	0.0	A	0.002	A	-34.13	A	-33.96	A
5	0.0208	0.002	A	0.0	A	-33.92	A	-34.13	A
6	0.0209	0.0	A	0.0	A	-34.13	A	-34.04	A
7	0.0210	0.0	A	0.0	A	-34.10	A	-34.08	A
8	0.0211	0.0	A	0.0	A	-34.11	A	-34.09	A
9	0.0212	0.0	A	0.0	A	-34.11	A	-34.13	A
10	0.0214	0.0	A	0.0	A	-34.08	A	-34.13	A
11	0.0215	0.0	A	0.003	A	-34.06	A	-33.82	A
12	0.0216	0.0	A	0.0	A	-34.08	A	-34.08	A
13	0.0217	0.0	A	0.0	A	-34.13	A	-34.13	A
14	0.0218	0.0	A	0.005	A	-34.07	A	-33.67	A
15	0.0220	0.0	A	0.002	A	-34.12	A	-33.93	A
16	0.0221	0.0	A	0.0	A	-34.13	A	-34.13	A
17	0.0222	0.004	A	0.0	A	-33.80	A	-34.10	A
18	0.0223	0.0	A	0.0	A	-34.13	A	-34.10	A
19	0.0225	0.0	A	0.0	A	-34.10	A	-34.13	A
20	0.0226	0.0	A	0.0	A	-34.09	A	-34.13	A

A = Accept the hypothesis that α_j is not significantly different from zero.
R = Reject the hypothesis that α_j is not significantly different from zero.

residuals of model H2 and those of model WAB at lags of 1, 10, 15 and 17 months. As the residuals from sets C and D are not significantly correlated, the final model for water levels in well Tc-9 is the same as model H3 given in Table 4.3.

4.3.6 Final Stochastic Models for Groundwater Levels

As discussed in the previous section the significant correlations observed between the two variables in each set at different lags should be incorporated into the appropriate univariate model to derive final stochastic models for groundwater levels. The procedure is briefly explained below.

First a stochastic difference equation model similar to that in Eq. 4.4 is formulated between the residuals of the two variables using the lags at which these residuals are significantly correlated. Let us designate this model as WX. The residuals from model WX are then tested for whiteness using the different validation tests described in Sec. 4.3.4. If the model WX is valid, the final model is given by the combination of the appropriate univariate model and the model WX.

In the present study, the residuals from model H2 for water levels in well Tc-7 are significantly correlated either with the residuals of the precipitation series or with those of the Wabash River stages

as described in Sec. 4.3.5. Consequently, two different final models are formulated for water levels in well Tc-7. The first of these is constructed using the univariate model H2 and the model resulting from the causal relationship with the residuals of model AGF for precipitation at the Agronomy Farm. The second model is the combination of model H2 and the model obtained for the causal relationship with the residuals of model WAB for the Wabash River stages.

(i)- *Model for Water Levels in Well Tc-7 Using the Causal Relationship with Precipitation at the Agronomy Farm.* The univariate model formulated for water levels in well Tc-7 is model H2 as shown in Table 4.3. The residuals from this model are given by $W_Y(\cdot)$. Model AGF (Table 4.3) is the valid univariate model for precipitation at the Agronomy Farm with residuals denoted as $W_A(\cdot)$. As the fluctuations in water levels at well Tc-7 are affected by precipitation, the former is the effect and the latter is the cause. The causal relationship between the whitened processes of $W_Y(\cdot)$ and $W_A(\cdot)$ was investigated in Sec. 4.3.5 where it was found that these residuals are significantly correlated at lags of 1, 8 and 15 months. Consequently, a stochastic difference equation model for the residuals from these two variables is given as,

$$W_Y(k+1) = \alpha_1 W_A(k) + \alpha_2 W_A(k-7) + \alpha_3 W_A(k-14) \quad (4.19)$$

In Eq. 4.19, the parameters α_1 , α_2 and α_3 are estimated as explained in Sec. 4.2.1. The resulting parameters and their standard errors are shown in Table 4.11. These parameters are significantly different from zero. The model for $W_Y(\cdot)$ is depicted in Eq. 4.20 and is designated as HWA.

$$W_Y(k+1) = 0.0177 W_A(k) + 0.0168 W_A(k-7) + 0.0222 W_A(k-14) + \eta_{YA}(k+1) \quad (4.20)$$

The residuals $\eta_{YA}(\cdot)$ are tested for whiteness by using the different validation tests as described in Sec. 4.3.4.

The correlogram of residuals $\eta_{YA}(\cdot)$ from Eq. 4.20 (model HWA) is plotted in Fig. 4.8 along with the 95% confidence limits. The residual correlation coefficients are within the confidence limits and hence these residuals are uncorrelated. The cumulative periodogram is shown in Fig. 4.9. This periodogram lies within the 25% confidence limits which indicates that the residuals $\eta_{YA}(\cdot)$ are free from deterministic sinusoidal trends. The results of the Portmanteau test, the F-test and the χ^2 -test are given in Table 4.12. These results show that the residuals $\eta_{YA}(\cdot)$ are uncorrelated upto 20 lags. As the residuals from model HWA satisfy all the validation tests, it can be concluded that this model is valid.

The final stochastic model for water levels in well Tc-7 is obtained (Eq. 4.21) by substituting Eq. 4.10 for $W_Y(k+1)$ into model H2.

$$y(k+1) = 2.772 + 1.310 y(k) - 0.351 y(k-1) + 0.025 y(k-10) + 0.019 \sin \omega_1 k - 0.187 \cos \omega_1 k \\ + 0.0177 W_A(k) + 0.0168 W_A(k-7) + 0.0222 W_A(k-14) + \eta_{YA}(k+1) \quad (4.21)$$

TABLE 4.11

PARAMETER ESTIMATES AND THEIR STANDARD ERRORS IN STOCHASTIC MODELS FOR RESIDUALS

MODEL	PARAMETERS AND STANDARD ERRORS			
	α_1	α_2	α_3	α_4
HWA	0.0177 (0.00082)	0.0168 (0.00083)	0.0222 (0.00083)	
HWB	0.0139 (0.00061)	0.0182 (0.00062)	0.0194 (0.00063)	-0.0166 (0.00063)

Numbers in parentheses indicate standard errors

TABLE 4.12

RESULTS OF PORTMANTEAU TEST, F-TEST AND CHI-SQUARE TEST ON RESIDUALS FROM MODELS HWA AND HWB

MODEL	LAG K	PORTMANTEAU TEST		F-TEST		CHI-SQ. TEST	
		STATISTIC	DECISION	STATISTIC	DECISION	STATISTIC	DECISION
HWA (p=0, q=3)	5	0.74	A	0.14	A	0.70	A
	10	9.76	A	0.84	A	8.47	A
	15	14.19	A	0.78	A	11.92	A
	20	21.65	A	0.80	A	16.22	A
HWB (p=0, q=4)	5	0.33	A	0.06	A	0.32	A
	10	8.44	A	0.77	A	7.80	A
	15	14.93	A	0.91	A	13.73	A
	20	22.24	A	0.93	A	18.64	A

p = no. of A.R. terms, q = no. of M.A. terms

A = accept the hypothesis that the residuals are uncorrelated at $\alpha=0.05$

R = reject the hypothesis that the residuals are uncorrelated at $\alpha=0.05$

The model given in Eq. 4.21 is designated HHX. The mean of the residuals $\eta_{YA}(\cdot)$ from model HHX is 0.001 and the variance is 0.1. The ratio of the residual variance to the signal variance is 0.0233. Thus the model HHX explains 97.67 percent of the variance of the residuals $\eta_{YA}(\cdot)$.

(ii) - Model for Water Levels in Well Tc-7 Using the Causal Relationship with the Wabash River Stages. The causal relationship between the whitened processes derived from models H2 and WAB is explained in Sec. 4.3.5. These results show that the residuals $W_Y(\cdot)$ of model H2 are significantly correlated with the residuals $W_S(\cdot)$ of model WAB at lags of 1, 10 15 and 17 months. A stochastic difference equation model for the residuals from these two variables can be written as

$$W_Y(k+1) = \alpha_1 W_S(k) + \alpha_2 W_S(k-9) + \alpha_3 W_S(k-14) + \alpha_4 W_S(k-16). \quad (4.22)$$

The parameters α_1 , α_2 , α_3 and α_4 given in Eq. 4.22 are estimated as explained in Sec. 4.2.1. The parameter estimates and their standard errors are given in Table 4.11. All these parameters are significantly different from zero. Equation 4.23 shows the relationship between $W_Y(\cdot)$ and $W_S(\cdot)$.

$$W_Y(k+1) = 0.0139 W_S(k) + 0.0182 W_S(k-9) + 0.0194 W_S(k-14) - 0.0167 W_S(k-16) + \eta_{YS}(k+1) \quad (4.23)$$

The model for $W_Y(\cdot)$ depicted in Eq. 4.23 is designated HWB. The correlogram and the cumulative periodogram of the residuals $\eta_{YS}(\cdot)$ from model HWB are respectively plotted in Figs. 4.8 and 4.9. The results from both these plots indicate that the residuals are uncorrelated as the test statistics are within their respective confidence limits. The results of the Portmanteau test, the F-test and the χ^2 -test (Table 4.12) also show that these residuals are white. Therefore model HWB is valid.

The final stochastic model for water levels in well Tc-7 which takes into account the effect of the Wabash River stages is

$$y(k+1) = 2.772 + 1.310 y(k) - 0.351 y(k-1) + 0.025 y(k-10) + 0.019 \sin \omega_1 k - 0.187 \cos \omega_1 k \\ + 0.0139 W_S(k) + 0.0182 W_S(k-9) + 0.0194 W_S(k-14) - 0.0167 W_S(k-16) + \eta_{YS}(k+1). \quad (4.24)$$

The above model (Eq. 4.24) is designated as HHY. The mean and variance of the residuals $\eta_{YS}(\cdot)$ are respectively 0.0026 and 0.0999. The ratio of the residual variance to the signal variance is 0.0233 which shows that the model HHY explains 97.67 percent of the variance of the residuals.

(iii) - *Model for Water Levels in Well Tc-9*. As explained in Sec. 4.3.5, the tests for causality did not show significant correlations between the residuals of model H3 (well Tc-9) and those of either model ONF (Rainfall, O'Neall Farm) or model WAB (Wabash River stages). Consequently, the final model for water levels in well Tc-9 is given by the univariate model H3 as shown in Table 4.3. The relationship is again given below as Eq. 4.25.

$$y(k+1) = 10.611 + 0.543 y(k) + 0.028 y(k-1) + 0.182 y(k-2) - 0.135 y(k-3) + 0.239 y(k-4) + W_Z(k+1) \quad (4.25)$$

The results of the validation tests on residuals $W_Z(\cdot)$ are already discussed in Sec. 4.3.4. The ratio of the residual variance to the signal variance is 41.3 percent. Therefore the variance explained by the residual $W_Z(\cdot)$ is only 58.7 percent.

4.3.7 Characteristics of Groundwater Levels Regenerated from the Final Stochastic Models

In this section, some of the statistical characteristics of groundwater levels regenerated from final stochastic models (Eqs. 4.21, 4.24 and 4.25) are compared with those of the observed data. The method used to regenerate groundwater levels is briefly explained below.

Let us assume that the water levels in well Tc-7 are to be regenerated using the final stochastic model (model HHX) shown in Eq. 4.21. Equation 4.21 is rewritten as in Eq. 4.26 in the present notation.

$$y_c(k+1) = 2.772 + 1.31 y_c(k) - 0.351 y_c(k-1) + 0.025 y_c(k-10) + 0.019 \sin \omega_1 k - 0.187 \cos \omega_1 k + 0.0177 W_A(k) + 0.0168 W_A(k-7) + 0.0222 W_A(k-14) + \eta_{YA}(k+1) \quad (4.26)$$

In Eq. 4.26, $y_c(\cdot)$ are the computed groundwater levels and $W_A(\cdot)$ are the residual sequence from model AGF. Values of y_c are recursively computed using the values computed from the previous times and the known values of $W_A(\cdot)$ series. As the maximum lag in Eq. 4.26 is 14 months, the first value of y_c corresponds to that of 15th observation. However, to initialize computations, the first 15 values of y_c are assumed to be the same as the observed water levels in well Tc-7. The residuals $\eta_{YA}(\cdot)$ are not included in these computations.

Some of the elementary statistics of the regenerated values from models HHX, HHY and H3 are tabulated in Table 4.13. The statistics of the corresponding observed data are also presented in Table 4.13 for comparison. All the statistics of models HHX and HHY for water levels in well Tc-7 are very close to those of the observed data. For example, the coefficient of skewness of the computed data from model HHX and HHY are respectively 0.15 and 0.12 as compared to 0.13 of the observed data. The mean of the computed values of model H3 is very close to that of the observed data from well Tc-9. However, the other statistics such as variance, coefficients of skewness and kurtosis are considerably different from those of the observed data.

TABLE 4.13
COMPARISON BETWEEN THE STATISTICS OF
OBSERVED AND REGENERATED GROUNDWATER LEVELS

STATISTIC	WELL Tc-7			WELL Tc-9	
	Observed	Model HHX	Model HHY	Observed	Model H3
Mean	168.06	168.25	168.25	73.96	74.01
Variance	4.28	4.26	4.15	3.46	2.03
Skew. Coeff.	0.13	0.15	0.12	0.51	2.35
Coeff. of Kurtosis	2.58	2.87	2.68	3.18	2.65

The correlograms and power spectra of the computed data resulting from different final stochastic models are compared with those of the respective observed data in Fig. 4.10. The correlograms of models HHX and HHY for water levels in well Tc-7 are very close to those of the observed data. The weak annual cycle is also reproduced in these correlograms. The spectral density plots of models HHX and HHY also show close agreement with those of the observed data. The computed correlogram of model H3 for water levels in well Tc-9 is slightly different from that of the historical data. However, the spectral density plot is in close agreement with that of the observed data. In general the weak annual cycle of the observed data at well Tc-9 is reproduced in the correlogram and the power spectral density plots.

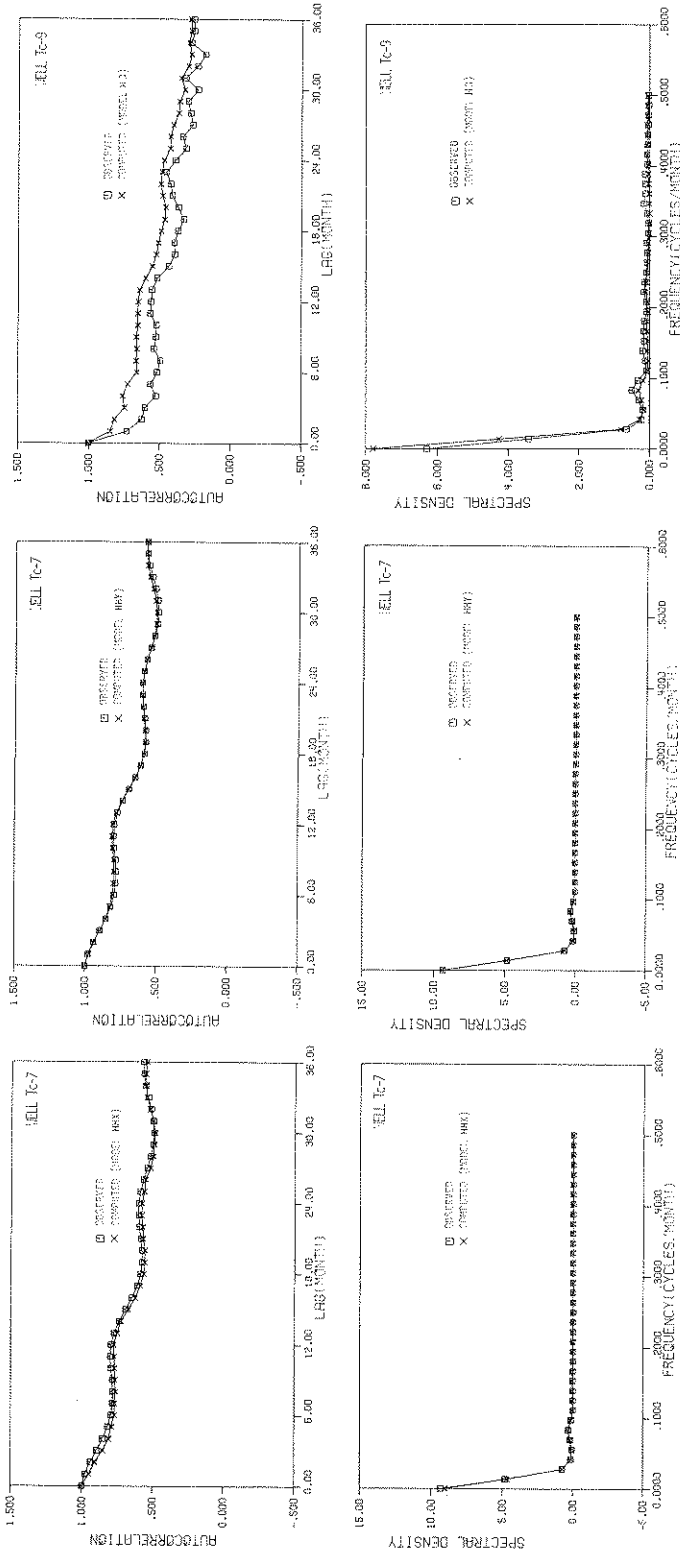


FIGURE 4.10 CORRELOGRAMS AND POWER SPECTRA OF OBSERVED AND REGENERATED GROUNDWATER LEVEL

A comparison between the monthly means and the standard deviations of the computed and the observed data are presented in Fig. 4.11. The computed monthly means from models HHX, HHY and H3 are close to those obtained from the respective observed data. The seasonal patterns exhibited by the monthly standard deviations of the observed data are reproduced by those of the computed data from different models. In particular, the monthly standard deviations computed from the results of model HHY are in close agreement with those from the observed water levels in well Tc-7.

The time series of the computed data resulting from different models are compared with the respective observed time series as shown in Fig. 4.12. The computed values obtained from models HHX and HHY for water levels in well Tc-7 correspond closely to that of the observed values. For example, the computed water level in well Tc-7 in December, 1963 from the models HHX and HHY are respectively 168.42 ft. and 168.37 ft. below land surface datum as compared with an observed value of 169.16 ft. The discrepancy is less than a foot. The observed water levels in well Tc-9 are also satisfactorily reproduced by those computed from model H3.

4.3.8 Simulation Results

The validity of the final stochastic models fitted to the groundwater level data from wells Tc-7 and Tc-9 are further tested by simulation. The first objective of the simulation study is to examine the characteristics of these simulated sequences and to determine the capability of the models to preserve some of the characteristics of the observed data. The second objective is to investigate the relative merits of the univariate model of the groundwater levels and the final models developed after considering the causal relationships for water levels in well Tc-7.

The univariate and the final stochastic model fitted to the groundwater level data from well Tc-7 (models H2, HHX and HHY) and well Tc-9 (model H3) are used to simulate monthly values on a digital computer. This is accomplished by using a procedure similar to that used for regenerating the groundwater levels (Sec. 4.3.7). However, in the simulation process, the residual series such as $W_Y(\cdot)$, $W_A(\cdot)$, $n_{YA}(\cdot)$, $W_S(\cdot)$, $n_{YS}(\cdot)$ and $W_Z(\cdot)$ from models H2, HHX, HHY and H3 are generated from their respective probability distributions.

The statistics of the residuals from models H2, HHX, HHY and H3 are given in Table 4.14. The means of these residuals are zero and the coefficients of kurtosis are approximately close to 3. The histograms of different residual series (Fig. 4.13) are symmetrical about their respective means and appear to fit a normal distribution satisfactorily. Consequently, random values of different residual series are generated from normal distributions and these values are used as inputs into the appropriate final models in order to simulate the monthly groundwater levels.

The above procedure is used to simulate monthly groundwater levels for well Tc-7 from models H2, HHX and HHY, and for well Tc-9 from model H3. From each model, three series of groundwater levels, each series

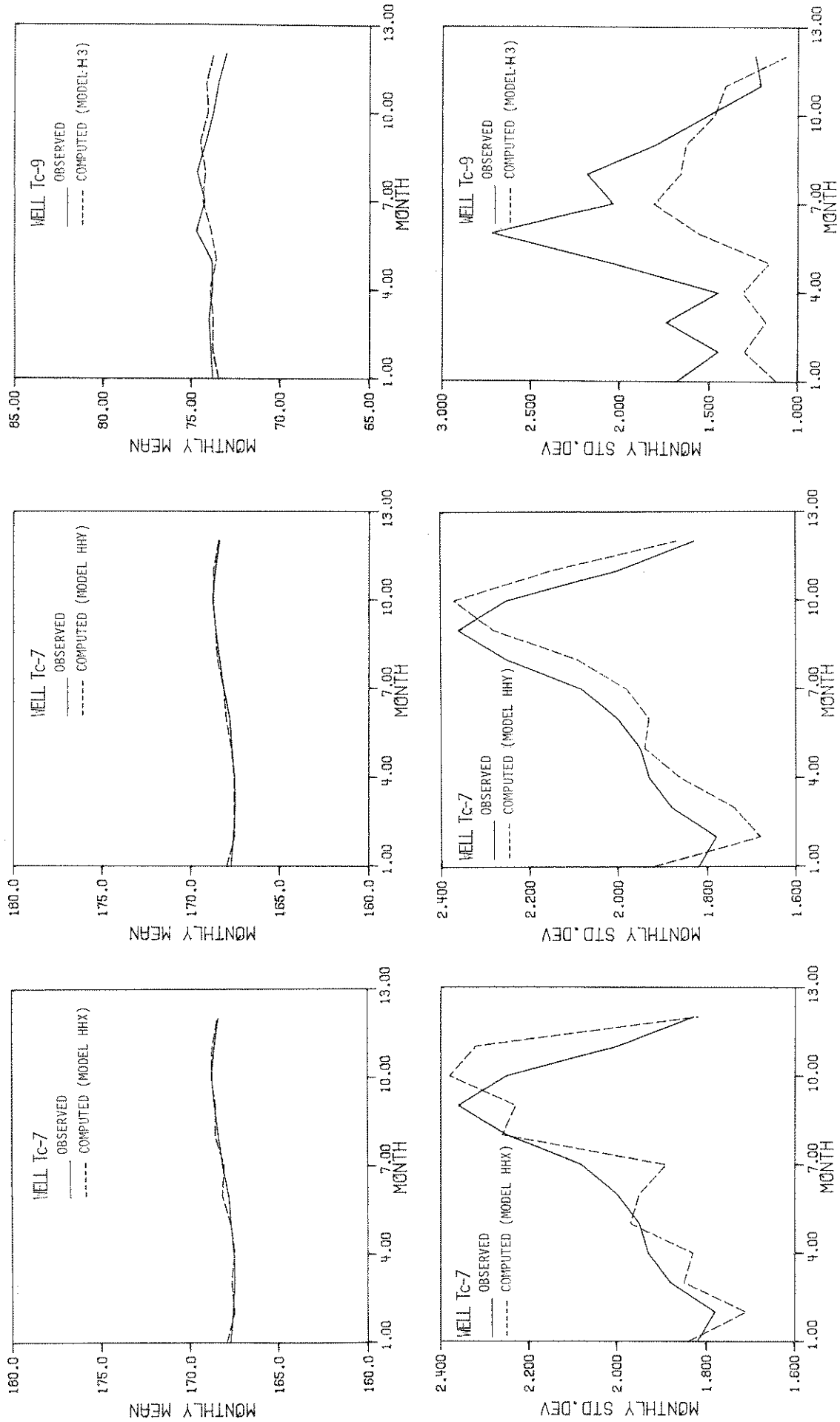


FIGURE 4.11 MONTHLY MEANS AND STANDARD DEVIATIONS OF OBSERVED AND REGENERATED GROUNDWATER LEVELS

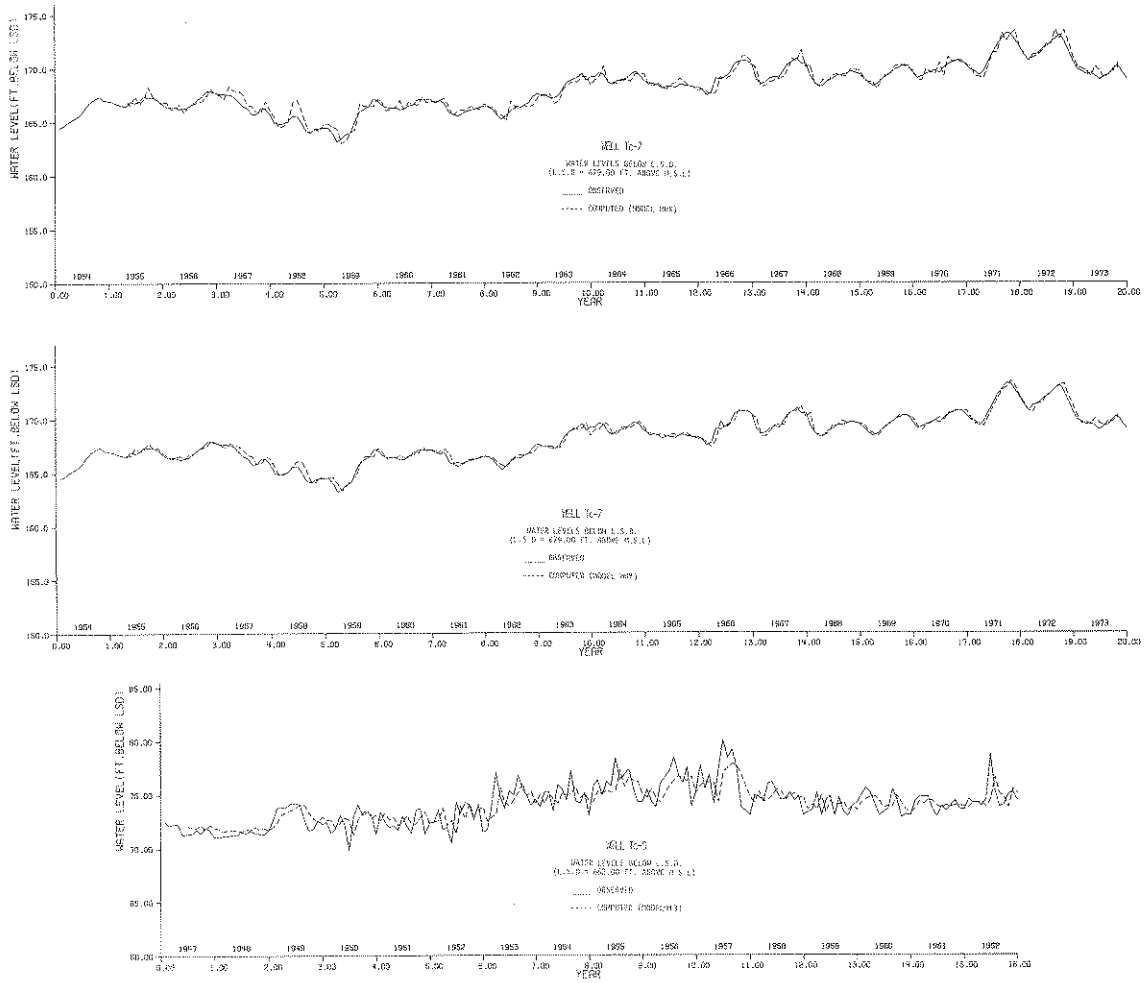


FIGURE 4.12 COMPARISON BETWEEN THE TIME SERIES OF OBSERVED AND REGENERATED GROUNDWATER LEVELS

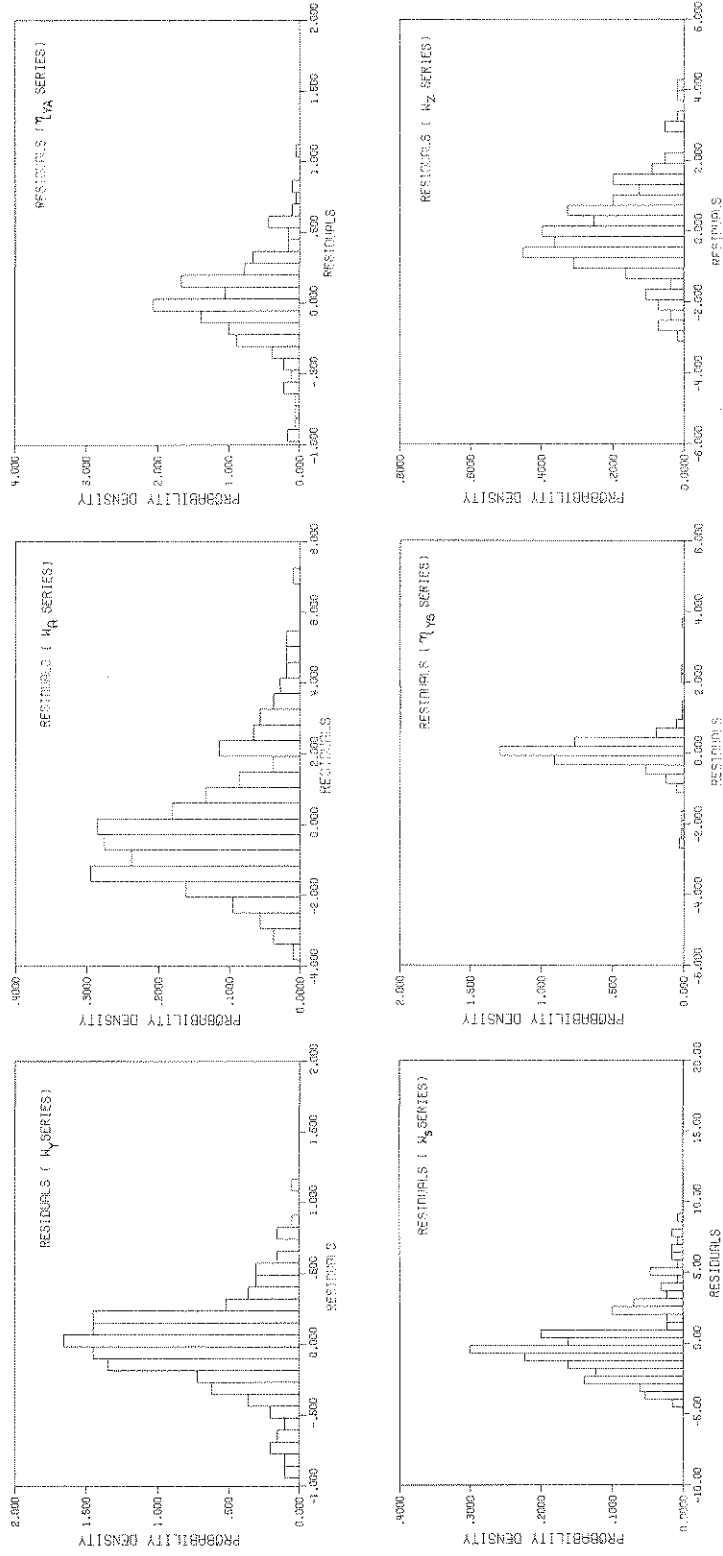


FIGURE 4.13 HISTOGRAMS OF RESIDUALS

TABLE 4.14
 STATISTICS OF RESIDUALS USED TO
 SIMULATE GROUNDWATER LEVELS

STATISTIC	MODEL H2	MODEL HHX		MODEL HHY		MODEL H3
	W_Y	W_A	η_{YA}	W_S	η_{YS}	W_Z
Mean	0.0	0.0	0.0	0.0	0.0	0.0
Variance	0.11	3.23	0.10	5.82	0.10	1.43
Mean Sq.	0.11	3.23	0.10	5.82	0.10	1.43
Skew. Coeff.	-0.07	0.93	-0.07	1.11	-0.03	0.49
Coeff. of Kurtosis	4.06	4.06	4.04	4.48	3.89	4.12

consisting of 1000 values, are simulated using different sets of initial values (Sec. 4.3.7) and the statistics of these different series are shown in Table 4.15. The statistics of the observed data are also included in Table 4.15 for comparison. The overall agreement between the statistics of the observed and the simulated data are satisfactory although the statistics of one of the three series from each model match better with the respective statistics of the observed data. These series are marked with an asterisk in Table 4.15.

A comparison between the statistics of the simulated series of models H2, HHX and HHY with those of the observed water levels in well Tc-7 reveals the following information. The statistics of series 2 from model HHY agree most closely with those of the observed data although the discrepancy between the means appear to be slightly larger than that for the other models. It is interesting to note that the variance and the coefficient of kurtosis are 3.97 ft^2 and 2.46 ft^4 as compared to 4.28 ft^2 and 2.58 ft^4 of the observed data respectively. The statistics of simulated series 3 of model HHX appear to be the next best match with those of the observed data. From the foregoing analysis, the models HHY and HHX which were developed after incorporating the causal relationships appear to be better models for water levels in well Tc-7 than the univariate model H2. This observation is further examined from a study of the histograms, correlograms and power spectra of the best fitted simulation series from different models.

The histograms of the best fitted simulation series are shown in Fig. 4.14 and those of the observed water levels in wells Tc-7 and Tc-9 are given in Fig. 4.4. The histogram of the observed data in well Tc-7 is rather flat with a double peak whereas, those of models H2 and HHX are single peaked. The histogram of model HHY is similar in shape to that of the observed data and can be considered acceptable. The simulated series of model H3 (well Tc-9) yields a histogram with a less pronounced peak as compared to

TABLE 4.15

STATISTICS OF OBSERVED AND SIMULATED GROUNDWATER LEVELS

(Number of values generated in each series = 1000)

STATISTIC	WELL Tc-7												WELL Tc-9		
	OBSERVED	MODEL H2			MODEL HHX			MODEL HHY			OBSERVED	MODEL H3			
		Series 1	Series 2	Series 3*	Series 1	Series 2	Series 3*	Series 1	Series 2*	Series 3		Series 1*	Series 2	Series 3	
		168.92	168.96	169.03	167.88	167.98	168.13	170.41	170.52	170.63		74.20	74.27	74.24	
Mean	168.06	168.96	169.03	167.88	167.98	168.13	170.41	170.52	170.63	73.96	74.20	74.24			
Variance	4.28	2.16	2.12	2.38	2.46	2.97	4.41	3.97	3.83	3.46	2.72	2.67			
Mean Sq.	28250	28548	28574	28185	28220	28271	29044	29083	29117	5474	5508	5514			
Skew. Coeff.	0.13	0.03	0.04	0.0	0.06	0.27	-0.05	0.03	-0.05	0.51	-0.02	-0.02			
Coeff. of Kurtosis	2.58	2.72	2.71	3.86	3.91	3.58	2.45	1.46	2.55	3.18	2.77	2.73			

*Best fitting simulation results

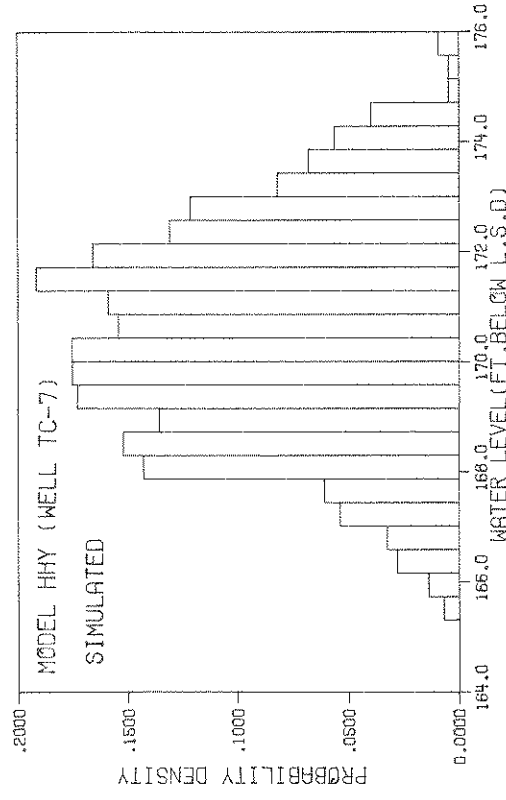
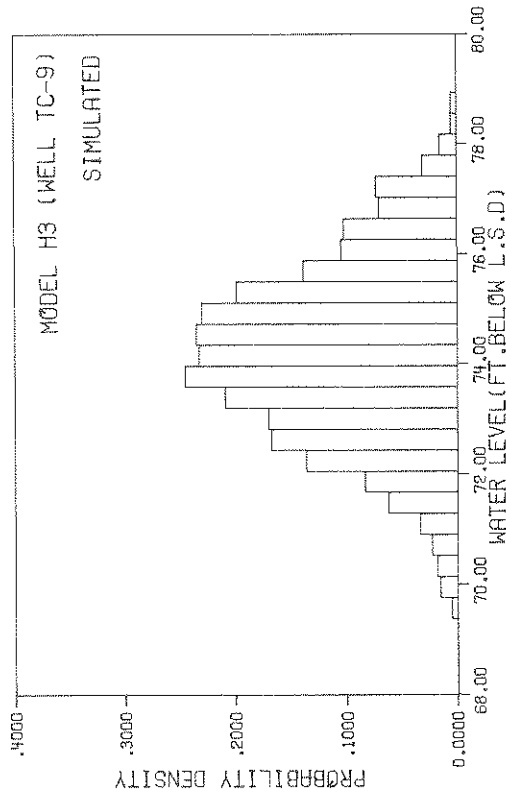
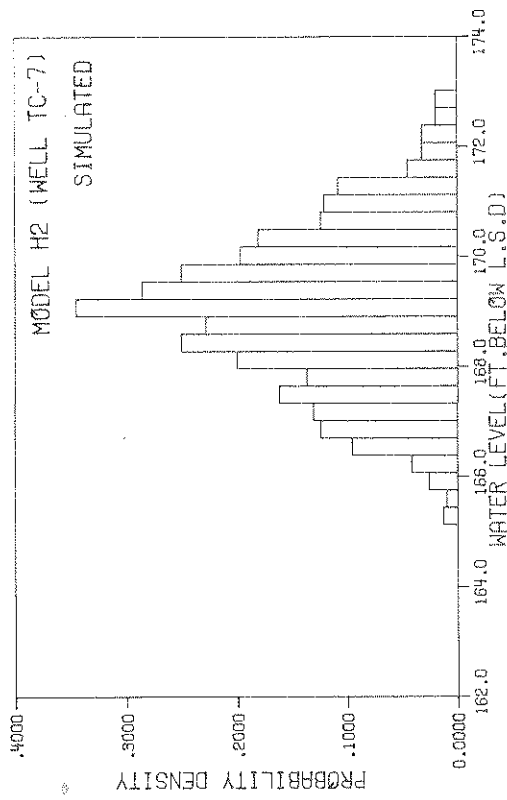
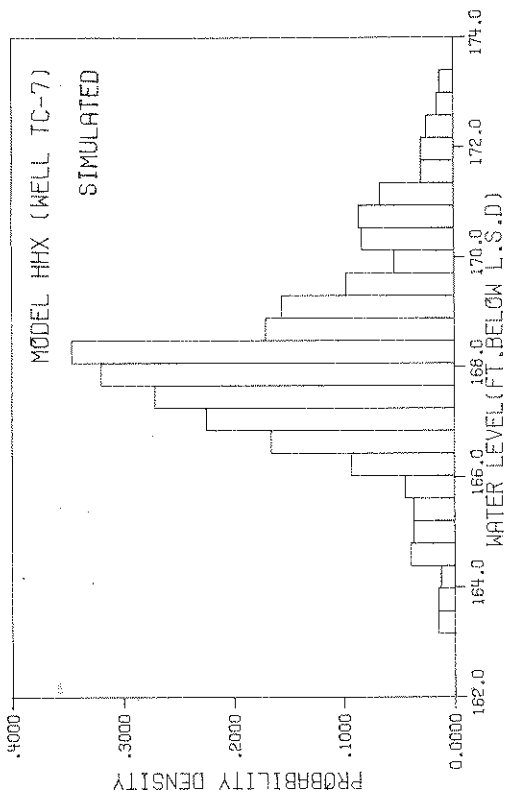


FIGURE 4.14 HISTOGRAMS OF SIMULATED GROUNDWATER LEVELS

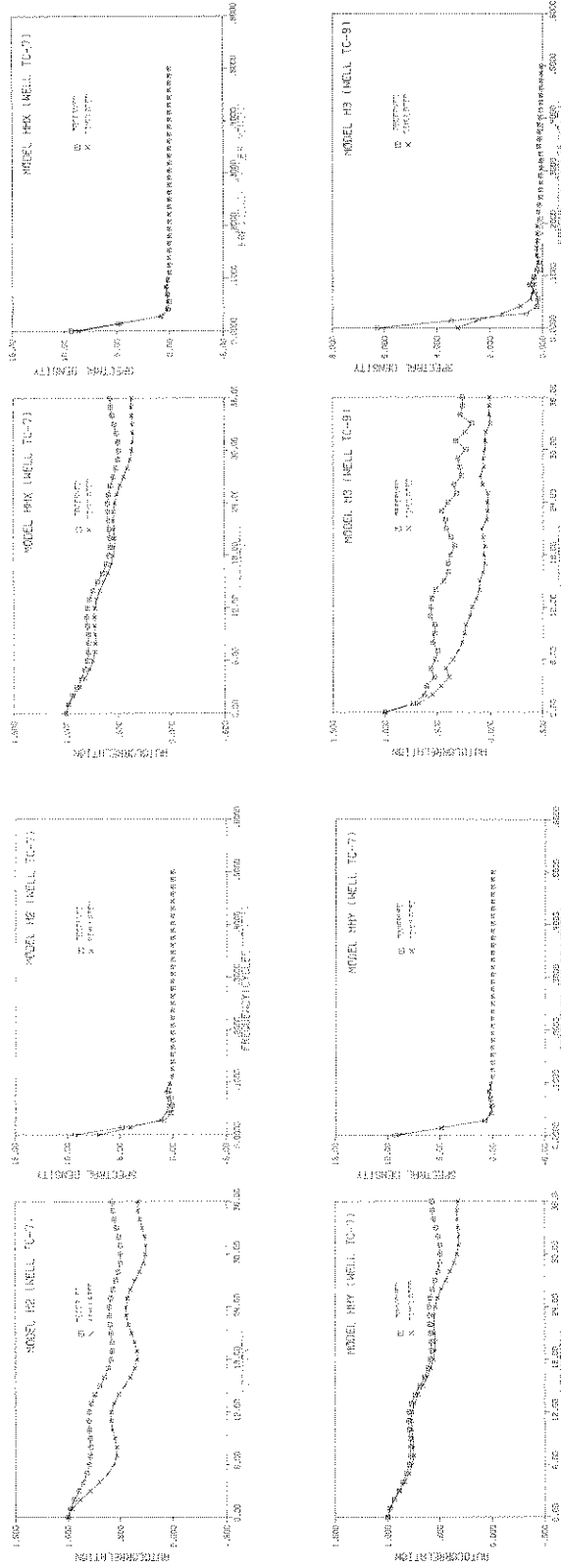


FIGURE 4.15 CORRELOGRAMS AND POWER SPECTRA OF SIMULATED DATA

that of the observed data. However, the peak probabilities are approximately equal to 25 percent in both the histograms.

A comparison between the correlograms and the power spectra of the simulated and the observed data for water levels in wells Tc-7 and Tc-9 are given in Fig. 4.15. The correlograms of models H2, HHX and HHY do not show any significant annual cycle just as in the correlogram for the observed water levels in well Tc-7. However, the correlogram of model HHY is very close to that of the observed data upto a lag of about 25 months. The match between the correlograms of model HHX and the observed data is also satisfactory. The correlogram of model H2 is considerably different from that of the observed data. The overall agreement between the power spectral density plots (Fig. 4.15) of the observed and the simulated data (models H2, HHX and HHY) is satisfactory. A close examination of these plots (Fig. 4.15) indicate that the best results are obtained from model HHY and the next best is the model HHX.

The correlograms and the power spectral density plots of the simulated data from model H3 (well Tc-9) do not show any pronounced periodicities just as their counterparts obtained from observed data. The discrepancies between the observed and the simulated correlograms and power spectra appear to be slightly large. However, the agreement can be considered to be satisfactory.

In conclusion, the results of the simulation study indicate that the data simulated by the models for water levels in wells Tc-7 and Tc-9 preserve the observed statistical characteristics of the data. The final stochastic models developed for well Tc-7 (models HHX and HHY) after considering the causal relationships are definitely better than the univariate model H2. The model HHY is the best of all the three models developed for water levels in well Tc-7.

CHAPTER 5
DISCUSSION AND CONCLUSIONS

The linear systems approach has been used in the present study to formulate deterministic models for analysing several types of groundwater flow problems. The stochastic nature of groundwater levels and the causal relationships between precipitation, river stages and groundwater levels have also been analysed. Some aspects of these models are further discussed in this chapter and a set of conclusions are presented.

5.1 Linear Systems Analysis of Aquifer Flow Problems

A generalized linear relationship (Eqs. 2.21 and 2.22) has been used to analyse groundwater flow in a stream-well-aquifer system. A general procedure has been developed to predict aquifer response by considering only the cause-and-effect relationships of the groundwater flow system. The method of solution and the data requirements of the above procedure need further explanation and analysis.

5.1.1 Modeling Regional Aquifer Systems

There are several models available for analysis of regional groundwater flow problems. Resistance-Capacitance (R-C) networks and numerical-digital computer techniques based on either finite difference or finite element approximations are quite popular as efficient tools for solving these problems. However, R-C networks, and finite difference and finite element methods have several limitations in terms of data and skilled manpower requirements, initial and operating costs as discussed in Sec. 1.2. On the other hand, the procedure discussed in the present study has several advantages over other commonly used methods. A few of these advantages are briefly described below.

- (1) In the present method, the locations of the existing and the planned wells constitute the number of nodes in the model. Consequently, the number of simultaneous equations to be solved at each observation is drastically reduced. The number of nodes increase only with the number of wells, and is independent of the areal extent of the aquifer.
- (2) As the number of nodes used in the present method is small compared to that in a finite difference model of the aquifer, the time required to determine and specify the input data at each nodal point is also much smaller in comparison with the corresponding effort in a finite difference model.
- (3) Unlike other deterministic models, the predetermined aquifer transmissivity values are not used as inputs in the present procedure. However, estimated storage coefficient values are used as one of the inputs. It is relatively easy to estimate the storage coefficients after examining the geology and the well logs of the area. Consequently, the expensive pumping tests which are usually required to determine aquifer transmissivities and storage coefficients are not needed in the present procedure.
- (4) A trial and error procedure is used to arrive at satisfactory solutions in both the traditional and the present methods. However, the number of trials needed in the present procedure are fewer than those

required in an R-C network or a finite difference model. Consequently, the computational expenditure is drastically reduced in the present procedure.

(5) The present procedure is analogous to the finite element method, in the sense that the nodal points can be spaced at irregular intervals.

(6) The deterministic relationships, such as the Theis nonequilibrium equation (Eq. 2.10a) and the stream-aquifer interaction formulas (Eqs. 2.1-2.6), which were used to analyse the groundwater flow problems in the present study are easier to program for a digital computer than the finite difference equations. Consequently, the complexity of the problem is considerably reduced in the present formulation.

Based on the foregoing discussion, the present procedure is a simple and less expensive method for the analysis of regional aquifer problems.

5.1.2 Estimation of Aquifer Storage Coefficients

In the present procedure (Chapter 3), the storage coefficients were initially estimated after examining the geology and the well logs of the aquifer region. These estimated values were then used as inputs into the model to compute transmissivity values by using each observation during the calibration period as explained in Sec. 3.1.1. The accuracy of the transmissivity values computed from calibration is directly dependent on "good" initial estimates of storage coefficients. If these initial estimates are not properly selected, the solution may not converge for each observation during the calibration period. A converging solution is obtained if these initial storage coefficients are reasonably close to the true values. However, when a split sample is used, the water levels computed from calibration and prediction should match reasonably close to the respective observed water levels. Consequently, the degree of accuracy needed in the estimated storage coefficients is limited to obtaining a converging solution which would give water levels which are close to observed water levels. This can be achieved after making a few trials by using refined estimates of storage coefficients during each trial. Therefore, for all practical purposes, the present procedure, unlike other conventional methods, does not rely upon predetermined values of aquifer transmissivity and storage coefficients.

5.1.3 Data Requirements

The input data required for solving a groundwater flow problem depend on the type of model considered in the study. For example, when a finite difference model is used for analysis, the historical records of pumping rates, groundwater levels, river stages and the aquifer properties, i.e., the transmissivity and the storage coefficient are used as primary inputs. The aquifer properties are usually determined from field pumping tests which are expensive. The input variables such as pumping rates, groundwater levels and river stages are also used for analysis in the present procedure. However, the aquifer storage coefficients and transmissivities are estimated and computed respectively as explained in Sec. 3.1.1.

Consequently, in the present procedure, the effort required for acquisition of data is much smaller as compared to the corresponding effort in a finite difference model.

Therefore, the historical inputs such as pumping rates, groundwater levels and river stages are very essential irrespective of the type of model used in the analysis. Hydrological data such as streamflow, river stage and precipitation are measured at many gaging stations in the United States and are extensively documented. However, pumping data and groundwater level information of few well fields are available in such detail. Groundwater levels are often recorded in one or two observation wells in a well field at irregular time intervals and pumping data are available as monthly or yearly averages. It is difficult to achieve meaningful results by using such sparse data in any model. A few of the difficulties experienced in formulating a numerical-digital computer model for regional aquifer evaluation studies by using such sparse data, and the accuracy of the results obtained from such a model are discussed in Bathala et al., (1976).

In view of these considerations, accurate and long-term records of historical data are very essential. Therefore, a book-keeping procedure or installation of continuous recorders for the measurement of groundwater levels and pumping rates is highly recommended.

5.1.4 Analysis of Pumping Test Data

The utility of the present procedure as a substitute for the traditional type curve method to determine the transmissivity and the storage coefficient has been demonstrated in Sec. 3.3. In this method, it is possible to improve the solution by comparing the discrepancies between the observed and the computed drawdowns from different trials. Unlike the type curve method, the possibility of human errors is small. Another disadvantage of the type curve solution, which is absent in the present method is that the storage coefficient value cannot be determined accurately when there is lack of early time-drawdown data. This is evident from the comparison of the results obtained from the present procedure with those obtained from the type curve method for different case studies illustrated in Sec. 3.3.2. Consequently, the present procedure appears to be more reliable than the type curve method to determine the aquifer transmissivity and the storage coefficient from pumping test data.

5.2 Causal Relationships Between Precipitation, River Stages and Groundwater Levels

The procedure for investigating the causal relationships between precipitation, river stages and groundwater levels have been presented in Chapter 4. Monthly precipitation, river stages and groundwater levels measured at different locations in Lafayette and West Lafayette, Indiana were used in the analysis.

5.2.1 Models for Water Levels in Well Tc-7

Three different models, viz. H2, HHX and HHY were fitted to the water levels in well Tc-7 in West Lafayette. The first of these was a univariate model (Table 4.3) and the second model (Eq. 4.21) was

developed after incorporating the causal relationship between the residuals of univariate model H2 and those of univariate model AGF for rainfall at the Agronomy Farm. The model HHY (Eq. 4.24) has been formulated after considering the causal relationship between the residuals of univariate model H2 and those of univariate model WAB for the Wabash River stages.

The statistical characteristics of the simulated sequences of models HHX and HHY were in close agreement with those of the observed data (Sec. 4.3.8). In particular, the higher order properties such as coefficients of skewness and kurtosis were also preserved in these simulated sequences. Consequently, the models HHX and HHY developed after considering the causal relationships are superior models than the model H2.

An added advantage of these two models for generating synthetic sequences of groundwater levels is in simulation. For example, models for groundwater levels are formulated by using rainfall as one of the inputs (Rao et al., 1975). A general form of this model is given as

$$Y(k+1) = \alpha_0 + \alpha_1 Y(k) + \dots + \beta_1 X(k) + \beta_2 X(k-1) + \dots + n(k+1), \quad (5.1)$$

where, $Y(\cdot)$ and $X(\cdot)$ represent the groundwater level and rainfall processes respectively and $n(\cdot)$ are the residuals. In the above model (Eq. 5.1), it is more difficult to simulate $X(\cdot)$ series than the random noise, $n(\cdot)$ series. On the other hand, the final stochastic models, HHX and HHY (Eqs. 4.21 and 4.24) are composed of the past values of groundwater levels and residual sequences such as $W_A(\cdot)$, $n_{YA}(\cdot)$, $W_S(\cdot)$ and $n_{YS}(\cdot)$. As explained earlier (Sec. 4.3.8), these residual sequences can be readily generated on a digital computer using the appropriate probability distributions. Consequently, the present formulation is better suited for generating synthetic sequences of groundwater levels.

5.2.2 Model for Water Levels in Well Tc-9

The final stochastic model for water levels in well Tc-9 (Eq. 4.25, model H3) does not include any terms of residuals from either precipitation or river stage models due to the reasons explained in Sec. 4.3.5. The characteristics of the simulated data from this model were considerably different from those of the observed data (Sec. 4.3.8). As explained earlier (Sec. 4.3.5) the aquifer in the vicinity of well Tc-9 is mostly under confined condition and hence the effects of the Wabash River stages and rainfall are considerably damped out. Consequently, these damped effects were not detected by the tests used for investigating the causal relationships.

5.3 Scope for Further Investigation

The foregoing analysis of groundwater flow problems and the investigation of causal relationships have given rise to several other problems which need further investigation. A few of these are briefly described below.

- (1) As discussed in Sec. 5.1.2, when the initial estimates of storage coefficients are very different from actual values, the simultaneous solution of the nonlinear equations may not converge to the desired accuracy. This aspect needs further analysis and investigation.
- (2) The present procedure for the determination of the aquifer response by considering only the cause-and-effect relationships of the system has given encouraging results when applied to a hypothetical groundwater flow problem and to a few field situations of small areal extent. However, the usefulness of the present procedure has not been tested using field input data on a regional basis. This aspect needs further investigation.
- (3) In the present analysis of the regional aquifer flow problem, the vertical recharge due to precipitation has not been considered. Most large aquifers receive major portion of their recharge from precipitation and this should be considered in the analysis. A theoretical relationship using the impulse response relationship between precipitation and groundwater levels would be of great use in introducing recharge due to rainfall. In the present study, a theoretical formulation has been presented (Sec. 2.2.1) on the basis of the theory of leaky artesian aquifers (Hantush, 1964). This formulation does not relate precipitation directly to groundwater levels, but considers only leakage from an overlying semi-permeable confining layer. Also no numerical example has been presented by using this theoretical formulation. Therefore, further analysis in this direction would be very useful in making the present procedure more general.
- (4) A few case histories of pumping test data have been analysed in the present study for the determination of the aquifer transmissivity and the storage coefficient. Several more pumping tests must be analysed to determine whether the present procedure is better than the traditional type curve method.
- (5) The present approach used for developing stochastic models for groundwater levels incorporating the causal relationships between groundwater levels and the precipitation and the river stage processes leads to better models. However, data from other locations should be used in this formulation to reinforce this conclusion.

5.4 Conclusions

The following conclusions can be presented on the basis of the study reported herein.

1. The linear systems approach can be usefully employed to analyse several types of groundwater flow problems.
2. The procedure developed in the present study for predicting aquifer response due to different hydrologic effects by considering only the cause-and-effect relationships of the system is satisfactory. For practical purposes, this procedure does not require a precise knowledge of the aquifer properties, viz. the transmissivity and the storage coefficient values.

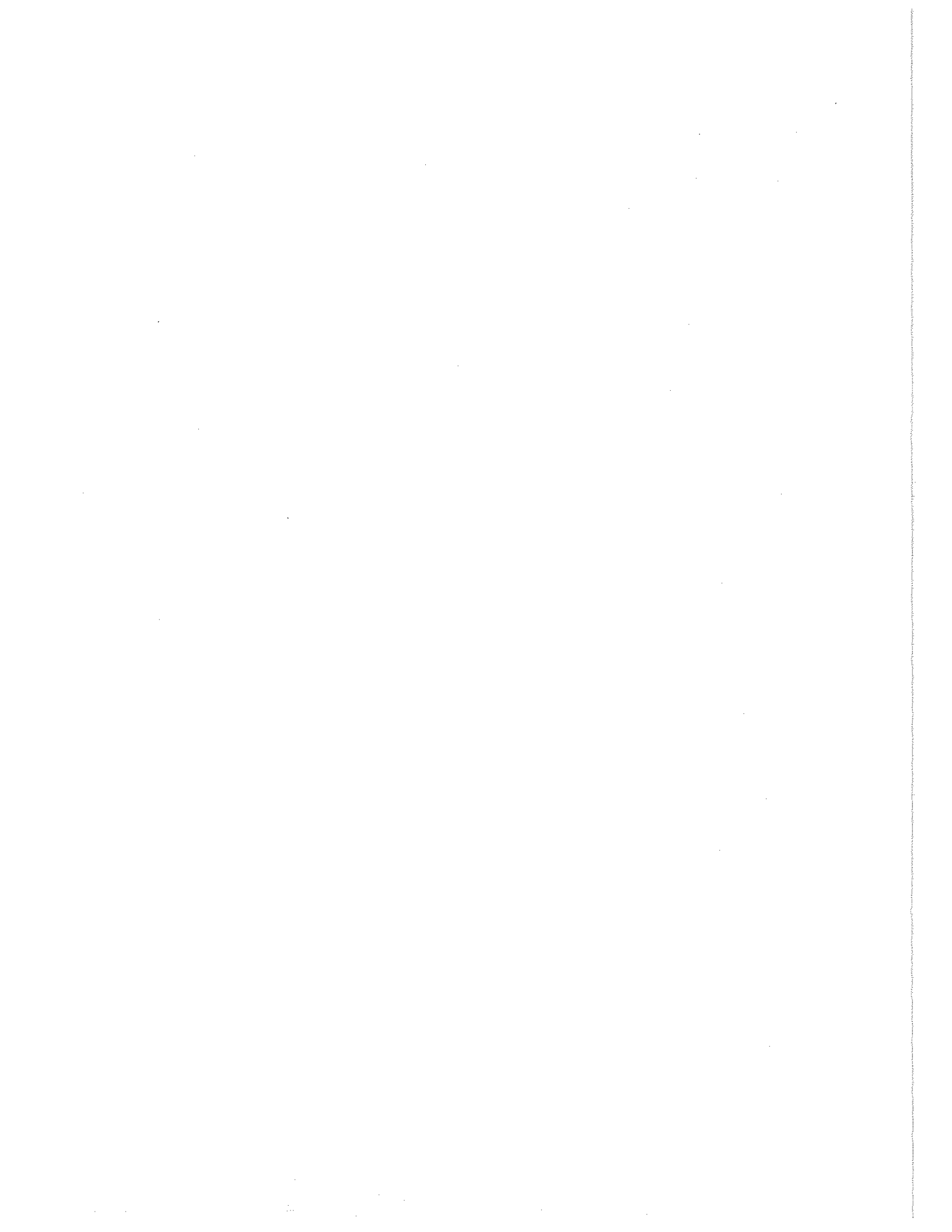
3. The computational expenditure and the complexity of the problem are considerably reduced in the present formulation compared to the R-C networks or the finite difference models.
4. The procedure detailed in the present study can be successfully used to predict response of regional aquifer systems. However, adequate and accurate input data are essential for the implementation of this procedure. A well integrated program for the measurement of groundwater levels and pumping rates at regular time intervals from different wells in the study area would be of great use not only for applying this procedure but also for the agencies which are involved in the evaluation of groundwater resources.
5. The present procedure for the prediction of aquifer response can also be employed to determine the aquifer transmissivity and the storage coefficient from pumping test data. This procedure appears to be more promising than the type curve method for pumping test analysis.
6. The causal relationships between precipitation, river stages and groundwater levels are very useful to formulate better stochastic models for groundwater levels.

BIBLIOGRAPHY

1. Abramowitz, M., and I. A. Stegun, Handbook of Mathematical Functions, pp. 1046, Dover Publications, Inc., New York, 1965.
2. Bartlett, M. S., An Introduction to Stochastic Processes, Cambridge Uni. Press, Cambridge, 1955.
3. Bathala, Chenchayya T., "The Application of Linear Systems Analysis to Groundwater Evaluation Studies," Ph.D thesis, Purdue University, West Lafayette, Indiana, August 1976.
4. Bathala, C. T., Spooner, J. A., and A. R. Rao, "Regional Aquifer Evaluation Studies with Stochastic Inputs," Tech. Report No. 72, Purdue University, Water Resources Res. Center, West Lafayette, Indiana, February 1976.
5. Bear, J., Dynamics of Fluids in Porous Media, American Elsevier Publishing Co., Inc., New York, 1972.
6. Box, G. E. P and G. M. Jenkins, Time Series Analysis, Forecasting and Control, Holden Day, San Francisco, 1970.
7. Box, G. E. P., and D. A. Pierce, "Distribution of Residual Auto Correlations in Autoregressive - Integrated Moving Average Time Series Models," Jour. of Am. Stat. Assoc., Vol. 64, 1970.
8. Bredehoeft, J. D., and R. A. Young, "The Temporal Allocation of Ground Water - A Simulation Approach," Water Resources Res., Vol. 6, No. 1, pp. 3-21, February, 1970.
9. Carnahan, B., Luther, H. A., and J. O. Wilkes, Applied Numerical Methods, pp. 604, John Wiley & Sons, Inc., New York, 1969.
10. Carslaw, H. S., and J. C. Jaeger, Conduction of Heat in Solids, pp. 510, Oxford University Press, London, 1959.
11. Cheng, D. K., Analysis of Linear Systems, pp. 431, Addison-Wesley Publishing Company, Inc., Reading, Massachusetts, 1959.
12. Cooper, H. H., Jr., and C. E. Jacob, "A Generalized Graphical Method for Evaluating Formation Constants and Summarizing Well-Field History," Trans. Am. Geophys. Union, Vol. 27, pp. 526-534, 1946.
13. Courant, R., "Variational Methods for the Solution of Problems of Equilibrium Vibrations," Bull. Am. Math. Soc., pp. 1-23, Vol. 49, 1943.
14. De Wiest, R. J. M., Geohydrology, John Wiley and Sons, Inc., New York, 1965.
15. Dixon, W. J., Biomedical Computer Programs, Uni. of California Press, Berkeley, California, 1971.
16. Dooge, J. C. I., "Linear Theory of Hydrologic Systems," U.S. Dept. Agri., Tech. Bull., 1968, pp. 327, 1973.
17. Eagleson, P. S., Mejia R. M., and F. March, "Computation of Optimum Realizable Unit Hydrographs," Water Res. Res., Vol. 2, No. 4, Fourth quarter 1966.
18. Eriksson, E., "Groundwater Time-Series: An Exercise in Stochastic Hydrology," Nordic Hydrology, pp. 181-205, 1970.
19. Gelhar, L. W., "Stochastic Analysis of Phreatic Aquifers," Water Resour. Res., Vol. 10, No. 3, June, 1974.
20. Granger, C. W. J., "Economic Processes Involving Feedback," Information and Control, 6, pp. 28-48, 1963.
21. Hall, F. R., and A. F. Moench, "Application of the Convolution Equation to Stream-Aquifer Relationships," Water Resour. Res., Vol. 8, No. 2, April 1972.
22. Hantush, M. S., "Hydraulics of Wells" in Advances in Hydroscience, edited by Chow, V. T., Academic Press Inc., New York, 1964.

23. Hantush, M. S., and C. E. Jacob, "Non-Steady Radial Flow in an Infinite Leaky Aquifer," *Trans. Am. Geophys. Union*, Vol. 36, No. 1, February 1955.
24. Jackson, R. E., Gilliland, J. A., and K. Adamowski, "Time Series Analysis of the Hydrologic Regimen of a Groundwater Discharge Area," *Water Resour. Res.*, Vol. 9, No. 5, October 1973.
25. Jenkins, G. M., and D. G. Watts, Spectral Analysis and Its Applications, Holden-Day, San Francisco, 1968.
26. Johnson, E. E., Groundwater and Wells, pp. 440, Edward E. Johnson, Inc., Saint Paul, Minnesota, 1966.
27. Kashyap, R. L., and A. R. Rao, "Real Time Recursive Prediction of River Flows," *Automatica*, The Journal of the International Federation of Automatic Control, Vol. 9, No. 2, pp. 175-183, Pergamon Press, Oxford, England, March 1973.
28. Kashyap, R. L., and A. R. Rao, Stochastic Dynamic Models from Empirical Data, Academic Press, New York, 1976.
29. Kisiel, C. C., "Time Series Analysis of Hydrologic Data," in Advances in Hydro-Science, edited by Chow, V. T., Vol. 5, Academic Press, Inc., New York, 1969.
30. Lohman, S. W., et al., "Definitions of Selected Ground-Water Terms - Revisions and Conceptual Refinements," Geological Survey Water-Supply Paper 1988, 1972.
31. Maarouf, A. M. S., and W. N. Melhorn, "Hydrogeology of Glacial Deposits in Tippecanoe County, Indiana," Tech. Rep. No. 61, Purdue University, Water Resour. Res. Center, West Lafayette, Ind., June 1975.
32. Maddock, T., III, "Algebraic Technological Function from a Simulation Model," *Water Resour. Res.*, Vol. 8, No. 1, pp. 129-134, February 1972.
33. Maddock, T., III, "The Operation of a Stream-Aquifer System Under Stochastic Demands," *Water Resour. Res.*, Vol. 10, No. 1, February 1974a.
34. Maddock, T., III, "A Program to Compute Response Coefficients for Algebraic Technological Functions," U.S. Geological Survey, Open File Report, November 1974b.
35. Maddock, T., III, "A Drawdown Prediction Model Based on Regression," Paper Presented at the Symposium on Hydraulic Engineering for Optimal Use of Water Resources, 23rd. Annual Specialty Conference, Hyd. Div., A.S.C.E., Univ. of Washington, Seattle, Washington, August 6-8, 1975.
36. Moench, A., "Groundwater Fluctuations in Response to Arbitrary Pumpage," *Ground Water*, Vol. 9, No. 2, pp. 4-8, March-April 1971.
37. Moench, A. F., and C. C. Kisiel, "Application of the Convolution Relation to Estimating Recharge from an Ephemeral Stream," *Water Resour. Res.*, Vol. 6, No. 4, August 1970.
38. Morel-Seytoux, H. J., "A Simple Case of Conjunctive Surface-Ground-Water Management," *Ground Water*, Vol. 13, No. 6, November - December 1975.
39. Morel-Seytoux, H. J., and C. J. Daly, "A Discrete Kernel Generator for Stream-Aquifer Studies," *Water Resources Research*, Vol. 11, No. 2, April 1975.
40. Muskat, M., The Flow of Homogeneous Fluids Through Porous Media, McGraw-Hill Book Company, New York, 1937.
41. Pinder, G. F., and J. D. Bredehoeft, "Application of the Digital Computer for Aquifer Evaluation," *Water Resour. Res.*, Vol. 4, No. 5, 1968.
42. Pinder, G. F., Bredehoeft, J. D., and H. H. Cooper, Jr., "Determination of Aquifer Diffusivity from Aquifer Response to Fluctuations in River Stage," *Water Resour. Res.*, Vol. 5, No. 4, August 1969.
43. Prickett, T. A., and C. G. Lonquist, "Selected Digital Computer Techniques for Groundwater Resource Evaluation," Bulletin 55, Illinois State Water Survey, Urbana, Ill., 1971.
44. Prickett, T. A., "Modeling Techniques for Groundwater Evaluation," in Advances in Hydrosience, edited by Chow, V. T., Academic Press, New York, 1975.
45. Rao, R. A., Kashyap, R. L. and R. G. S. Rao, "Stochastic Models for the Interaction of Rainfall and Groundwater Levels," Proc. of the International Symposium on Development of Groundwater Resources, College of Engineering, Guindy, Madras, India, 1973.

46. Rao, A. R., Rao, R. G. S., and R. L. Kashyap, "Stochastic Models for Ground Water Levels," Tech. Rept. No. 67, Purdue University, Water Resour. Res. Center, West Lafayette, Ind., August 1975.
47. Remson, I., Hornberger, G., and F. J. Molz, Numerical Methods in Subsurface Hydrology, Wiley-Interscience, New York, 1971.
48. Rosenshein, J. S., "Ground-Water Resources of Tippecanoe County, Indiana," Bull. No. 8, Division of Water Resources, Indiana Dept. of Conservation, 1958.
49. Suter, M., Bergstrom, R. E., Smith, H. F., et al., "Preliminary Report on Ground-Water Resources of the Chicago Region, Illinois," State Water Survey and State Geol. Survey Coop. Ground-Water Report 1, Illinois, 1959.
50. Theis, C. V., "The Relation Between the Lowering of the Piezometric Surface and the Rate and Duration of Discharge of a Well Using Groundwater Storage," Trans. Am. Geophys. Union, 16, pp. 519-524, 1935.
51. Todd, D. K., Ground Water Hydrology, John Wiley & Sons, Inc., New York, 1959.
52. Venetis, C., "Finite Aquifers: Characteristic Responses and Applications," Jour. Hydrol, 12, pp. 53-62, 1970.
53. Venetis, C., "Estimating Infiltration and/or the Parameters of Unconfined Aquifers From Ground Water Level Observations," Jour. Hydrol., 12, pp. 161-169, 1971.
54. Walton, W. C., Groundwater Resource Evaluation, McGraw-Hill Book Company, New York, 1970.
55. Wenzel, L. K., "The Theim Method for Determining Permeability of Water-Bearing Materials and Its Application to the Determination of Specific Yield," Water Supply Paper 679-A, 1936.
56. Wenzel, L. K., "Methods of Determining Permeability of Water-Bearing Materials, with Special Reference to Discharging Well Methods," U. S. Geol. Survey, Water - Supply Paper, 887, 1942.
57. Wolfe, P., "The Secant Method for Simultaneous Nonlinear Equations," Communications of the ACM, Vol. 2, pp. 12-13, 1959.



APPENDIX A

A.1 Single Well in an Infinite Nonleaky Artesian Aquifer Pumped at a Constant Rate

Consider the basic form of the Theis equation, 2.7 which is again shown below for convenience.

$$s(r,t) = \int_0^t q(\tau) \frac{\exp\left[-\frac{r^2 S}{4T(t-\tau)}\right]}{4\pi T(t-\tau)} d\tau \quad (2.7)$$

When the well is pumped at a constant rate Q during the pumping period t , Eq. 2.7 can be written as

$$s(r,t) = \frac{Q}{4\pi T} \int_0^t \frac{\exp\left[-\frac{r^2 S}{4T(t-\tau)}\right]}{t-\tau} d\tau \quad (A.1)$$

Let,

$$v = \frac{r^2 S}{4T(t-\tau)} \quad (A.2)$$

$$dv = \frac{r^2 S}{4T(t-\tau)^2} d\tau \quad (A.3)$$

$$d\tau = (t-\tau) dv/v \quad (A.4)$$

with the limits of integration:

$$\left. \begin{array}{l} \text{as } \tau \rightarrow 0, \text{ lower limit } \rightarrow u = \frac{r^2 S}{4Tt} \\ \text{as } \tau \rightarrow t, \text{ upper limit } \rightarrow \infty \end{array} \right\} \quad (A.5)$$

Equation 2.10a is obtained after substituting Eqs. A.1, A.4 and A.5 into Eq. A.1 (Theis, 1935).

$$s(r,t) = \frac{Q}{4\pi T} \int_u^\infty \frac{e^{-v}}{v} dv \quad (2.10a)$$

A.2 Single Well in an Infinite Nonleaky Artesian Aquifer Pumped at a Variable Rate

Let a single well located in an artesian aquifer of infinite areal extent be pumped at different rates during different times as shown in Fig. A.1. Then, Eq. 2.7 can be written for each time step as shown in Eqs. A.7 by using the method of superposition illustrated in Fig. A.2. The following notation (Eqs. A.6) is used in formulating Eqs. A.7.

$$\alpha_i = \frac{1}{4\pi T} \int_{u_i}^\infty \frac{e^{-v}}{v} dv \quad (i = 1, 2, \dots, N) \quad (A.6a)$$

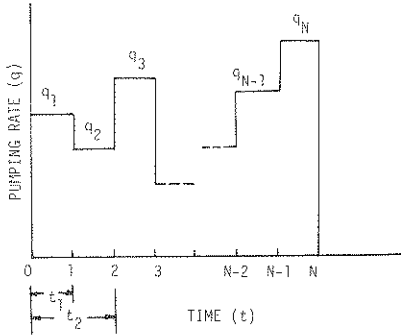


FIGURE A.1 STEP PUMPING SCHEME

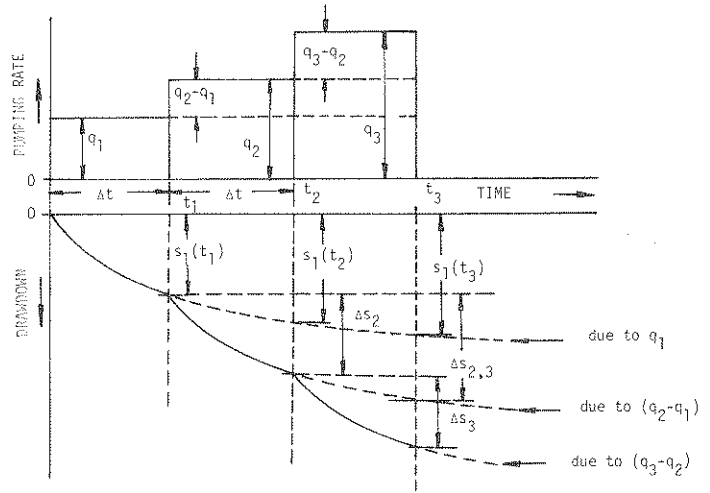


FIGURE A.2 METHOD OF SUPERPOSITION

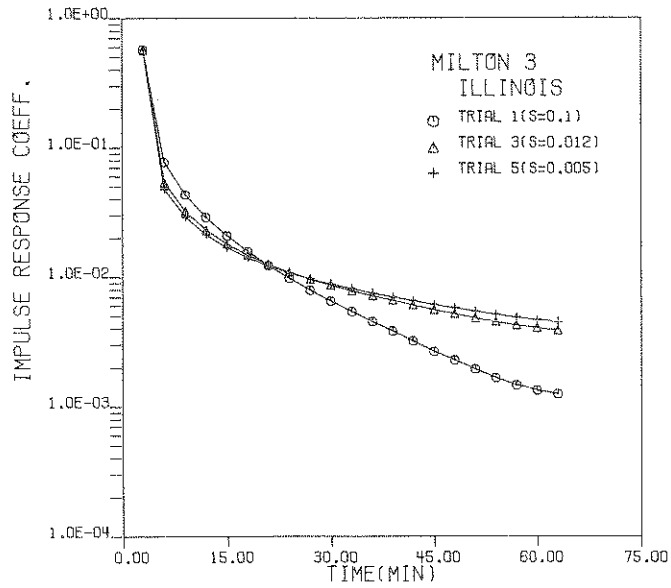


FIGURE A.3 UNIT IMPULSE RESPONSE COEFFICIENTS FOR WELL 3, MILTON, JUNE 1969

$$u_i = \frac{r^2 S}{4Tt_i} \quad (\text{A.6b})$$

$$\beta_i = \alpha_i - \alpha_{i-1} \quad (\text{A.6c})$$

$$\alpha_{i-1} = 0 \quad \text{when } i = 1 \quad (\text{A.6d})$$

(i) First time step ($t=t_1$)

$$s(r, t_1) = s_1(t_1) = q_1 \alpha_1 = q_1 \beta_1 \quad (\text{A.7a})$$

(ii) Second time step ($t=t_2$)

$$s(r, t_2) = s_1(t_2) + \Delta s_2 = q_1 \alpha_2 + (q_2 - q_1) \alpha_1 = \beta_1 q_2 + \beta_2 q_1 \quad (\text{A.7b})$$

(iii) Third time step ($t=t_3$)

$$s(r, t_3) = s_1(t_3) + \Delta s_{2,3} + \Delta s_3 = q_1 \alpha_3 + (q_2 - q_1) \alpha_2 + (q_3 - q_2) \alpha_1 = \beta_1 q_3 + \beta_2 q_2 + \beta_3 q_1 \quad (\text{A.7c})$$

(iv) N^{th} time step ($t=t_N$)

$$\begin{aligned} s(r, t_N) &= s_1(t_N) + \Delta s_{N-1,N} + \Delta s_{N-2,N} + \dots + \Delta s_N \\ &= q_1 \alpha_N + (q_2 - q_1) \alpha_{N-1} + (q_3 - q_2) \alpha_{N-2} + \dots + (q_N - q_{N-1}) \alpha_1 \\ &= \beta_1 q_N + \beta_2 q_{N-1} + \beta_3 q_{N-2} + \dots + \beta_N q_1 \end{aligned} \quad (\text{A.7d})$$

In general,

$$s(r, t_N) = \sum_{i=1}^N \beta_i q_{N-i+1} \quad (\text{A.8})$$

A.3 Multiple Well System in an Infinite Nonleaky Artesian Aquifer

The drawdown at any well k in a multiple well system consisting of M wells is equal to the sum of the drawdowns caused by each well at the k^{th} well. This relationship is expressed as shown in Eq. A.9.

$$s(k, N) = \sum_{j=1}^M s(j, N) \quad (\text{A.9})$$

where, $s(k, N)$ is the resultant drawdown of the k^{th} well at N^{th} time step, and $s(j, N)$ is the drawdown at the k^{th} well due to pumping in the j^{th} well at N^{th} time step.

Eq. A.9 is written as in Eq. 2.17 by using Eq. A.8 and appropriate notation to distinguish each of the M wells.

$$s(k, N) = \sum_{j=1}^M \sum_{i=1}^M \beta(k, j, i) q(j, N-i+1) \quad (\text{2.17})$$

A.4 Relationship Between Unit Impulse Response Coefficients and Beta Coefficients

Eqs. 2.33 and 2.31 can be expanded as shown for the first two time steps (Eqs. A.10).

$$s_1 = q_1 U_1 \Delta_1 = q_1 \beta_1 \quad (i=1) \quad (\text{A.10a})$$

$$s_2 = q_1 U_2 \Delta_1 + q_2 U_1 \Delta_2 = q_1 \beta_2 + q_2 \beta_1 \quad (i=2) \quad (\text{A.10b})$$

Using Eqs. A.10 the relationships for U-coefficients are obtained as shown in Eqs. A.11.

$$U_1 = \beta_1 / \Delta_1 \quad (\text{A.11a})$$

$$U_2 = \frac{(q_1 \beta_2 + q_2 \beta_1) - q_2 U_1 \Delta_2}{q_1 \Delta_1} \quad (\text{A.11b})$$

It follows from the above equation that a general recursive relationship between U-coefficients and β -coefficients can be expressed for any time step N as shown in Eq. A.12.

$$U_N = \frac{\sum_{j=1}^N q_j \beta_{N-j+1} - \sum_{i=2}^N U_{i-1} q_{n-i+2} \Delta_{N-i+2}}{q_1 \Delta_1} \quad (\text{A.12})$$

The above relationship is used to compute U-coefficients from β -coefficients obtained for the pumping test analysis at Milton, Illinois (Sec. 3.3.2(a)). The β -coefficients computed for each observation during the period of calibration are plotted in Fig. 3.14 for trials 1, 3 and 5. The unit impulse response coefficients computed by using the recursive relationship given in Eq. A.12 and the known values of computed β -coefficients (Fig. 3.14) and pumping rates (Table 3.11) are shown in Fig. A.3. These plots of U-coefficients also show an exponential decay and become asymptotic to the time axis with increasing time.

TABLE B.1

TIME-DRAWDOWN, WELL 4, MILTON, ILLINOIS

Pumping Well: Well No. 4
 Diameter: 12", Depth: 56 ft., Ground El.: 621.00
 Location: 30'S, 2250'E, N.W. Corner of Sec. 9, T.6S., R.2W
 Obs. Well: Well No. 3, 10 ft. west of Well No. 4
 Diameter: 8", Depth: 63 ft., Ground El.: 630.00
 Date of Test: 10:10 a.m., November 24, 1969

Date and Time	Time Since Pumping Started (Min)	Pumping Rate (gpm)	Drawdown (ft.)	
			Pumping Well	Obs. Well
1	2	3	4	5
Nov. 24, 1969				
10:10 A.M.	0	0	0.	0
10:11	1	30	4.40	
10:12	2	30	4.47	
10:13	3	30	5.33	
10:14	4	30	5.50	
10:15	5	30	5.63	4.22
10:16	6	30	5.77	
10:17	7	30	5.90	
10:18	8	30	5.99	
10:19	9	30	6.08	
10:20	10	30	6.20	4.54
10:22	12	30	6.30	
10:25	15	32	6.39	
10:30	20	33	6.58	
10:35	25	30	6.59	
10:40	30	30	6.70	5.00
10:50	40	30	6.83	
11:00	50	30	6.94	5.25
11:10	60	30	7.01	
11:20	70	30	7.05	5.37
11:35	85	30	7.16	
11:40	90	30	7.19	
11:50	100	30	7.27	
12:10 P.M.	120	30	7.29	5.64
12:40	150	30	7.35	5.72
12:42	152	0	2.42	
12:43	153	0	2.06	
12:44	154	0	1.87	
12:45	155	0	1.71	
12:46	156	0	1.56	
12:47	157	0	1.49	
12:48	158	0	1.45	
12:49	159	0	1.37	
12:50	160	0	1.34	
12:52	162	0	1.26	
12:55	165	0	1.15	
1:00	170	0	1.07	
1:05	175	0	0.97	
1:10	180	0	0.91	
1:12	182	10	2.06	
1:14	184	10	2.10	
1:16	186	10	2.10	
1:18	188	10	2.10	
1:20	190	10	2.10	
1:22	192	20	3.95	
1:24	194	20	4.25	
1:26	196	20	4.37	
1:28	198	20	4.46	
1:30	200	20	4.51	
1:32	202	30	6.44	
1:34	204	30	6.71	
1:36	206	30	6.82	
1:38	208	30	6.95	
1:40	210	30	7.01	

TABLE B.2

TIME-DRAWDOWN DATA, WELL 3, MILTON, ILLINOIS

Pumping Well: Well No. 3
 Diameter: 8", Depth: 63 ft., Ground El.: 630.00
 Location: 2250'E, 39'S of NW Corner of Sec. 9, T.6S., R.2W.
 Date of Test: 11:45 A.M., June 5 to 3:43 P.M., June 7, 1969

Date and Time	Time Since Pumping Started (min)	Pumping Rate (gpm)	Drawdown (ft.)
1	2	3	4
6-5-1969			
11:45 A.M.	0	0	0
11:49	4	105	25.25
11:50	5	105	26.12
11:51	6	105	26.77
11:52	7	105	27.32
11:53	8	105	27.76
11:54	9	105	28.28
11:55	10	105	28.52
11:56	11	105	28.86
11:58	13	105	29.23
12:00	15	105	29.73
12:05 P.M.	20	105	30.58
12:06	21	105	30.74
12:12	27	105	31.63
12:15	30	105	31.94
12:22	37	105	32.65
12:25	40	105	32.88
12:30	45	105	32.86
12:31	46	105	33.40
12:36	51	105	33.49
12:38	53	105	33.44
12:42	57	105	33.96
12:47	62	105	34.62
12:49	64	105	34.65
12:56	71	101	35.34
12:57	72	101	35.41
1:00	75	101	35.58
1:11	86	101	35.38
1:12	87	101	34.48
1:14	89	101	34.75
1:16	91	101	35.49
1:18	93	101	35.56
1:23	98	101	35.71
1:25	100	101	35.76
1:40	115	100	36.44
1:49	124	100	36.67
1:51	126	100	36.70
2:13	148	100	37.75
2:20	155	100	37.92
2:27	162	100	38.02

TABLE B.3

TIME-DRAWDOWN DATA, WELL 1, GRIDLEY, ILLINOIS

Pumping Well: Well No. 3
 Depth: 300 ft.
 Location: Village of Gridley, Sec. 4, T.26N., R.3E.
 Obs. Well: Well No. 1
 Distance: 824 ft. from Well No. 3
 Date of Test: 9:45 A.M., July 2, 1953

Time Since Pumping Started (min)	Pumping Rate (gpm)	Drawdown (ft.) Well No. 1
0	0	0
3	220	0.3
5	220	0.7
8	220	1.3
12	220	2.1
20	220	3.2
24	220	3.6
30	220	4.1
38	220	4.7
47	220	5.1
50	220	5.3
60	220	5.7
70	220	6.1
80	220	6.3
90	220	6.7
100	220	7.0

TABLE B.4

TIME-DRAWDOWN DATA, WELL 5,
GRAND ISLAND, NEBRASKA

Pumping Well: Well 83
 Diameter: 24", Depth - 40 ft., Ground El: 1812.16 ft.
 Location: NW $\frac{1}{4}$, Sec. 17, T.11N., R.8W.
 Obs. Well: Well 5, 229 ft. away from Well 83
 Diameter: 1", Depth - 12.9 ft., Ground El.: 1814.43 ft.
 Date of Test: 6:05 A.M., July 29, 1931 to 6:04 A.M., July 31, 1931

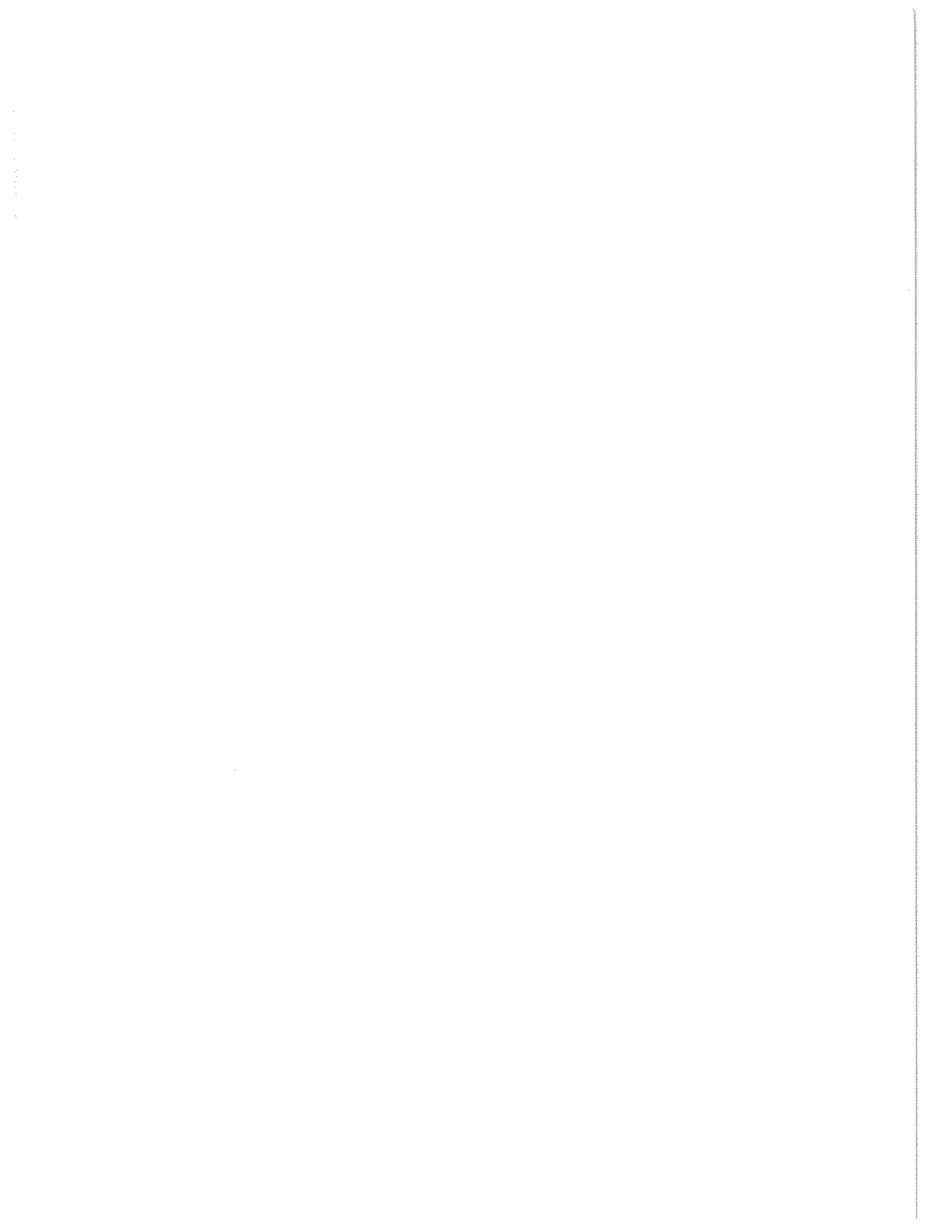
Date and Time	Pumping Rate (gpm)	Drawdown (ft.) Well 5
July 29, 1931		
6:05 A.M.	0.0	0.0
7:00	540.0	0.09
8:00	540.0	0.19
9:00	540.0	0.28
10:00	540.0	0.34
11:00	540.0	0.39
12:00	540.0	0.44
1:00 P.M.	540.0	0.49
2:00	540.0	0.54
3:00	540.0	0.58
4:00	540.0	0.62
5:00	540.0	0.66
6:00	540.0	0.69
7:00	540.0	0.72
8:00	540.0	0.74
9:00	540.0	0.76
10:00	540.0	0.78
11:00	540.0	0.80

TABLE B.5

GROUNDWATER LEVELS AND RIVER STAGES NEAR
THE KANKAKEE RIVER, DUNNS BRIDGE, INDIANA

Date	River Stage (Ft. above datum)	Water Levels in Well No. 1 (ft. above M.S.L.)
October 1972		
24	8.19	658.11
25	9.00	658.50
26	9.22	658.67
27	9.33	658.77
28	9.32	658.82
29	9.07	658.72
30	8.72	658.55
31	8.40	658.40
November 1972		
1	8.14	658.21
2	7.95	658.13
3	7.93	658.03
4	7.97	657.99
5	8.02	657.97
6	7.88	657.92
7	7.65	657.82

Datum of river gage = 649.65 ft. above mean sea level



Water Resources Research Center
Lilly Hall of Life Sciences
Purdue University
West Lafayette, Indiana 47907

BULK RATE

Non-profit Organization
U. S. Postage
PAID
Permit No. 121
Lafayette, Indiana